# GENETIC DISSECTION OF NEGATIVE REGULATION ON DISEASE RESISTANCE GENES IN ARABIDOPSIS

A Dissertation

Presented to the Faculty of the Graduate School

of Cornell University

In Partial Fulfillment of the Requirements for the Degree of

Doctor of Philosophy

by

ZHILONG BAO

August 2013

# GENETIC DISSECTION OF NEGATIVE REGULATION ON DISEASE RESISTANCE GENES IN ARABIDOPSIS

ZHILONG BAO, Ph. D.

Cornell University 2013

Plant defense responses are repressed under non-pathogenic conditions to ensure optimal plant growth and development. *R* (Disease Resistance) genes are central regulators mediating robust disease resistance. An *R* gene *SNC1* is negatively regulated by an evolutionarily conserved copine gene *BON1* in Arabidopsis. The loss of *BON1* function leads to enhanced disease resistance but a growth defect in a *SNC1* dependent manner. To understand how the *R* gene *SNC1* is regulated, I analyzed enhancers and suppressors of *bon1* mutants.

The study of *bon1* enhancer *ebo30* reveals an effect on *R* gene expression by cell cycle progression. The *ebo30* mutant is an overexpression allele of *OSD1* (*omission of second division 1*). Both *OSD1* gene and its homolog *UVI4* are negative regulators of anaphase-promoting complex/cyclosome (APC/C), a multisubunit ubiquitin E3 ligase that regulates the progression of cell cycles. Overexpression of *OSD1* or *UVI4* as well as down regulation of *APC10* confers enhanced resistance to a bacterial pathogen. Further, enhanced immune response induced by *OSD1* overexpression is dependent on *CYCB1;1* and the *R* gene *SNC1*. Together, this study suggests that mis-regulated cell cycle progression has an impact on *R* gene expression and plant immunity.

This notion is reinforced by the study of interaction of *UVI4* and *OSD1* with *CPR5*, a gene involved in both defense and cell cycle regulation. The *cpr*5 mutant was reported to have reduced endoreduplication and enhanced disease resistance. These cell cycle defects of *osd1* and

*uvi4* single and double mutants can be suppressed by *cpr5* mutation. Therefore, the *CPR5* gene may have a direct role in cell cycle regulation and subsequently affect plant immunity.

The study of *mos1*, a suppressor of *bon1* reveals a new transcriptional regulator for plant immunity, flowering time and endoreduplication. The *mos1* mutant has compromised defense responses, is late flowering, and has enhanced endoreduplication. These phenotypes are due to the change of expression of *SNC1*, *FLC*, and potentially *CYCD3;1* respectively. The function of *MOS1* in modulating flowering time and cell cycle progression is dependent on SUF4, a previously known transcription factor for flowering time control. MOS1 is found to physically interact with SUF4, and may thus repress its function. The interaction of MOS1 and SUF4 might be influenced by MAD2, a component in the spindle assembly checkpoint complex. The interactions among MOS1, MAD2 with SUF4 suggest an intriguingly possibility that checkpoint machinery might have a direct impact on flowering time control.

In sum, this study provides insights into complex regulation on R genes in plants, and discusses potential connections among regulations of defense, cell cycle, and flowering time.

BIOGRAPHICAL SKETCH

| | |
|---|---|
| December 31st, 1980 | Born, Changzhou Jiangsu, China |
| 1999-2003 | B.S., Biotechnology<br>Nanjing Agricultural University |
| 2003 – 2005 | M.S., Plant Pathology<br>Nanjing Agricultural University |
| 2009 – 2013 | Ph.D., Plant Biology<br>Cornell University |

This dissertation is dedicated to my parents, Aoxing Bao and Qinqin Qu.

献给我的父母，包敖兴和瞿琴琴。

ACKNOWLEDGMENTS

I would like to express my deepest appreciation to my advisor, Dr. Jian hua, who has greatest knowledge on science. Without her guidance and persistent help, I would never be able to complete this dissertation.

I would like to thank my committee members, Dr. Gregory Martin and Dr. Wojciech Pawlowski. Without their guidance and suggestions, I would never be able to complete this dissertation.

I would like to thank Dr. Wingking Yip and Dr. Lailiang Cheng. Dr. Wingking Yip was my former advisor when I was a graduate student in the University of Hong Kong and he supported me as a visiting student outside Hong Kong. Dr. Lailiang Cheng recommended me to work with my advisor Dr. Jian Hua as a visiting student. Without their help, I would not be a graduate student at Cornell.

I would like to thank all my former labmates, especially Huijun Yang, Ying Zhu, Weiqiang Qian, Mingyue Gou, Donglei Yang, Zhenying Shi, Jun Qian, Yi Wang and Yongqing Li. Ying Zhu and Yongqing Li gave me greatest help on my life and research work when I had trouble. Without their help, I would not be a graduate student at Cornell.

I would like to thank two of my best friends, Dr. Shixian Chen and her husband Tingzheng Chen. Without their help, I would not be able to conduct experiments efficiently.

I would like to thank all graduate students in Plant Biology program, especially Xian Qu, Sun Tao, Haiyi Wang and Margaret Frank. Their suggestions and technical support helped me conduct experiments efficiently.

I would like to thank my girlfriend, Dr. Fangfang Ma, whose consideration and help support me to complete this dissertation.

Last but not the least, I would like to thank my loving parents, Aoxing Bao and Qinqin Qu. Their love helps me get through every step in the life and study and brings me hope and faith of persistence when I was in trouble.

TABLE OF CONTENTS

LIST OF FIGURES

LIST OF TABLES

LIST OF ABBREVIATIONS

BON: BONZAI

SNC1: SUPPRESSOR OF *NPR1-1*, CONSTITUTIVE 1

EBO: ENHANCER OF *BON1-2*

OSD1: OMISSION OF THE SECOND DIVISION 1

UVI4: ULTRAVIOLET-B-INSENSITIVE 4

APC/C: ANAPHASE-PROMOTING COMPLEX/CYCLOSOME

CDC20: CELL DIVISION CYCLE 20

CCS52: CELL CYCLE SWITCH 52

CPR5: CONSTITUTIVE EXPRESSION OF *PR* GENES 5

SBO: SUPPRESSOR OF *BON1*-1

MOS1: MODIFIER OF *SNC1*, 1

SUF4: SUPPRESSOR OF FRIGIDA, 4

MAD: MITOTIC ARREST DEFICIENT

BUB: BUDDING UNINHIBITED BY BENZYMIDAZOL

# CHAPTER 1

# INTRODUCTION

Plant immune responses are repressed by negative regulators to protect the growth and development under the normal growth condition. There is a larger coordination of various biotic responses, abiotic responses, plant growth and plant development. Regulators of plant defenses might modulate other processes in plant growth and development. Studying the functions of these regulators will enable a better understanding of how plants fine-tune different processes to achieve the best fitness under the stress condition.

## 1.1 Plant immune responses

Plants are often subjected to pathogen invasions. To protect themselves, they use at least two layers of immune systems. The primary defense response, pathogen associated molecular pattern (PAMP) triggered immunity (PTI), is mediated by the pattern recognition receptors (PRRs) that recognize PAMPs which are essential components of pathogens such as bacterial flagellin, elongation factor (EF-Tu) or fungal chitin (Zipfel, 2009). PTI is sometimes overcome by effectors secreted from pathogens. To counteract this, plants monitor the effectors and activate a more robust immune response called effector trigged immunity (ETI) to limit bacterial growth. ETI is generally mediated by resistance (R) genes and associated with elevated production of reactive oxygen species (ROS) and activation of defense related genes such as *pathogenesis-related* (*PR*) genes (Jones and Dangl, 2006; Vlot et al., 2009; Dodds and Rathjen, 2010).

During the process of defense against pathogen invasion, oxidative burst is one of the earliest responses induced in plants. The increase in ROS such as hydrogen peroxide ($H_2O_2$), superoxide ion and nitric oxide (NO) contributes to programmed cell death (PCD), also called

hypersensitive response (HR) or hypersensitive cell death in plants. The Arabidopsis genome has at least 158 genes that regulate ROS production and scavenging (Van Breusegem and Dat, 2006). Two respiratory burst oxidase homologues (*Rbohs*), *AtrbohD* and *AtrbohF* play pivotal roles in the production of ROS during ETI (Torres et al., 2002). *AtrbohD* functions to restrict cell death at the infection site and is also required for a rapid, cell-to-cell propagation of systemic signals through the accumulation of ROS (Torres et al., 2002; Miller et al., 2009; Pogany et al., 2009). The *rbohD rbohF* double mutant suppresses the cell death phenotype but does not induce more susceptibility to virulent or avirulent bacterial pathogens (Torres et al., 2002). However, PCD is still the major contributor in disease resistance against downy mildew in Arabidopsis (Wang et al., 2011). Cysteine aspartate-specific proteases (caspases) are critical effectors in animal PCD, but no caspase function has been well demonstrated in plant PCD. How PCD affects plant defense signaling remains largely unknown.

The plant hormone salicylic acid (SA) plays a crucial role in plant defense signaling. SA was found to enhance the accumulation of $H_2O_2$ in systemic tissues. SA biosynthesis is carried out through two pathways mediated by ISOCHORISMATE SYNTHASE (ICS) and PHENYLALANINE AMMONIA LYASE (PAL) respectively. Arabidopsis has two ICS encoding genes but ICS1 has the major role in SA production during pathogen infection and UV light stress (Vlot et al., 2009; Dempsey et al., 2011). SA plays an important role in the activation of both PTI and ETI. Callose deposition induced by *Pseudomonas syringae* ΔCEL (conserved effector loci) mutant is SA dependent in Arabidopsis (DebRoy et al., 2004). In L*er* (Landsberg *erecta*)-*NahG* plants expressing *NahG* transgene which encodes the SA degradation enzyme salicylate hydroxylase, the resistance to *Pseudomonas syringae* pv. *tomato* DC3000/*avrRps2* or *avrRpm1* was significantly reduced (Feys et al., 2001). SA is also the pivotal signal in the

systemic acquired resistance (SAR). The *NahG* transgenic tobacco not only has an enhanced susceptibility to TMV at the infection site but also has an abolished SAR. Under conditions where there is little light exposure after infection, methyl salicylate (MeSA) was found to be the systemic signal which acted as the source of SA in SAR signaling through the conversion of MeSA by the esterase activity of SA-binding protein 2 (SABP2) (Park et al., 2007). Two lipase–like proteins Enhanced Disease Susceptibility 1 (EDS1) (Falk et al., 1999) and Phytoalexin Deficient 4 (PAD4) (Jirage et al., 1999) are involved in regulating SA accumulation in both PTI and ETI. EDS1 and PAD4 together function in defense responses mediated by TIR-NBS-LRR (Toll/Interleukin1 receptor–nucleotide binding site–leucine-rich repeat) type of *R* proteins. Defense responses mediated by the CC-NBS-LRR type (Coiled-Coil–nucleotide binding site–leucine-rich repeat) R proteins are mainly regulated by *Nonspecific Disease Resistance 1* (*NDR1*) which also regulates SA accumulation (Vlot et al., 2009).

It is critical to tightly control defenses as constitutive activation of defense responses likely arrests plant growth and development (Heil and Baldwin, 2002; Li et al., 2007). A number of negative regulators of plant defense responses have been uncovered. *BON1*, an evolutionarily conserved copine gene, is one such negative regulator and it negatively affects plant defense via the regulation of an *R* gene *SNC1* (*suppressor of npr1-1, constitutive 1*). Loss of function mutant *bon1-1* had an enhanced *SNC1* expression and displayed a dwarf morphological phenotype. *BON1* has two homologs in Arabidopsis, *BON2* and *BON3*, which also act as negative regulators in plant defense (Yang et al., 2006b). In Col-0 background, at least 4 *Lesion Cell Death* (*LCD*) genes in addition to *SNC1* contribute to the seedling lethality of *bon1 bon3* double mutant (Li et al., 2009). In contrast, a *bon1* mutant allele in Ws, *bon1-2*, did not show *bon1-1* phenotype due to a lack of functional *SNC1* allele in Ws (Hua et al., 2001; Yang and Hua, 2004). Although

enhanced *SNC1* expression is the major cause for *bon1-1* phenotype, loss of function mutation *snc1-11* does not completely suppress *bon1-1* suggesting that *BON1* has other downstream targets besides *SNC1*.

*SNC1* is a TIR-NR-LRR type R gene. Its gain of function mutation, *snc1-1*, leads to constitutive defense responses including enhanced *PR* gene expression, increased disease resistance to bacterial pathogens and elevated SA accumulation (Li et al., 2001; Zhang et al., 2003). Like other TIR-NB-LRR type *R* genes, all the defense phenotypes in *snc1-1* are dependent on the function of *EDS1* and *PAD4*. To understand how SNC1 regulates defense signaling, more than 13 *mos* (*modifier of snc1*) mutants which completely or partially suppress *snc1-1* phenotypes were isolated in the past decade (Johnson et al., 2013). Among these *MOS* genes, *MOS1* was identified as *SBO3* (*suppressor of bon1 3*) in chapter 4 of this thesis. MOS1 contains HLA-B ASSOCIATED TRANSCRIPT2 (BAT2) domain which is conserved in plants and animals and MOS1 is postulated to regulate *SNC1* expression possibly through chromatin remodeling (Li et al., 2010). Loss of *MOS1* function also induces a late flowering phenotype, but how *MOS1* regulates the flowering time control was not studied. All the studies suggest that MOS1 is a general regulator involved in multiple biological processes. Detailed analyses of MOS1 function in the flowering time control and cell cycle regulation are described in chapter 4.

**1.2 Cell cycle regulation**

Cell cycle regulation plays a pivotal role in the regulation of cell proliferation and division and affects the whole plant growth and development (Inze and De Veylder, 2006). The typical mitotic cell cycle includes four phases, Gap phase 1 (G1), DNA synthesis (S) phase, G2, and mitotic (M) phase. S- and M-phase are separated by G1 and G2. The combination of G1, S and G2 is also called interphase. M phase is relatively short during cell cycle and is divided into

seven stages in plant cells: preprophase, prophase, premetaphase, metphase, anaphase, telophase and cytokinesis. The endoreduplication, also called endocycle is a special mitotic cell cycle that skips cell division after DNA replication, and it occurs in both plants and animals (Lee et al., 2009). Endoreduplication was found to play important roles in the regulation of cell size and cell morphology (Roodbarkelari et al., 2010). In general, an increased DNA content by endoreduplication is associated with a larger cell size (Lee et al., 2009). The promoted endoreduplication at or adjacent to the infection site during biotroph-plant interactions is associated with more nutrient exchange which supports the growth of biotrophs (Chandran et al., 2009; Wildermuth, 2010). Moreover, an increase of endoreduplication is a stress response to retain genome integrity under the genomic stresses (Adachi et al., 2011).Therefore, accurate and appropriate cell cycle progression is important for plant growth and development and stress responses.

The regulation of cell cycle progression is governed by activities of cyclin dependent kinases (CDKs). Two classes of CDKs are found in plants: CDKA and CDKB. In Arabidopsis, only one CDKA was identified and it is encoded by the *CDKA;1* gene. CDKB is plant specific and has CDKB1 and CDKB2 subgroups. Arabidopsis has two CDKB1 (CDKB1;1 and CDKB1;2) and two CDKB2 (CDKB2;1 and CDKB2;2) (Inze and De Veylder, 2006; Inagaki and Umeda, 2011). *CDKB1;1* expression is increased in dividing cells and reduced at the onset of endoreduplication, indicating that CDKB1;1 activity is critical for the transition between the mitotic cell division and endocycle (Inze and De Veylder, 2006). Cyclins are activators of CDKs. Cyclins bind to CDKs and activate CDKs at different cell cycle phases to promote cell cycle progression. In Arabidopsis, 32 cyclins including 10 CYCAs, 11 CYCBs, 10 CYCDs and 1 CYCH have putative functions in the regulation of cell cycle progression at different cell cycle

phases (Inagaki and Umeda, 2011). Different CDK-cyclin complexes phosphorylate a number of substrates to regulate G1/S and G2/M transitions (Inze and De Veylder, 2006). CYCAs mainly regulate S to M progression, CYCBs mainly control G2/M transition phase, and CYCDs have functions in but are not specific to the regulation of G1/S transition phase (Figure 1.1) (Inagaki and Umeda, 2011). In addition to the regulation of cell cycle progression, CDK-cyclin may also phosphorylate the RNA polymerase II or other transcription factors to modulate gene transcription and RNA splicing (Loyer et al., 2005).

Regulation of G2-to-M phase transition is critical for the choice between mitotic cell cycle and endocycle (Inze and De Veylder, 2006). To promote the transition from mitotic cell cycle to endocycle, the activity of CDK-cyclin complex at G2/M needs to be repressed. Anaphase-promoting complex/cyclosome (APC/C), a conserved ubiquitin E3 ligase in eukaryotes, degrades cyclins at G2/M to downregulate the activity of CDK-cyclin complex (Figure 1.1). APC/C is a large protein complex containing 11 subunits, among which APC2 and APC11 are the subunits minimally required for the E3 ligase activity.

The activation and substrate specificity of APC/C is determined by two groups of activator genes, *CDC20* and *CDH1*. In yeast and animals, $APC/C^{CDC20}$ functions in mitosis and triggers metaphase/anaphase transition, while $APC/C^{CDH1}$ plays important roles in the metaphase/anaphase transition and keeps active in the subsequent G1 phase (Lee et al., 2009). The kinase activity of CDK-Cyclin complex antagonistically affects the activation of CDC20 and CDH1. CDC20 only targets phosphorylated APC/C for activation, and the phosphorylation of CDH1 blocks its activity (Kramer et al., 2000). Thus, $APC/C^{CDC20}$ may repress the kinase activity of CDK-cyclin complex to facilitate the function of $APC/C^{CDH1}$ on the endocycle onset and progression. $APC/C^{CDH1/FZR/CCS52}$ was reported to regulate the onset of endocycle by

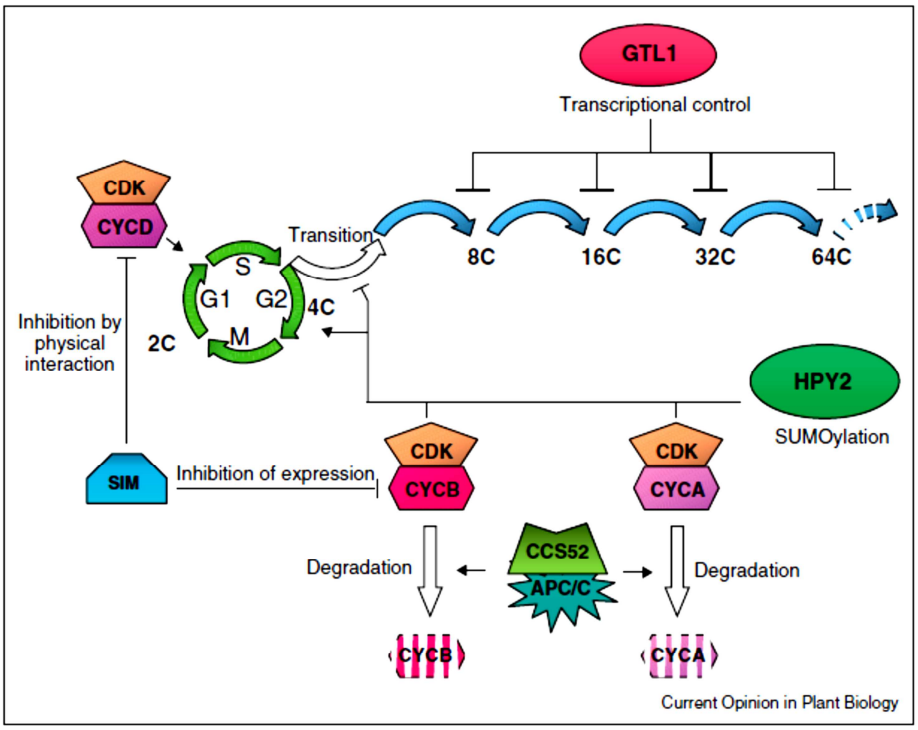


**Figure 1.1 Cell cycle regulation in plants.** The diagram is taken from a previous review (Breuer et al., 2010).

The cell cycle progression is governed by different CDK-cyclin complexes at different phases. CDK-CYCD controls G1/S transition, CDK-CYCB controls G2/M transition, and CDK-CYCA controls the progression from S phase to M phase. The activities of CDK-cyclin complexes are controlled by a multisubunit ubiquitin E3 ligase, APC/C and CDK inhibitors. APC/C is activated by two activators, CDC20 and CCS52, and activated APC/C degrades different cyclins at different cell cycle phases. CCS52 mediated activation of APC/C triggers degradation of CYCB and CYCA to prevent the entry to M phase. Consequently, cells keep replicated for several rounds without the division, which is called endocycle or endoreduplication. SIM (SIAMESE), a type of plant specific CDK inhibitor family, prevents the cell cycle progression by inhibiting the transcription of CYCB and the activity of CDK-CYCD complex through the physical interaction. A SUMO E3 ligase, HPY2 (HIGH PLOIDY2) protects the mitotic cell cycle progression and prevents the entry of endoreduplication. GTL1(GT-2-LIKE1), a trihelix transcription factor inhibits the successive progression of endoreduplication.

degrading mitotic cyclins in human, Drosophila and Arabidopsis (Lammens et al., 2008; Larson-Rabin et al., 2009b; Lee et al., 2009). APC/C also targets Germinin protein which is an inhibitor of DNA replication for the degradation in mitotic cycles (Lee et al., 2009). Arabidopsis contains five CDC20 homologs and three CDH1 homologs that are also named cell cycle switch proteins (CCS52), CCS52A1, CCS52A2 and CCS52B (Inze and De Veylder, 2006). Both CCS52A1 and CCS52A2 are activators of the onset of endoreduplication and show similar high expression in G1 and S phase (Lammens et al., 2008; Larson-Rabin et al., 2009b). *CCS52A2* has a high expression in late S and G2 phases, while *CCS52B* has an increased expression at the end of G2 and the beginning of M phase (Fulop et al., 2005; Inze and De Veylder, 2006).

In contrast to the function of APC/C activators, *OSD1/GIG1* (*Omission of the Second Division/ gigas cell 1*) and its homolog *UVI4* (*UV Insensitive 4*) are negative regulators of APC/C in Arabidopsis (Heyman et al., 2011a; Iwata et al., 2011). A number of defective cell cycle phenotypes have been observed in the mutants of *OSD1* and *UVI4*. The loss of *OSD1* function abolishes the second meiotic division and subsequently produces diploid gametes (d'Erfurth et al., 2009). The *cycA1;2* null mutant fails to enter the meiosis II, and the double mutant *cycA1;2 osd1* does not have chromosome segregation during male meiosis, indicating that *CYCA1;2* and *OSD1* are required to promote transitions in both meiotic divisions (d'Erfurth et al., 2010). *gig1*, a loss of function allele of *OSD1*, has gigantic cotyledon epidermal cells with higher ploidy, indicating that *osd1* mutation leads to endoreduplication or endomitosis in cotyledons (Iwata et al., 2011). The loss of *UVI4* function enhanced resistance to UV-B and had increased ploidy level in somatic tissues, indicating that *UVI4* negatively regulates endocycles (Perazza et al., 1999; Hase et al., 2006).

Both OSD1 and UVI4 interact with the APC/C complex (Van Leene et al., 2010). Their interactions with APC/C activators CCS52A1, CCS52B, CDC20.1, and CDC20.5 were further confirmed by the yeast two-hybrid system (Heyman et al., 2011a; Iwata et al., 2011). The CCS52 genes appear to mediate the function of OSD1 and UVI4. The *ccs52a1* mutation is epistatic to *uvi4* in the regulation of endoreduplication (Heyman et al., 2011a). Cyclins accumulated of higher levels in *UVI4* or *OSD1* overexpression plants, and accumulated of lower levels in loss of function mutant *uvi4* compared to that in wild type (Heyman et al., 2011a; Iwata et al., 2011; Iwata et al., 2012b), indicating *OSD1* and UVI4 negatively regulate APC/C activity in degrading cell cycle proteins.

In addition to playing a major role in the cell cycle regulation, APC/C is required for the recruitment of RNA polymerase II to the promoter of *miRNA159* and stimulates the expression of *miRNA159*. *miRNA159* was reported to target DUO POLLEN 1 (DUO1) which downregulates the transcription of *CYCB1;1* (Zheng et al., 2011). Therefore, APC/C affects the accumulation of cell cycle proteins not only at translational level but also through the transcriptional regulation.

Another mechanism in cell cycle regulation is through the checkpoint machinery that senses DNA damages and subsequently either stalls the cell cycle or triggers apoptosis. Checkpoints occur at G1/S, S and G2/M phases. Spindle assembly checkpoint (SAC) functions during metaphase to anaphase transition. SAC is a protein complex with 6 subunits including mitotic arrest deficient 1 (MAD1), MAD2, budding uninhibited by benzimidazole 1 (BUB1), BUB1-related protein kinase (BUBR1), BUB3, and centromere protein E (CENP-E) (Holland and Cleveland, 2009). In yeast and animals, MAD1 is predominantly localized at the unattached kinetochore and recruits MAD2 to form a MAD1-MAD2 complex (Figure 1.2). MAD2 has two distinct conformations, open and closed. Closed MAD2 bound to MAD1 serves as a template to

convert open MAD2 into closed MAD2 which would bind to CDC20 (De Antoni et al., 2005). The formation of MAD2-CDC20 complex promotes the binding of BUB3 and MAD3 to form a mitotic checkpoint complex (MCC) (Kulukian et al., 2009; Kim et al., 2012). MCC stabilizes the binding between MAD2 and CDC20 and prevents the interaction between CDC20 and APC/C as MAD2 and APC/C binds to the same motif KILR in CDC20 (Figure1.2) (Izawa and Pines, 2012). Without CDC20, APC/C could not be activated and anaphase is not triggered. Thus, MAD2 is a negative regulator of APC/C. When all of the kinetochores are properly attached, MCC is inactivated. Consequently, CDC20 activates APC/C to allow sister chromatid separation. In plants, SAC machinery has not been well studied, but homologous SAC components were isolated and characterized on their subcellular localizations (Caillaud et al., 2009). MAD2 is the first SAC protein characterized on its subcellular localization during meiosis and mitosis in maize (Yu et al., 1999). In Arabidopsis, *MAD2* was recently reported to regulate the root elongation and the growth of root meristem (Gudmundsdottir and Ashworth, 2004). No further studies on *MAD2*-associated cell cycle regulation have been reported in plants.

When checkpoint detects DNA damage, signals are transmitted to downstream components likely by ATM (ataxia telangiectasia-mutated) and ATR (ataxia telangiectasia-mutated and Rad3-related), resulting in arrested cell cycle, DNA repair, or programmed cell death (Meier and Ahmed, 2001; Sakamoto et al., 2009). ATM is critical for responses to double strand breaks and also required for the immediate transcriptional responses to γ-irradiation (Culligan et al., 2006). On the other hand, ATR responds to both DNA damage and replication-blocking agents such as UV-B lights, hydroxyurea (HU) and aphidicolin, and it controls G2 phase checkpoint in Arabidopsis (Sakamoto et al., 2009). The *atr atm* loss of function double

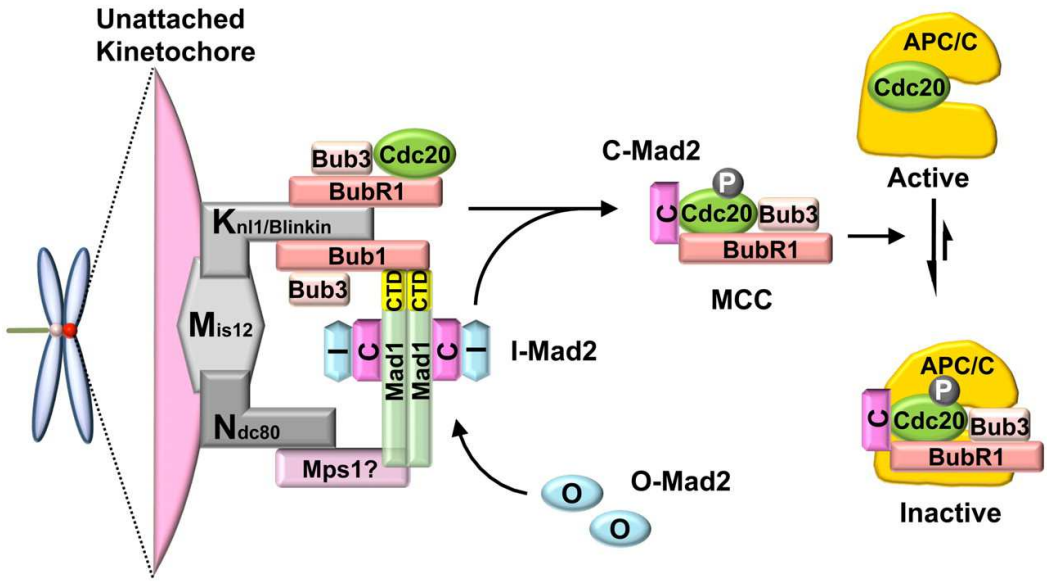


**Figure 1.2 Spindle assembly checkpoint (SAC) machinery.** The diagram is taken from a previous paper (Kim et al., 2012).

In the unattached kinetochore, SAC protein complex or proteins including BUBR1 (MAD3)-BUB3, BUB1-BUB3and MPS1 are first assembled to the kinetochore through the interaction with KMN ((Knl1/Blinkin-Mis12-Ndc80) network of proteins. Dimerized MAD1 resides to the kinetochore by binding with BUB1 and MPS1. MAD2 has two conformers, open-MAD2 (O-MAD2) and closed-MAD2 (C-MAD2). The kinetochore-localized MAD1 recruits O-MAD2 and convert it into C-MAD2. The MAD1-C-MAD2 complex severs as a template to recruit more cytosolic O-MAD2 to convert them into intermediate MAD2 (I-MAD2) and C-MAD2. C-MAD2 interacts with CDC20 and BUBR1-BUB3 to form a stable mitotic checkpoint complex (MCC) which consequently inhibit the activity of APC/C and prevent the entry to anaphase.

mutant is completely sterile (Culligan et al., 2004). Interestingly, *CYCB1;1* is strongly upregulated by γ-irradiation induced genomic stress, and this activation is depended on both ATM and ATR kinases (Culligan et al., 2006). Nevertheless, the function of *CYCB1;1* in genomic stress responses is largely unknown.

**1.3 Flowering time control**

Flowering time is controlled by at least four major pathways including the autonomous pathway, vernalization, gibberellin and photoperiod. FLC is central regulator of flowering time. The *flc* null mutant exhibits early flowering and overexpression of *FLC* leads to late flowering (Michaels and Amasino, 1999). Vernalization and genes in the autonomous pathway and pathway repress the expression of *FLC* (*Flowering Locus C*) to control flowering time. In the autonomous pathway, *FLC* expression is repressed through RNA-mediated chromatin silencing (Kim et al., 2009; Crevillen and Dean, 2011). Vernalization, a prolonged cold treatment, represses the FLC expression through a deposition of repressive histone mark H3K27me3 (Kim et al., 2009; Crevillen and Dean, 2011).

FLC controls flowering time through several target genes. As a MADS-box transcription factor, FLC directly binds to CArG box in *SOC1* (*SUPPRESSOR OF OVEREXPRESSION OF CO 1*) promoter and the first intron of *FT* (*FLOWERING LOCUS T*) and consequently represses both *SOC1* and *FT* expression (Helliwell et al., 2006). FLC may also bind to the CArG box of the *FD* (*FLOWERING LOCUS D*) promoter to repress *FD* expression (Searle et al., 2006). *SOC1*, *FT* and *FD* are all floral integrator genes which positively regulate the expression of floral meristem identity genes such as *LEAFY* (*LFY*), *APETALA1* (*AP1*), *FRUITFUL* (*FUL*) and *SEPALATA 3* (*SEP3*) (Kim et al., 2009). Floral meristem identity genes control the formation of floral meristems.

*FRIGIDA* (*FRI*) is a regulator of *FLC* (Kim et al., 2009). *FRI* is responsible for the natural variations of Arabidopsis ecotypes in flowering time: most of early flowering ecotypes do not have a functional *FRI* allele (Johanson et al., 2000). *FRI*-mediated late flowering phenotype is *FLC*-dependent, and functional *FRI* allele significantly activates *FLC* expression (Michaels and Amasino, 1999). FRI is a plant specific nuclear protein (Johanson et al., 2000) and it presumably is a regulator of transcription. FRI interacts with a small subunit of the nuclear cap-binding complex (CBC), CBC20, to regulate the *FLC* mRNA level (Geraldo et al., 2009).

Several suppressors of *FRIGIDA* (*suf*) were identified. Loss of *FRL1* (*FRIGIDA LIKE 1*) (Michaels et al., 2004) and *FES1* (*FRIGIDA ESSENTIAL 1* ) (Schmitz et al., 2005) function each specifically suppresses *FRI*-mediated activation of *FLC* expression. The *suf4 mutant* was identified as a suppressor of *FRIGIDA*, but it also suppresses the late flowering phenotype of *ld* (*luminidependens*) mutant in the autonomous pathway (Kim et al., 2006). SUF4 is a nuclear localized protein containing two C2H2-type zinc finger motifs. SUF4 interacts with FRI and FRL to form a complex and activates the *FLC* expression by binding to the *FLC* promoter region (Kim et al., 2006). In the absence of *FRI*, LD may interact with SUF4 to inhibit the *FLC* expression (Kim et al., 2006). Recent study shows that FRI interacts with FRL, FES1, SUF4 and FLX to form a transcription activator complex (FRI-C), and SUF4 binds to a *cis*-element of the *FLC* promoter (Choi et al., 2011).

**1.4 Potential connections between plant immune responses and cell cycle regulation**

In animal and fungal systems, cell cycle progression is tightly linked to cell survival. Cell damage is assessed at various cell cycle checkpoints and may cause cell cycle arrest for DNA repair or cell death (Stevens and La Thangue, 2004). In plants, few examples exist for the association of cell cycle arrest and cell death, and the connection between the two processes is

not clear. The *CPR5* (*Constitutive expresser of PR genes 5*) gene is implicated in both defense regulation and endoreduplication. The loss-of-function (l-o-f) *cpr5* mutant has increased disease resistance to virulent bacterial pathogens and has a high accumulation of salicylic acid and ectopic cell death (Bowling et al., 1997; Boch et al., 1998). The *cpr5* mutant also has abnormal trichomes due to reduced endoreduplication and cell death (Kirik et al., 2001). The CPR5 protein has a predicted transmembrane segment and is localized to both cytoplasm and nucleus (Perazza et al., 2011). It is not known how *CPR5* regulates both defense responses and cell cycle.

The connection of cell cycle and disease resistance has been observed in some pathosystems. Powdery mildew infection in Arabidopsis promoted endocycle at or adjacent to infection sites, possibly to enhance nutrient exchange for more pathogen growth. Reduced endoreduplication in cells distant from infection site was associated with less pathogen growth (Chandran et al., 2009; Wildermuth, 2010). However, it is not known how plant defense response and endoreduplication are connected. Compromised systemic acquired resistance (SAR) is one possible explanation for the reduced pathogen growth in distal tissues. The plant hormone essential for SAR is SA, and SA plays a role in the regulation of cell cycle progression. SA represses the expression of *cyclin D3* (*CYCD3;1*) that drives G1/S phase transition (Xia et al., 2009). Ectopic expression of *CYCD3;1* in trichome promotes both S-phase entry and mitosis (Schnittger et al., 2002b). Therefore, SA might affect mitosis by regulating *CYCD3* expression.

All these studies suggest that plant defense signaling and cell cycle regulation may share some components whose alterations may affect both plant defense response and cell cycle progression.

### 1.5 Potential connections between flowering time control and cell cycle regulation

There is little evidence for the regulation of flowering time by cell cycle. However, a *cycd3;1-3* triple mutant exhibited slightly late flowering (Dewitte et al., 2007) suggesting that perturbed cell cycle progression may affect the flowering time. It is conceivable that cell cycle progression has a general role in gene expression regulation. Cell cycle progression is associated with the histone deposition and histone modification and consequently expression of genes (Sanchez Mde et al., 2008). The *FLC* locus is extensively regulated at the chromatin level (Crevillen and Dean, 2011) and presumably perturbed cell cycle progression may affect the *FLC* expression. In addition, general regulators of gene expression can affect both cell cycle progression and flowering time. One example is that *hub1* (*histone monoubiquitination 1*) mutation led to early entry of endocycle and reduced *FLC* expression and subsequent early flowering (Fleury et al., 2007; Cao et al., 2008). It remains to be determined whether cell cycle progression affects chromatin modification or chromatin modification affects the cell cycle progression.

### 1.6 Goal of my research

The purpose of my research is to determine how the immune receptor *R* gene *SNC1* is regulated. To dissect this regulation, I took two genetic approaches using the sensitive genetic system of the *bon* mutants. The first approach was to isolate and functionally analyze an enhancer of *bon1-2.* This would help me identify components that likely function in parallel to *BON1* to repress *R* genes. Here I isolated an overexpression allele of *OSD1* which has a function in the regulation of cell cycle progression. This unexpected finding led to further studies on the link between cell cycle progression and plant defense responses. Results are described in chapter 2 and 3. The second approach was to isolate and functionally analyze a suppressor of *bon1-1*.

This would potentially identify components that are required for *SNC1* activation in *bon1-1*. Indeed, we isolated a loss of function allele of *MOS1* which is required for the transcriptional activation of *SNC1* expression. MOS1 is found to regulate flowering time, endocycle in addition to defense responses. Molecular basis for its function is characterized utilizing the flowering time phenotype where transcriptional regulation of FLC is better characterized. This study is described in chapter 4. It gives us an entry point to further investigate the potential connection between regulations of defense, cell cycle, and flowering time.

## Reference


**Adachi, S., Minamisawa, K., Okushima, Y., Inagaki, S., Yoshiyama, K., Kondou, Y., Kaminuma, E., Kawashima, M., Toyoda, T., Matsui, M., Kurihara, D., Matsunaga, S., and Umeda, M.** (2011). Programmed induction of endoreduplication by DNA double-strand breaks in Arabidopsis. Proceedings of the National Academy of Sciences of the United States of America.

**Boch, J., Verbsky, M.L., Robertson, T.L., Larkin, J.C., and Kunkel, B.N.** (1998). Analysis of resistance gene-mediated defense responses in Arabidopsis thaliana plants carrying a mutation in CPR5. Mol Plant Microbe In **11,** 1196-1206.

**Bowling, S.A., Clarke, J.D., Liu, Y., Klessig, D.F., and Dong, X.** (1997). The cpr5 mutant of Arabidopsis expresses both NPR1-dependent and NPR1-independent resistance. Plant Cell **9,** 1573-1584.

**Breuer, C., Ishida, T., and Sugimoto, K.** (2010). Developmental control of endocycles and cell growth in plants. Current opinion in plant biology **13,** 654-660.

**Caillaud, M.C., Paganelli, L., Lecomte, P., Deslandes, L., Quentin, M., Pecrix, Y., Le Bris, M., Marfaing, N., Abad, P., and Favery, B.** (2009). Spindle assembly checkpoint protein dynamics reveal conserved and unsuspected roles in plant cell division. PLoS One **4,** e6757.

**Cao, Y., Dai, Y., Cui, S., and Ma, L.** (2008). Histone H2B monoubiquitination in the chromatin of FLOWERING LOCUS C regulates flowering time in Arabidopsis. The Plant cell **20,** 2586-2602.

**Chandran, D., Inada, N., Hather, G., Kleindt, C.K., and Wildermuth, M.C.** (2009). Laser microdissection of Arabidopsis cells at the powdery mildew infection site reveals site-specific processes and regulators. Proc Natl Acad Sci U S A **107,** 460-465.

**Choi, J., Hyun, Y., Kang, M.J., In Yun, H., Yun, J.Y., Lister, C., Dean, C., Amasino, R.M., Noh, B., Noh, Y.S., and Choi, Y.** (2009). Resetting and regulation of Flowering Locus C expression during Arabidopsis reproductive development. Plant J **57,** 918-931.

**Choi, K., Kim, J., Hwang, H.J., Kim, S., Park, C., Kim, S.Y., and Lee, I.** (2011). The FRIGIDA complex activates transcription of FLC, a strong flowering repressor in Arabidopsis, by recruiting chromatin modification factors. The Plant cell **23,** 289-303.

**Crevillen, P., and Dean, C.** (2011). Regulation of the floral repressor gene FLC: the complexity of transcription in a chromatin context. Current opinion in plant biology **14,** 38-44.

**Culligan, K., Tissier, A., and Britt, A.** (2004). ATR regulates a G2-phase cell-cycle checkpoint in Arabidopsis thaliana. The Plant cell **16,** 1091-1104.

**Culligan, K.M., Robertson, C.E., Foreman, J., Doerner, P., and Britt, A.B.** (2006). ATR and ATM play both distinct and additive roles in response to ionizing radiation. Plant J **48,** 947-961.

**d'Erfurth, I., Jolivet, S., Froger, N., Catrice, O., Novatchkova, M., and Mercier, R.** (2009). Turning meiosis into mitosis. PLoS biology **7,** e1000124.

**d'Erfurth, I., Cromer, L., Jolivet, S., Girard, C., Horlow, C., Sun, Y., To, J.P., Berchowitz, L.E., Copenhaver, G.P., and Mercier, R.** (2010). The cyclin-A CYCA1;2/TAM is required for the meiosis I to meiosis II transition and cooperates with OSD1 for the prophase to first meiotic division transition. PLoS Genet **6,** e1000989.

**De Antoni, A., Pearson, C.G., Cimini, D., Canman, J.C., Sala, V., Nezi, L., Mapelli, M., Sironi, L., Faretta, M., Salmon, E.D., and Musacchio, A.** (2005). The Mad1/Mad2 complex as a template for Mad2 activation in the spindle assembly checkpoint. Current biology : CB **15,** 214-225.

**DebRoy, S., Thilmony, R., Kwack, Y.B., Nomura, K., and He, S.Y.** (2004). A family of conserved bacterial effectors inhibits salicylic acid-mediated basal immunity and promotes disease necrosis in plants. Proceedings of the National Academy of Sciences of the United States of America **101,** 9927-9932.

**Dempsey, D.A., Vlot, A.C., Wildermuth, M.C., and Klessig, D.F.** (2011). Salicylic Acid biosynthesis and metabolism. Arabidopsis Book **9,** e0156.

**Dewitte, W., Scofield, S., Alcasabas, A.A., Maughan, S.C., Menges, M., Braun, N., Collins, C., Nieuwland, J., Prinsen, E., Sundaresan, V., and Murray, J.A.** (2007). Arabidopsis CYCD3 D-type cyclins link cell proliferation and endocycles and are rate-limiting for cytokinin responses. Proceedings of the National Academy of Sciences of the United States of America **104,** 14537-14542.

**Ding, D., Muthuswamy, S., and Meier, I.** (2012). Functional interaction between the Arabidopsis orthologs of spindle assembly checkpoint proteins MAD1 and MAD2 and the nucleoporin NUA. Plant molecular biology **79,** 203-216.

**Dodds, P.N., and Rathjen, J.P.** (2010). Plant immunity: towards an integrated view of plant-pathogen interactions. Nature reviews **11,** 539-548.

**Falk, A., Feys, B.J., Frost, L.N., Jones, J.D., Daniels, M.J., and Parker, J.E.** (1999). EDS1, an essential component of R gene-mediated disease resistance in Arabidopsis has homology to eukaryotic lipases. Proceedings of the National Academy of Sciences of the United States of America **96,** 3292-3297.

**Feys, B.J., Moisan, L.J., Newman, M.A., and Parker, J.E.** (2001). Direct interaction between the Arabidopsis disease resistance signaling proteins, EDS1 and PAD4. The EMBO journal **20,** 5400-5411.

**Fleury, D., Himanen, K., Cnops, G., Nelissen, H., Boccardi, T.M., Maere, S., Beemster, G.T., Neyt, P., Anami, S., Robles, P., Micol, J.L., Inze, D., and Van Lijsebettens, M.** (2007). The Arabidopsis thaliana homolog of yeast BRE1 has a function in cell cycle regulation during early leaf and root growth. The Plant cell **19,** 417-432.

**Fulop, K., Tarayre, S., Kelemen, Z., Horvath, G., Kevei, Z., Nikovics, K., Bako, L., Brown, S., Kondorosi, A., and Kondorosi, E.** (2005). Arabidopsis anaphase-promoting complexes: multiple activators and wide range of substrates might keep APC perpetually busy. Cell cycle (Georgetown, Tex **4,** 1084-1092.

**Geraldo, N., Baurle, I., Kidou, S., Hu, X., and Dean, C.** (2009). FRIGIDA delays flowering in Arabidopsis via a cotranscriptional mechanism involving direct interaction with the nuclear cap-binding complex. Plant physiology **150,** 1611-1618.

**Hase, Y., Trung, K.H., Matsunaga, T., and Tanaka, A.** (2006). A mutation in the uvi4 gene promotes progression of endo-reduplication and confers increased tolerance towards ultraviolet B light. Plant J **46,** 317-326.

**Heil, M., and Baldwin, I.T.** (2002). Fitness costs of induced resistance: emerging experimental support for a slippery concept. Trends in plant science **7,** 61-67.

**Helliwell, C.A., Wood, C.C., Robertson, M., James Peacock, W., and Dennis, E.S.** (2006). The Arabidopsis FLC protein interacts directly in vivo with SOC1 and FT chromatin and is part of a high-molecular-weight protein complex. Plant J **46,** 183-192.

**Heyman, J., Van den Daele, H., De Wit, K., Boudolf, V., Berckmans, B., Verkest, A., Kamei, C.L., De Jaeger, G., Koncz, C., and De Veylder, L.** (2011). Arabidopsis

ULTRAVIOLET-B-INSENSITIVE4 Maintains Cell Division Activity by Temporal Inhibition of the Anaphase-Promoting Complex/Cyclosome. The Plant cell.

**Holland, A.J., and Cleveland, D.W.** (2009). Boveri revisited: chromosomal instability, aneuploidy and tumorigenesis. Nat Rev Mol Cell Biol **10,** 478-487.

**Hua, J., Grisafi, P., Cheng, S.H., and Fink, G.R.** (2001). Plant growth homeostasis is controlled by the Arabidopsis BON1 and BAP1 genes. Genes & development **15,** 2263-2272.

**Inagaki, S., and Umeda, M.** (2011). Cell-cycle control and plant development. Int Rev Cell Mol Biol **291,** 227-261.

**Inze, D., and De Veylder, L.** (2006). Cell cycle regulation in plant development. Annual review of genetics **40,** 77-105.

**Iwata, E., Ikeda, S., Matsunaga, S., Kurata, M., Yoshioka, Y., Criqui, M.C., Genschik, P., and Ito, M.** (2011). GIGAS CELL1, a Novel Negative Regulator of the Anaphase-Promoting Complex/Cyclosome, Is Required for Proper Mitotic Progression and Cell Fate Determination in Arabidopsis. The Plant cell.

**Iwata, E., Ikeda, S., Abe, N., Kobayashi, A., Kurata, M., Matsunaga, S., Yoshioka, Y., Criqui, M.C., Genschik, P., and Ito, M.** (2012). Roles of GIG1 and UVI4 in genome duplication in Arabidopsis thaliana. Plant Signal Behav **7,** 1079-1081.

**Izawa, D., and Pines, J.** (2012). Mad2 and the APC/C compete for the same site on Cdc20 to ensure proper chromosome segregation. J Cell Biol **199,** 27-37.

**Jirage, D., Tootle, T.L., Reuber, T.L., Frost, L.N., Feys, B.J., Parker, J.E., Ausubel, F.M., and Glazebrook, J.** (1999). Arabidopsis thaliana PAD4 encodes a lipase-like gene that is important for salicylic acid signaling. Proceedings of the National Academy of Sciences of the United States of America **96,** 13583-13588.

**Johanson, U., West, J., Lister, C., Michaels, S., Amasino, R., and Dean, C.** (2000). Molecular analysis of FRIGIDA, a major determinant of natural variation in Arabidopsis flowering time. Science (New York, N.Y **290,** 344-347.

**Johnson, K.C., Dong, O.X., Huang, Y., and Li, X.** (2013). A Rolling Stone Gathers No Moss, but Resistant Plants Must Gather Their MOSes. Cold Spring Harb Symp Quant Biol.

**Jones, J.D., and Dangl, J.L.** (2006). The plant immune system. Nature **444,** 323-329.

**Kim, S., Choi, K., Park, C., Hwang, H.J., and Lee, I.** (2006). SUPPRESSOR OF FRIGIDA4, encoding a C2H2-Type zinc finger protein, represses flowering by transcriptional activation of Arabidopsis FLOWERING LOCUS C. The Plant cell **18,** 2985-2998.

**Kim, S., Sun, H., Tomchick, D.R., Yu, H., and Luo, X.** (2012). Structure of human Mad1 C-terminal domain reveals its involvement in kinetochore targeting. Proceedings of the National Academy of Sciences of the United States of America **109,** 6549-6554.

**Kirik, V., Bouyer, D., Schobinger, U., Bechtold, N., Herzog, M., Bonneville, J.M., and Hulskamp, M.** (2001). CPR5 is involved in cell proliferation and cell death control and encodes a novel transmembrane protein. Curr Biol **11,** 1891-1895.

**Kramer, E.R., Scheuringer, N., Podtelejnikov, A.V., Mann, M., and Peters, J.M.** (2000). Mitotic regulation of the APC activator proteins CDC20 and CDH1. Mol Biol Cell **11,** 1555-1569.

**Kulukian, A., Han, J.S., and Cleveland, D.W.** (2009). Unattached kinetochores catalyze production of an anaphase inhibitor that requires a Mad2 template to prime Cdc20 for BubR1 binding. Developmental cell **16,** 105-117.

**Lammens, T., Boudolf, V., Kheibarshekan, L., Zalmas, L.P., Gaamouche, T., Maes, S., Vanstraelen, M., Kondorosi, E., La Thangue, N.B., Govaerts, W., Inze, D., and De Veylder, L.** (2008). Atypical E2F activity restrains APC/CCCS52A2 function obligatory for endocycle onset. Proceedings of the National Academy of Sciences of the United States of America **105,** 14721-14726.

**Larson-Rabin, Z., Li, Z., Masson, P.H., and Day, C.D.** (2009). FZR2/CCS52A1 expression is a determinant of endoreduplication and cell expansion in Arabidopsis. Plant physiology **149,** 874-884.

**Lee, H.O., Davidson, J.M., and Duronio, R.J.** (2009). Endoreplication: polyploidy with purpose. Genes & development **23,** 2461-2477.

**Li, X., Clarke, J.D., Zhang, Y., and Dong, X.** (2001). Activation of an EDS1-mediated R-gene pathway in the snc1 mutant leads to constitutive, NPR1-independent pathogen resistance. Mol Plant Microbe Interact **14,** 1131-1139.

**Li, Y., Pennington, B.O., and Hua, J.** (2009). Multiple R-like genes are negatively regulated by BON1 and BON3 in arabidopsis. Mol Plant Microbe Interact **22,** 840-848.

**Li, Y., Yang, S., Yang, H., and Hua, J.** (2007). The TIR-NB-LRR gene SNC1 is regulated at the transcript level by multiple factors. Mol Plant Microbe Interact **20,** 1449-1456.

**Li, Y., Tessaro, M.J., Li, X., and Zhang, Y.** (2010). Regulation of the expression of plant resistance gene SNC1 by a protein with a conserved BAT2 domain. Plant physiology **153,** 1425-1434.

**Loyer, P., Trembley, J.H., Katona, R., Kidd, V.J., and Lahti, J.M.** (2005). Role of CDK/cyclin complexes in transcription and RNA splicing. Cellular signalling **17,** 1033-1051.

**Meier, B., and Ahmed, S.** (2001). Checkpoints: chromosome pairing takes an unexpected twist. Curr Biol **11,** R865-868.

**Michaels, S.D., and Amasino, R.M.** (1999). FLOWERING LOCUS C encodes a novel MADS domain protein that acts as a repressor of flowering. The Plant cell **11,** 949-956.

**Michaels, S.D., Bezerra, I.C., and Amasino, R.M.** (2004). FRIGIDA-related genes are required for the winter-annual habit in Arabidopsis. Proceedings of the National Academy of Sciences of the United States of America **101,** 3281-3285.

**Miller, G., Schlauch, K., Tam, R., Cortes, D., Torres, M.A., Shulaev, V., Dangl, J.L., and Mittler, R.** (2009). The plant NADPH oxidase RBOHD mediates rapid systemic signaling in response to diverse stimuli. Science signaling **2,** ra45.

**Park, S.W., Kaimoyo, E., Kumar, D., Mosher, S., and Klessig, D.F.** (2007). Methyl salicylate is a critical mobile signal for plant systemic acquired resistance. Science (New York, N.Y **318,** 113-116.

**Perazza, D., Herzog, M., Hulskamp, M., Brown, S., Dorne, A.M., and Bonneville, J.M.** (1999). Trichome cell growth in Arabidopsis thaliana can be derepressed by mutations in at least five genes. Genetics **152,** 461-476.

**Perazza, D., Laporte, F., Balague, C., Chevalier, F., Remo, S., Bourge, M., Larkin, J., Herzog, M., and Vachon, G.** (2011). GeBP/GPL transcription factors regulate a subset of CPR5-dependent processes. Plant physiology **157,** 1232-1242.

**Pogany, M., von Rad, U., Grun, S., Dongo, A., Pintye, A., Simoneau, P., Bahnweg, G., Kiss, L., Barna, B., and Durner, J.** (2009). Dual roles of reactive oxygen species and NADPH oxidase RBOHD in an Arabidopsis-Alternaria pathosystem. Plant physiology **151,** 1459-1475.

**Roodbarkelari, F., Bramsiepe, J., Weinl, C., Marquardt, S., Novak, B., Jakoby, M.J., Lechner, E., Genschik, P., and Schnittger, A.** (2010). Cullin 4-ring finger-ligase plays a key role in the control of endoreplication cycles in Arabidopsis trichomes. Proceedings of the National Academy of Sciences of the United States of America **107,** 15275-15280.

**Sakamoto, A.N., Lan, V.T., Puripunyavanich, V., Hase, Y., Yokota, Y., Shikazono, N., Nakagawa, M., Narumi, I., and Tanaka, A.** (2009). A UVB-hypersensitive mutant in Arabidopsis thaliana is defective in the DNA damage response. Plant J **60,** 509-517.

**Sanchez Mde, L., Caro, E., Desvoyes, B., Ramirez-Parra, E., and Gutierrez, C.** (2008). Chromatin dynamics during the plant cell cycle. Semin Cell Dev Biol **19,** 537-546.

**Schmitz, R.J., Hong, L., Michaels, S., and Amasino, R.M.** (2005). FRIGIDA-ESSENTIAL 1 interacts genetically with FRIGIDA and FRIGIDA-LIKE 1 to promote the winter-annual habit of Arabidopsis thaliana. Development **132,** 5471-5478.

**Schnittger, A., Schobinger, U., Bouyer, D., Weinl, C., Stierhof, Y.D., and Hulskamp, M.** (2002). Ectopic D-type cyclin expression induces not only DNA replication but also cell division in Arabidopsis trichomes. Proceedings of the National Academy of Sciences of the United States of America **99,** 6410-6415.

**Searle, I., He, Y., Turck, F., Vincent, C., Fornara, F., Krober, S., Amasino, R.A., and Coupland, G.** (2006). The transcription factor FLC confers a flowering response to vernalization by repressing meristem competence and systemic signaling in Arabidopsis. Genes Dev **20,** 898-912.

**Stevens, C., and La Thangue, N.B.** (2004). The emerging role of E2F-1 in the DNA damage response and checkpoint control. DNA Repair (Amst) **3,** 1071-1079.

**Torres, M.A., Dangl, J.L., and Jones, J.D.** (2002). Arabidopsis gp91phox homologues AtrbohD and AtrbohF are required for accumulation of reactive oxygen intermediates in the plant defense response. Proceedings of the National Academy of Sciences of the United States of America **99,** 517-522.

**Van Breusegem, F., and Dat, J.F.** (2006). Reactive oxygen species in plant cell death. Plant physiology **141,** 384-390.

**Van Leene, J., Hollunder, J., Eeckhout, D., Persiau, G., Van De Slijke, E., Stals, H., Van Isterdael, G., Verkest, A., Neirynck, S., Buffel, Y., De Bodt, S., Maere, S., Laukens, K., Pharazyn, A., Ferreira, P.C., Eloy, N., Renne, C., Meyer, C., Faure, J.D., Steinbrenner, J., Beynon, J., Larkin, J.C., Van de Peer, Y., Hilson, P., Kuiper, M., De Veylder, L., Van Onckelen, H., Inze, D., Witters, E., and De Jaeger, G.** (2010). Targeted interactomics reveals a complex core cell cycle machinery in Arabidopsis thaliana. Molecular systems biology **6,** 397.

**Vlot, A.C., Dempsey, D.A., and Klessig, D.F.** (2009). Salicylic Acid, a multifaceted hormone to combat disease. Annual review of phytopathology **47,** 177-206.

**Wang, W., Barnaby, J.Y., Tada, Y., Li, H., Tor, M., Caldelari, D., Lee, D.U., Fu, X.D., and Dong, X.** (2011). Timing of plant immune responses by a central circadian regulator. Nature **470,** 110-114.

**Wildermuth, M.C.** (2010). Modulation of host nuclear ploidy: a common plant biotroph mechanism. Current opinion in plant biology **13,** 449-458.

**Xia, J., Zhao, H., Liu, W., Li, L., and He, Y.** (2009). Role of cytokinin and salicylic acid in plant growth at low temperatures. Plant Growth Regulation **57,** 211-221.

**Yang, S., and Hua, J.** (2004). A haplotype-specific Resistance gene regulated by BONZAI1 mediates temperature-dependent growth control in Arabidopsis. The Plant cell **16,** 1060-1071.

**Yang, S., Yang, H., Grisafi, P., Sanchatjate, S., Fink, G.R., Sun, Q., and Hua, J.** (2006). The BON/CPN gene family represses cell death and promotes cell growth in Arabidopsis. Plant J **45,** 166-179.

**Yu, H.G., Muszynski, M.G., and Kelly Dawe, R.** (1999). The maize homologue of the cell cycle checkpoint protein MAD2 reveals kinetochore substructure and contrasting mitotic and meiotic localization patterns. J Cell Biol **145,** 425-435.

**Zhang, Y., Goritschnig, S., Dong, X., and Li, X.** (2003). A gain-of-function mutation in a plant disease resistance gene leads to constitutive activation of downstream signal transduction pathways in suppressor of npr1-1, constitutive 1. The Plant cell **15,** 2636-2646.

**Zheng, B., Chen, X., and McCormick, S.** (2011). The anaphase-promoting complex is a dual integrator that regulates both MicroRNA-mediated transcriptional regulation of cyclin B1 and degradation of Cyclin B1 during Arabidopsis male gametophyte development. The Plant cell **23,** 1033-1046.

**Zipfel, C.** (2009). Early molecular events in PAMP-triggered immunity. Current opinion in plant biology **12,** 414-420.

## CHAPTER 2

**Perturbation of cell cycle regulation triggers the plant immune response via activation of disease resistance genes**

Zhilong Bao[1], Huijun Yang[1], and Jian Hua

This chapter has been published on *PNAS*.

### Abstract

The Arabidopsis *OSD1* gene and its homolog *UVI4* are negative regulators of anaphase-promoting complex/cyclosome (APC/C), a multisubunit ubiquitin E3 ligase that regulates the progression of cell cycles. Here we report the isolation of an activation tagging allele of *OSD1* as an enhancer of a mutant of *BON1*, a negative regulator of plant immunity. Overexpression of *OSD1* and *UVI4* each leads to enhanced immunity to a bacterial pathogen, which is associated with a higher expression of disease resistance (*R*) genes similar to the animal NOD1-receptor like immune receptor genes. In addition, the reduction of function of one subunit of the APC complex *APC10* exhibited a similar phenotype to that of overexpression of *OSD1* or *UVI4*, indicating that altered APC function induces immune responses. The enhanced immune response induced by *OSD1* overexpression is dependent on *CYCB1;1* which is a degradation target of APC/C. It is also associated with upregulation of *R* genes and is dependent on the *R* gene *SNC1*. Together, our study reveals an unexpected link between cell cycle progression and plant immunity, suggesting that misregulated cell cycle could have an impact on expression of genes including *R* genes in plant immunity.

## Introduction

Cell divisions, including meiosis, mitosis, and endoreduplication, are essential for both vegetative and reproductive development in plants (Inze and De Veylder, 2006). The anaphase-promoting complex/cyclosome (APC/C) is an evolutionarily conserved E3 ubiquitin-ligase critical for cell cycle progression by degrading cell cycle proteins (Peters, 2006; Marrocco et al., 2010). APC/C contains at least 11 different subunits (named APC1 to APC11) including the catalytic core subunits APC2 and APC11. It requires one of the two proteins, Cell division cycle 20/Fizzy (CDC20/FZY) and CDC20 homolog/Fizzy-related (CDH1/FZR), for activation and substrate specificity. Both CDC20 and CDH1 regulate the progression of mitotic cell cycle, and CDH1 additionally controls the onset and progression of endocycles. In Arabidopsis, there are five CDC20 homologs, namely CDC20.1 to CDC20.5, as well as three CDH1 homologs, namely CCS52A1/FZR2, CCS52A2/FZR1, and CCS52B/FZR3. Both CCS52A1 and CCS52A2 are reported to regulate the onset of endoreduplication (Lammens et al., 2008; Larson-Rabin et al., 2009b; Vanstraelen et al., 2009; Kasili et al., 2010). APC/C activity is essential for cell cycle transition, and total loss of APC/C activity results in lethality. Knocking down APC/C subunits such as APC6, APC10, and APC13 by RNAi in Arabidopsis results in growth defects including dwarf statue and multiple lateral shoots (Saze and Kakutani, 2007; Marrocco et al., 2009).

Two negative regulators of APC/C have been identified in Arabidopsis, and they are the homologous genes *OSD1* (*Omission of the Second Division*) and *UVI4* (*UV Insensitive 4*). *OSD1* functions in both divisions of meiosis, and the loss of its function led to omission of the second meiotic division by itself and the omission of the first meiotic division as well when combined with *cycA1;2* (d'Erfurth et al., 2009) (d'Erfurth et al., 2010). *OSD1* is also involved in endoreduplication or endomitosis in cotyledons and the loss-of-function (l-o-f) mutant *osd1* or

*gig1* (*gigas cell 1*) had gigantic cotyledon epidermal cells with higher ploidy (Iwata et al., 2011). *UVI4* inhibits endoreduplication as well, and the l-o-f *uvi4* mutant had enhanced resistance to UV-B and increased ploidy level in somatic tissues (Perazza et al., 1999; Hase et al., 2006). A co-immunoprecipitation study identified an association of both OSD1 and UVI4 with the APC/C complex (Van Leene et al., 2010), and this association was further revealed in two recent studies. In the yeast-two-hybrid system, UVI4 could directly interact with some core subunits of APC/C such as APC5 (Heyman et al., 2011b) while UVI4 and OSD1 could interact with APC/C activators CCS52A1, CCS52A2, CCS52B, CDC20.1, and CDC20.5 (Heyman et al., 2011a; Iwata et al., 2011; Cromer et al., 2012). The physical interaction is corroborated by their genetic interaction. The *ccs52A1* mutant acted epistatically to *uvi4* while overexpression of *CDC20.1* or *CCS52B* promoted endoreduplication/endomitosis in *osd1/gig1* and *uvi4* mutants (Heyman et al., 2011b; Iwata et al., 2011) . In addition, overexpression of *APC10* suppressed endomitosis defects in *osd1*/*gig1* (Iwata et al., 2011). Furthermore, over-expression of *OSD1*/*GIG1* or *UVI4* transiently caused an increase of protein but not RNA levels of cyclins such as *CYCB1;2* and *CYCA2;3*, demonstrating their function in regulating cell cycle genes at the protein level through APC/C.

Programmed cell death (PCD) is also a mechanism in controlling cell proliferation and fate (Jacobson et al., 1997). Upon recognition of specific pathogens, plant disease resistance (*R*) genes are activated to trigger a form of PCD named hypersensitive response (HR) to control the spread of biotrophic pathogens (Chisholm et al., 2006; Jones and Dangl, 2006). Most of the *R* genes encode nucleotide binding (NB) leucine rich repeat (LRR) proteins similar to animal NOD like immune receptors (Ausubel, 2005). *R* gene activation also induces systemic acquired resistance at distal locations (Durrant and Dong, 2004; Vlot et al., 2008). The *EDS1* (*Enhanced*

*Disease Susceptibility 1*) and *PAD4* (*Phytoalexin Deficient 4*) genes, encoding lipase like proteins, are critical for PCD and disease resistance mediated by many NB-LRR type of *R* genes (Wiermer et al., 2005).

The Arabidopsis *BON1* (*BONZAI1*) and its homologs *BON2* and *BON3* are negative regulators of cell death and disease resistance (Hua et al., 2001; Yang et al., 2006b; Li et al., 2009). A l-o-f allele *bon1-1* in the Col-0 accession has a dwarf phenotype and constitutive defense responses due to activation of a Col-0 specific NB-LRR type of *R* gene *SNC1* (*Suppressor of npr1 constitutive 1*) (Hua et al., 2001; Jambunathan et al., 2001; Yang and Hua, 2004). The l-o-f *bon1-2* mutant in the Wassileskija (Ws) background has no obvious defects under normal growth conditions due to the lack of *SNC1* in this accession, but the triple mutant of *bon1 bon2 bon3* in Ws is lethal resulting from cell death triggered by activation of multiple *R* genes (Yang et al., 2006b). During the course of isolating enhancers of *bon1-2*, an impact of altered expression of *OSD1* and *UVI4* on defense response regulation was discovered. Mis-regulation of APC/C triggers plant immune responses through upregulating expression of *R* genes including *SNC1*, which is dependent on one of the APC/C target protein CYCB1;1. These findings reveal an unexpected effect of APC/C activity on plant immunity, suggesting a cell cycle dependent expression of immunity genes.

## Results

### Identification of *ebo30* as an *enhancer of bon1-2*

To investigate the mechanisms underlying the repression of cell death and defense/immune responses, we carried out a sensitized enhancer mutant screen of *bon1-2* in the Ws accession through activation tagging (Weigel et al., 2000). One putative *enhancer of bon1-2*,

*ebo30*, induced a dwarf and bushy phenotype with many lateral shoots in the *bon1-2* background (Figure 2.1*A*). This mutation was dominant and the homozygous *bon1-2 ebo30* double mutant was lethal. We will refer to the heterozygous *ebo30* mutant as *ebo30* unless specified otherwise. The dwarf phenotype of *bon1-2 ebo30* was dependent on *bon1-2*, as the single mutant of *ebo30* had a close to wild-type appearance except for an increase of lateral shoot numbers later in development (Figure 2.1*A*).

The *bon1-2 ebo30* double mutant, unlike the *bon1-2* or *ebo30* single mutants in Ws, had an upregulation of immune responses similarly to the *bon1-1* mutant in Col-0. When challenged with virulent pathogen *Pseudomonas syringae pv. tomato* (*Pst*) DC3000, the *ebo30* single mutant was as susceptible as the wild-type Ws and the *bon1-2* mutant exhibited only a slight increase of resistance or sometimes no increase of resistance to the pathogen (Figure 2.1*B*). In contrast, the *bon1-2 ebo30* double mutant is much more resistant to *Pst* DC3000, supporting ten-fold less bacterial growth compared to the wild type (Figure 2.1*B*). In addition, *PR1*, a marker gene for salicylic acid mediated defense responses, was upregulated in the *bon1-2 ebo30* mutant (Figure 2.1*C*). Thus *ebo30* enhances both the morphological and the defense response phenotypes of *bon1-2*.

The enhanced immune response in *bon1-2 ebo30* is mediated by *EDS1* and is associated with upregulation of *R*-like genes and cell death. The *bon1-2 ebo30 eds1* triple mutant was largely wild-type looking (Figure 2.1*A*), indicating that the growth defect of *bon1-2 ebo30* is mainly due to activation of defense responses. Because *EDS1* mediates defense responses triggered by NB-LRR type of *R* genes, we assessed the expression of such genes by low stringency hybridization with the *SNC1* gene as a probe based on the sequence similarity among these *R* genes. Compared to Ws, both the *bon1-2* and the *ebo30* single mutants showed an

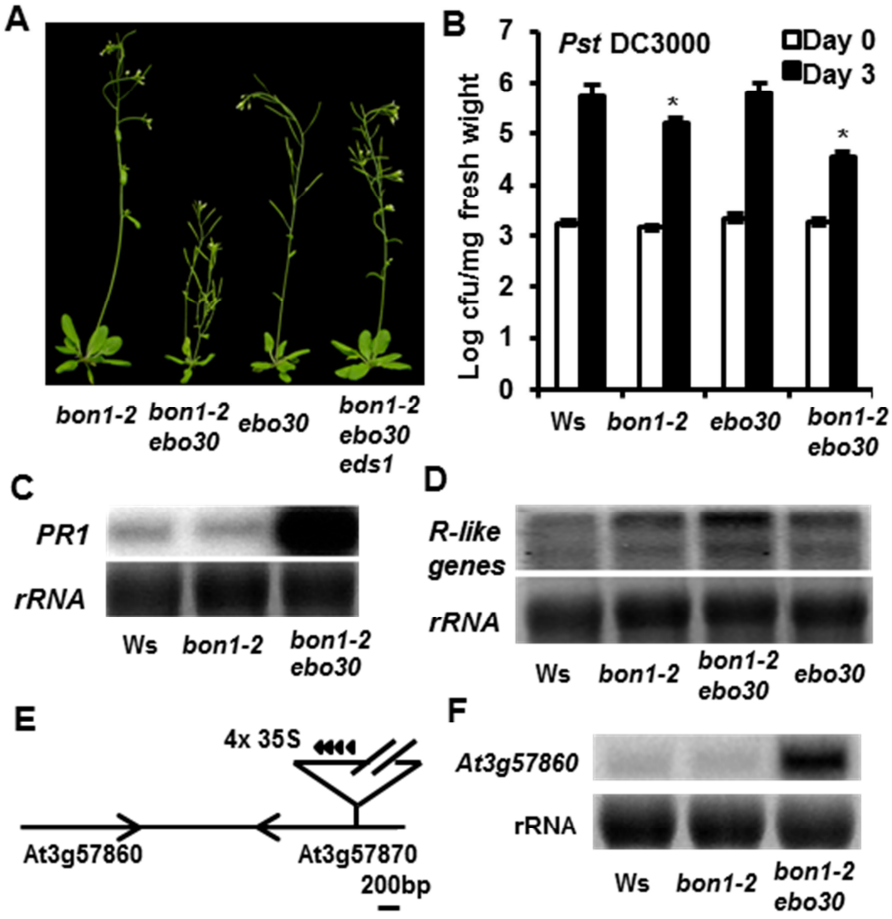


**Figure 2.1 The *ebo30* mutation enhances the *bon1-2* phenotype.** (*A*) Morphology of *bon1-2, bon1-2 ebo30, ebo30* and *bon1-2 ebo30 eds1* plants grown at 22°C for 4 weeks. (*B*) Growth of virulent bacterial pathogen *Pseudomonas syringae* pv. *tomato* (*Pst*) DC3000 in Ws, *bon1-2, ebo30*, and *bon1-2 ebo30* at day 0 and day 4 after inoculation. The asterisk indicates a statistically significant difference from Col-0 determined by Student's *t* test ($P<0.05$). (*C and D*) Expression of *PR1* (*C*) and *R* genes (*D*) in Ws, *bon1-2* and *bon1-2 ebo30* were analyzed by RNA blotting. *rRNA*s were used as loading controls. (*E*) Diagram of the genomic region around the *ebo30* mutation. The activation tag is inserted in At3g57870 which is adjacent to At3g57860. (*F*) Expression of *At3g57860* in *bon1-2 ebo30* analyzed by RNA blotting.

increase of hybridization signals and the *bon1-2 ebo30* double mutant exhibited an even stronger signal (Figure 2.1*D*). The increase of total expression of NB-LRR genes indicates a much stronger upregulation of some *R* genes already induced in the single mutants or an upregulation of more *R* genes in the double mutant. Consistent with the idea that *R* genes are upregulated in the *bon1-2 ebo30* mutant, the growth defect of the double was suppressed by elevated temperature which could often inhibit *R*-mediated disease resistance (Wang et al., 2009; Zhu et al., 2010). At 28ºC, the *bon1-2 ebo30* mutant did not have a stunted growth, but instead exhibited a close to wild-type appearance resembling the *ebo30* single mutant (Figure 2.2*A*).

**Cloning of the *EBO30* gene**

We cloned the *EBO30* gene based on a tight linkage of the *bon1-2 ebo30* phenotype with the T-DNA used in activation tagging (Figure 2.1*E*). The T-DNA was located within the gene At3g57870 encoding SUMO-conjugation enzyme 1 that is essential for embryogenesis (Saracco et al., 2007). The essential function of this gene would account for the lethality of the homozygous *ebo30* mutants but does not readily explain the defense response phenotype of the *bon1-2 ebo30* mutant. As activation tagging may cause overexpression of genes close to the T-DNA, we analyzed RNA expression levels of genes within 10 kb on both sides of the insertion by RNA blots and found an increase of At3g57860 expression in *ebo30* compared to the wild type (Figure 2.1*F*). We confirmed that overexpression of At3g57860 is the cause of the *bon1-2 ebo30* phenotype. A RNA interference (RNAi) construct designed to reduce the expression of At3g57860 was transformed into the *bon1-2 ebo30* mutant, and 25 lines out of a total of 32 transgenic lines showed rescued phenotype with the stronger suppression correlated with a lower expression of At3g57860 (Figure 2.2*B*). Further, over-expression of the At3g57860 gene tagged by GFP (green fluorescent protein) caused a dwarf phenotype in transgenic lines and this

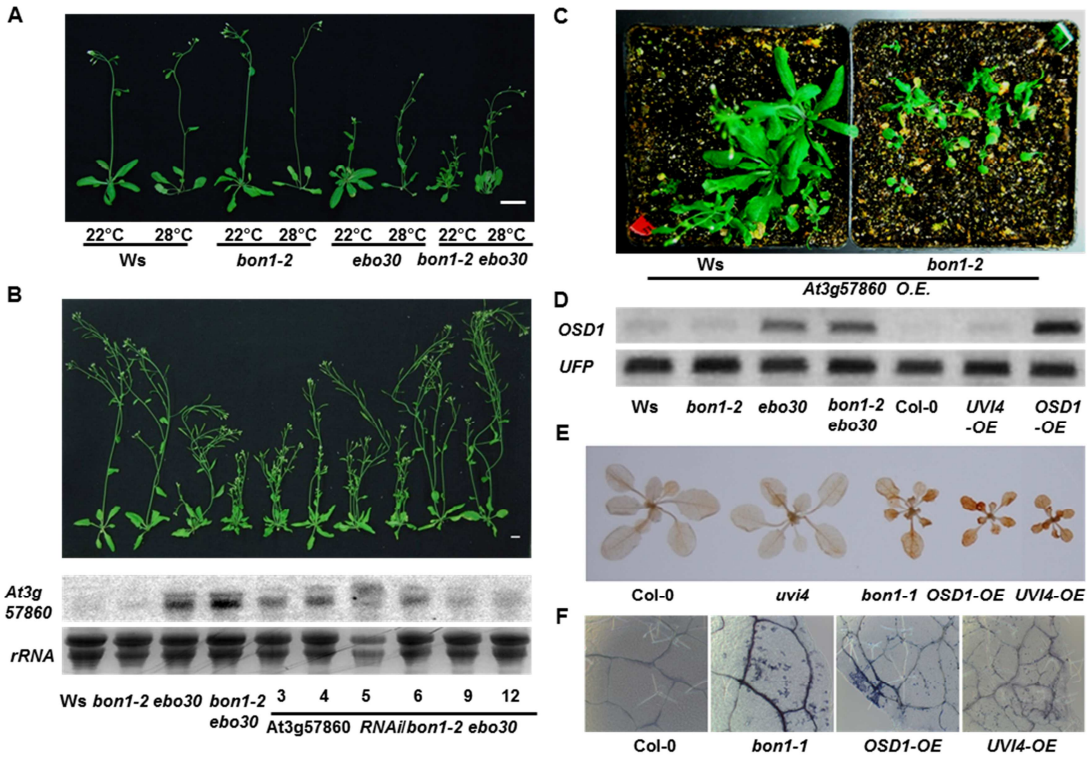


**Figure 2.2 Overexpression of *OSD1* enhances disease resistance.** (*A*) Suppression of the *bon1-2 ebo30* phenotype by a higher temperature. Shown are the Ws, *bon1-2*, *ebo30*, and *bon1-2 ebo30* plants grown at 22°C and 28°C. (*B*) Rescue of the *bon1-2 ebo30* phenotype by RNAi of the At3g57860 (*OSD1*) gene. Shown are the growth phenotypes (top panel) and expression of At3g57860 (middle panel) of six *RNAi* lines (#3, #4, #5, #6, #9 and #12) of At3g57860 in *bon1-2 ebo30* compared to Ws, *bon1-2*, *ebo30* and *bon1-2 ebo30*. rRNA expression (bottom panel) was used as a loading control. (*C*) Over-expression (OE) of a GFP fusion of At3g57860 induces dwarf phenotypes. Shown are multiple T1 plants generated in the wild-type Ws and *bon1-2*. Of the 19 overexpression lines in Ws, 15 (79%) showed a dwarf phenotype. Of the 23 lines in *bon1-2*, all showed a very severe dwarf phenotype. The majority of the T1 lines in *bon1-2* died at seedling stage, and only 3 lines (13%) were able to set seeds. In contrast, all lines in Ws could survive and set seeds. (*D*) Relative expression of At3g57860 in *ebo30* (*osd1-4*) and *OSD1-OE* lines analyzed by semi-quantitative RT-PCR. (*E*) Accumulation of $H_2O_2$ in OE lines shown by diaminobenzidine staining. (*F*) Cell death in leaves from Col-0, *bon1-1*, *OSD1-OE* and *UVI4-OE* revealed by trypan blue staining. Scale bar = 1cm.

phenotype was more severe in the *bon1-2* background than in the wild-type Ws background (Figure 2.2*C*). Thus, a high expression of At3g57860 enhances the *bon1-2* mutant phenotype and *ebo30* is an overexpression allele of the At3g57860 gene which was later reported as *OSD1* and *GIG1*. We thereafter renamed *ebo30* as *osd1-4* (Table 2.1).

**Over-expression of *OSD1* or its homolog *UVI4* confers growth defects and enhances defense responses**

The *UVI4* gene is a close homolog of *OSD1* in Arabidopsis, and their encoded proteins share 61% identity and 68% similarity (Hase et al., 2006). This prompted us to ask if overexpression of *UVI4* could enhance disease resistance similarly to *OSD1*. The *OSD1* and *UVI4* genes tagged by GFP were expressed under the control of the strong 35S promoter in wild-type Col-0 plants. Similarly to transgenic lines in Ws, 32 out of the 34 *p35S::GFP:OSD1* transgenic lines (named *OSD1-OE*, Table 2.1) in Col-0 were dwarf with water-soaked looking leaves and multiple lateral shoots (Figure 2.3*A*). All (more than 20) of the *p35S::GFP:UVI4* transgenic lines (named *UVI4*-OE) in Col-0 showed similar morphological phenotypes to the *OSD1-OE* lines (Figure 2.3*A*). The *OSD1-OE* plants exhibited a more severe phenotype than *osd1-4*, likely due to a higher expression of *OSD1* in *OSD1-OE* than in *osd1-4* or *bon1-2 osd1-4* (Figure 2.2*D*). Both the *UVI4-OE* and *OSD1-OE* plants exhibited enhanced disease resistance to the virulent bacterial pathogen *Pst* DC3000 (Figure 2.3*B*). The proliferation of the pathogen was 100-fold and 10-fold less in *OSD1-OE* and *UVI4-OE* lines, respectively, compared to the wild-type Col-0. In addition, the defense marker gene *PR1* was expressed at a much higher level in the *UVI4-OE* and *OSD1-OE* lines compared to the wild type (Figure 2.3*C*).

The growth phenotypes of *UVI4-OE* and *OSD1-OE* are largely dependent on *PAD4*. All of the fifteen transgenic lines of *OSD1-OE* generated in *pad4* showed wild-type morphologies in

**Table 2.1 Summary of mutants of *OSD1*.** Shown are name of the *osd1* alleles, accession background, characteristics of mutation, and references.

| Names | Accession background | Characteristics of mutation | References |
|---|---|---|---|
| *osd1-1* | Nooseen (No-0) | Ds transposon insertion<br>Loss of function | d'Erfurth I, et al. (2009) PLoS Biol 7: e1000124. |
| *osd1-2* | Landsberg *erecta* (L*er*-0) | Ds transposon insertion<br>Loss of function | d'Erfurth I, et al. (2009) PLoS Biol 7: e1000124. |
| *osd1-2*$^{C}$ | Columbia (Col-0) | *osd1-2* introgressed into Col-0 | this study |
| *osd1-4* | Wassilewskija (Ws-0) | Activation tagging mutant<br>Overexpression of *OSD1* | this study |
| *osd1-4*$^{C}$ | Col-0 | *osd1-4* introgressed into Col-0 | this study |
| *OSD1-OE* | Ws-0 or Col-0 | *p2x35s::GFP:OSD1* transgenic | this study |

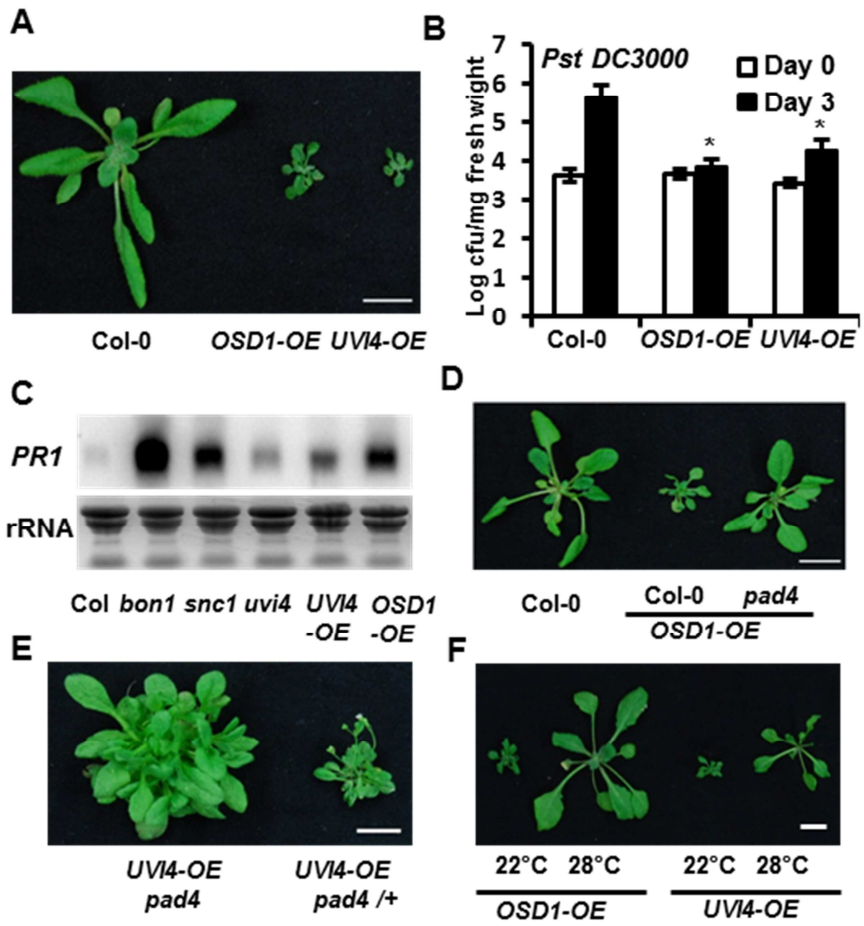


**Figure 2.3 Over-expression (OE) of *OSD1* and *UVI4* each confers enhanced disease resistance.** (*A*) Growth phenotypes of *OSD1-OE* and *UVI4-OE* plants before bolting. A representative line from each OE is shown. (*B*) Growth of *Pst* DC3000 in OE plants at day 0 and day 3 after inoculation. The asterisk indicates a statistically significant difference from Col-0 determined by Student's *t* test ($P<0.05$). (*C*) *PR1* expression analyzed by RNA blots for OE lines at 3-week old. (*D*) Growth phenotypes of *OSD1-OE* in Col-0 and *pad4*. (*E*) Growth phenotypes of the same *UVI4*-OE transgenic line in *pad4* and *pad4/+* (from a cross to the wild type Col-0). (*F*) Growth phenotypes of OE lines at 22°C and 28°C.

contrast to those generated in the wild type Col-0 (Figure 2.3*D*). All four *UVI4-OE* transgenic lines generated in *pad4* produced wild-type looking leaves rather than the small compact leaves produced in the wild-type Col-0 or a *pad4* heterozygous background, although they still had over-proliferation of lateral shoots (Figure 2.3*E*). Expression levels of *UVI4* in *UVI4-OE* lines were comparable in Col-0 and *pad4* indicating that weaker growth defect in *pad4* is not due to lower expression of *UVI4* (Figure 2.4*A*). Similarly, expression of *OSD1* in *osd1-4* is the same in *eds1* background as in *EDS1* wild-type background (Figure 2.4*B*). In addition, the growth defects of *OSD1-OE* and *UVI4-OE* lines exhibited at 22ºC were largely or partially suppressed at 28ºC respectively (Figure 2.3*F*). Thus, overexpression of *UVI4*, similarly to that of *OSD1*, confers constitutive defense responses mediated by *PAD4*.

Over-expression of *OSD1* or *UVI4* induces a higher accumulation of reactive oxygen species and cell death often associated with defense responses. Both the *OSD1-OE* and *UVI4-OE* lines had a higher level of hydrogen peroxide compared to the wild type indicated by a darker stain with 3,3'-diaminobenzidine (Figure 2.2*E*). The higher accumulation of $H_2O_2$ in *UVI4-OE* and *bon1-2 osd1-4* was abolished by *pad4* and *eds1* respectively (Figure 2.4). The *OSD1-OE* and *UVI4-OE* lines also had more spontaneous cell death revealed by a strong trypan blue staining especially on leaf edges (Figure 2.2*F*).

*OSD1* has a lower expression than *UVI4* in vegetative tissues as revealed by promoter reporter gene analysis as well as RNA transcript analysis on leaves at different stages of development (Figure 2.5 *A* and *B*). *UVI4* was slightly induced upon infection of the virulent pathogen *Pst* DC3000 as assayed in transgenic plants containing the reporter gene beta-glucuronidase (GUS) under the control of the *UVI4* promoter (*pUVI4::GUS*) (Figure 2.5*C*). No

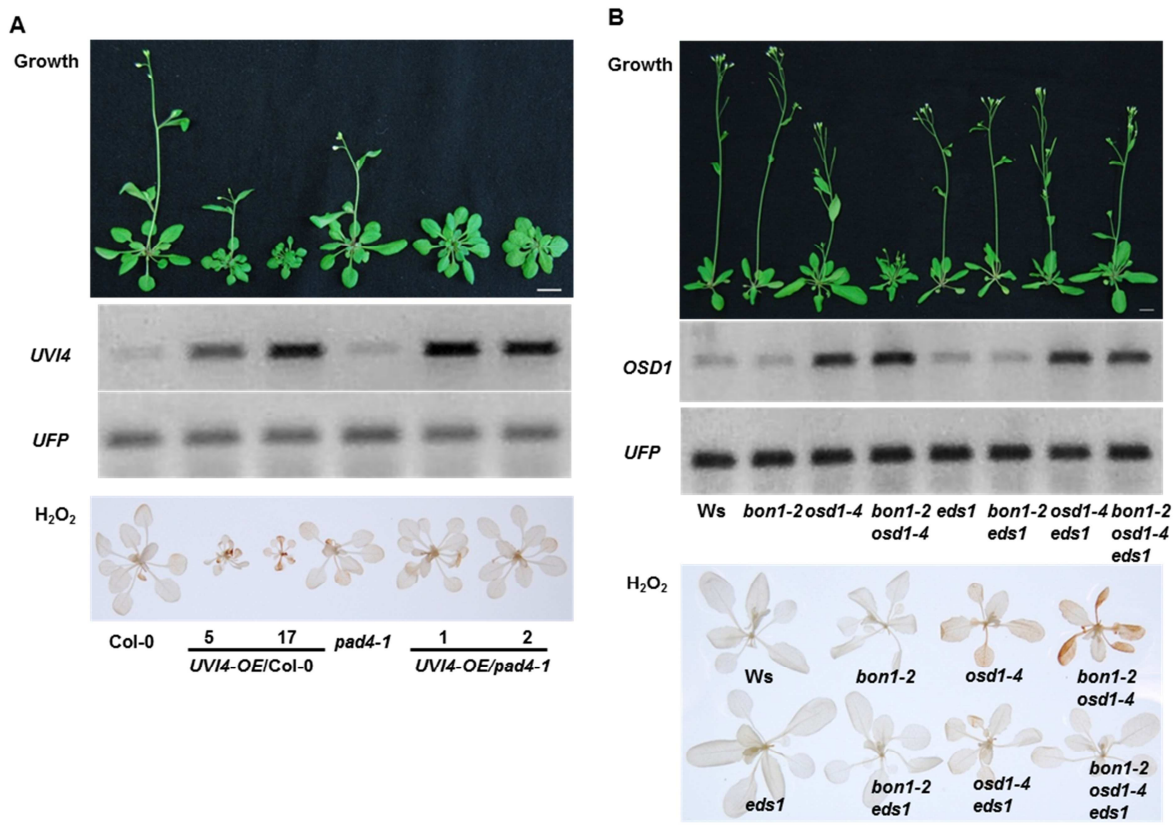


**Figure 2.4 Characterization of *UVI4* and *OSD1* overexpression mutants in wild type, *pad4*, and *eds1*.** Shown are the growth phenotypes, gene expression, and $H_2O_2$ accumulation in *UVI4* (A) and *OSD1* (B) overexpression lines in the wild type and *pad4* or *esd1* mutants. Expression levels of *UVI4* and *OSD1* were analyzed by reverse transcription (RT)-PCR and that of *UFP* was used as a control. Expression levels of *UVI4* were equivalent in *PAD4* and *pad4* backgrounds, and those of *OSD1* were equivalent in *EDS1* and *eds1* backgrounds. Accumulation of $H_2O_2$ was analyzed by DAB staining.

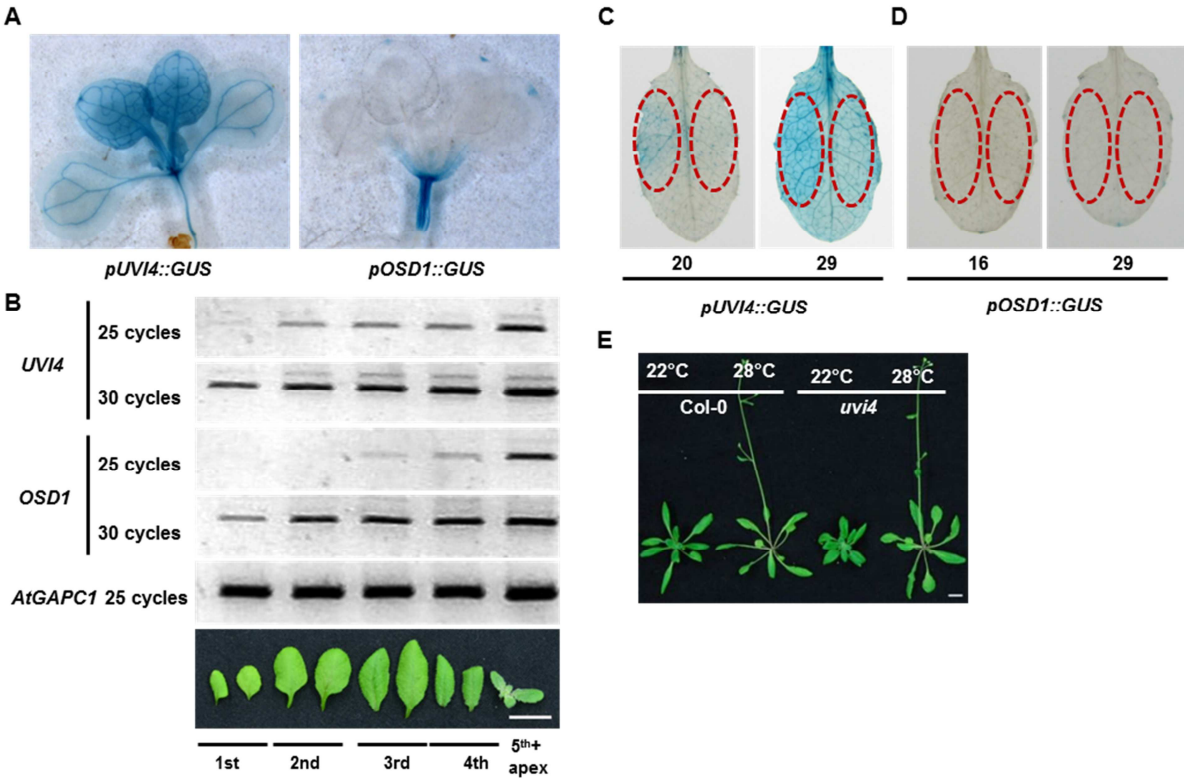


**Figure 2.5 Expression patterns of *OSD1* and *UVI4*.** (*A*) GUS staining of transgenic lines of *pUVI4::GUS* (left) and *pOSD1::GUS* (right) at 9 days after germination. (*B*) Expression of *UVI4* and *OSD1* in the $1^{st}$, $2^{nd}$, $3^{rd}$, $4^{th}$ pairs of leaves and central shoot apex analyzed by RT-PCR. *AtGAPC1* was used as a control. Scale bar = 1 cm. (*C* and *D*) Expression of *UVI4* (*C*) and *OSD1* (*D*) in response to pathogen infection. Shown are the third pairs of leaves from *pUVI4::GUS* and *pOSD1::GUS* transgenic plants. The left half of the leaves was infiltrated with *Pst* DC3000 at 0.05 of $OD_{600}$ and the right half was infiltrated with 10 mM $MgCl_2$ as a control. Leaves were collected 24 hours after the infiltration for GUS activity analysis. Infiltrated areas are indicated by red circles. (*E*) Growth phenotypes of the *uvi4* mutant at 22°C and 28°C.

GUS activity was detected in *pOSD1::GUS* lines (Figure 2.5*D*), indicating a low expression of *OSD1* that is probably not affected by this pathogen.

As overexpression of these two genes confers enhanced defense responses, we tested if loss of their gene functions affects plant immunity. Diploid homozygous l-o-f mutant named *osd1-2*$^{C}$ was generated by six-time consecutive introgression from *osd1-2* heterozygous mutants from L*er*-0 into Col-0 (Table 2.1). The *osd1-2*$^{C}$ plants were, to our surprise, more resistant to *Pst* DC3000 compared to the diploid wild-type Col-0 plants. Interestingly, the *uvi4* plants also showed an enhanced resistance to *Pst* DC3000 in three of the five tests we carried out while the other two times it was not significantly different from the wild type (Figure 2.6 *A* and *B*). The *uvi4* l-o-f mutant may therefore have a slight upregulation of defense responses which sometimes reach the threshold to confer measurable enhanced resistance. This is supported by a higher accumulation of *PR1* in the *uvi4* mutant compared to the wild type (Figure 2.3*C*). That the compact rosette phenotype of *uvi4* mutant was suppressed by a higher growth temperature also suggests an upregulation of immune response in *uvi4* (Figure 2.5*E*). It thus appears that higher or lower expression of *OSD1* or *UVI4* both trigger increased defense responses although the effect of overexpression is more drastic.

**Misregulation of APC/C activity results in enhanced defense responses**

Because *OSD1* and *UVI4* were identified as interacting proteins of some APC/C components [15], we tested their interaction with the APC subunits and the APC activators. We found that both UVI4 and OSD1 interacted with CCS52A1 and CCS52B, which was independently reported recently (Iwata et al., 2011). Though not identified as positive interactors with OSD1 or UVI4 previously, APC8 also showed weak interaction with UVI4 and OSD1 in

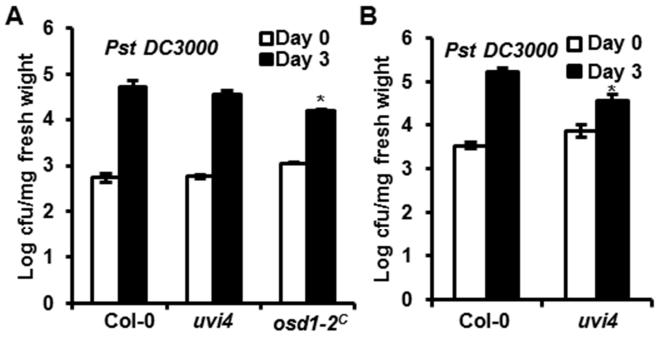


**Figure 2.6 Effects on defense responses from the loss of *UVI4* or *OSD1* function.** (A) Growth of *Pst* DC3000 in *uvi4* and *osd1-2*$^{C}$ at day 0 and day 3 after the inoculation. In this test, *uvi4* was not significantly different from the wild type. (B) Growth of *Pst* DC3000 in *uvi4* at day 0 and day 3 after the inoculation. In this test, *uvi4* is significantly more resistant to pathogen than the wild type. The asterisk indicates a statistically significant difference from Col-0 determined by Student's t test ($P<0.05$).

the yeast two-hybrid assay (Figure 2.7*A*). To determine if the effect of *OSD1* and *UVI4* on plant immunity is mediated by APC/C components, we analyzed disease resistance in APC/C mutants and CSS52 mutants. As most of the components of APC/C are essential, we analyzed reduction of function mutants of *APC10, APC8,* and *APC13*. The *APC10* RNAi lines had a dwarf phenotype (Marrocco et al., 2009) (Figure 2.7*B*); a weak allele of *APC8, apc8-1,* exhibited slight growth defects after the floral transition (Zheng et al., 2011)); and a weak allele of *APC13, apc13-2,* showed normal growth phenotype under our growth conditions although it was reported to have a more compact inflorescences than the wild-type (Zheng et al., 2011) (Figure 2.8*A*). Among these three mutants, the *APC10* RNAi line supported 10-fold less of bacterial growth than the wild type at 3 days after inoculation (Figure 2.7*C*) while *apc8-1* and *apc13-2* exhibited a defense phenotype similar to the wild-type Col-0 plants (Figure 2.8*B*). The *ccs52a1-1* and *ccs52b-1* mutants are l-o-f alleles of *CCS52A1* and *CCS52B* genes respectively. The *ccs52a1-1* mutant has reduced endoreduplication (Larson-Rabin et al., 2009a), but no obvious growth defects were observed in either *ccs52a1-1* or *ccs52b-1*. While *ccs52b-1* behaved like the wild type in response to *Pst* DC3000, *ccs52a1-1* had five-fold more bacterial growth than the wild type (Figure 2.7*D*). Therefore, perturbation of APC/C or APC/C activators can affect disease resistance.

**Loss of function mutation of *CYCB1;1* largely suppresses *osd1-4$^C$* phenotypes**

As CYCB1;1 is a target of APC/C (Zheng et al., 2011) and overexpression of *OSD1* resulted in high accumulation of CYCB1;1 protein (Iwata et al., 2012a), we asked if the defense response phenotype is due to over-accumulation of CYCB1;1. To avoid complication caused by different accession background in double mutant analysis, we generated an *osd1-4$^C$* mutant by introgressing the activation tagged allele *osd1-4* in Ws into Col-0 (Table 2.1). This *osd1-4$^C$*

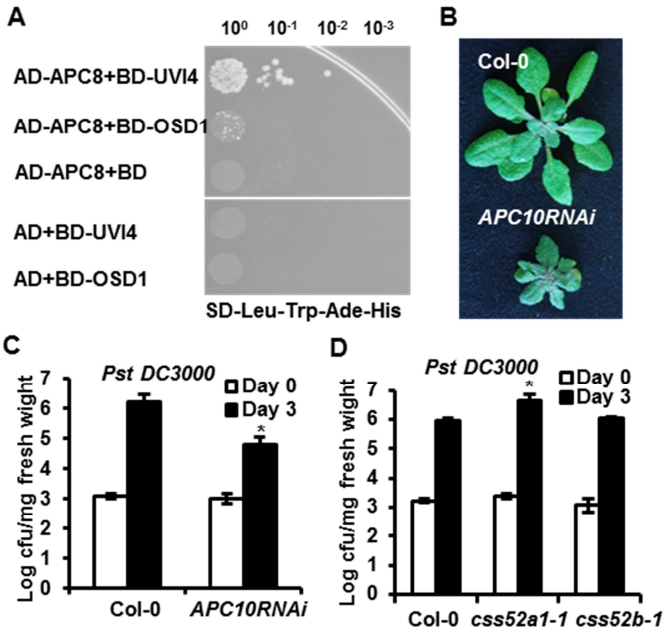


**Figure 2.7 Perturbation of APC/C and its activators affects defense responses.** (*A*) Interaction of APC8 with UVI4 and OSD1 assayed by yeast two-hybrid. Shown are serial dilutions of yeast cells containing the fusions proteins with GAL4 AD (activation domain) and GAL4 BD (DNA binding) plated on interaction selection plates. (*B*) Growth phenotypes of *APC10RNAi* plants under 12 hour-light per day condition for 4 weeks (*C and D*) Growth of *Pst* DC3000 in the *APC10RNAi* line (*C*), *css52a1-1*(*D*), and *css52b-1* (*D*) compared to the wild-type Col-0 at 0 and 3 days after inoculation. The asterisks indicate statistically significant differences from Col-0 determined by Student's *t* test ($P<0.05$).

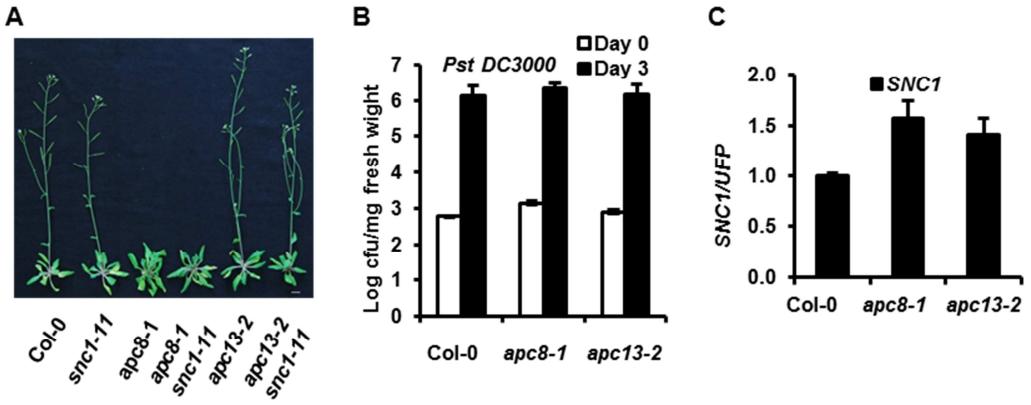


**Figure 2.8 Characterization of *apc8-1* and *apc13-2***. (*A*) Growth phenotypes of the wild-type Col-0, *snc1-1*, *apc8-1*, *apc13-2*, *apc8-1 snc1-11* and *apc13-2 snc1-11*. (*B*) Growth of pathogen *P.s.t.* DC3000 in *apc8-1* and *apc13-2*. Neither showed more disease resistant than the wild type. (*C*) *SNC1* expression in *apc8-1* and *apc13-2* analyzed by qRT-PCR. The error bar indicates standard deviation determined from three replicas. The error bar indicates standard deviation determined from three measurements.

mutant is more stable that the *OSD1-OE* lines and is in the Col-0 background where most of mutants used in this study reside in. Unlike *osd1-4* in Ws with a wild-type appearance, the *osd1-4*$^{C}$ mutant in Col-0 was dwarf and had multiple lateral shoots. These phenotypes were similar to *bon1-2 osd1-4* in Ws but were less severe than *OSD1-OE* in Col-0. We also isolated a *cycb1;1* l-o-f mutant where a T-DNA insertion in the intron results in an absence of a full length transcript of *CYCB1;1* (Figure 2.9*A*). This mutant had no obvious growth defects compared to the wild-type Col-0 (Figure 2.9*B*). When this *cycb1;1* mutation is introduced into *osd1-4*$^{C}$, the morphological defects of *osd1-4*$^{C}$ was largely suppressed (Figure 2.9*B*). Similarly, defense response phenotypes exhibited by *osd1-4*$^{C}$ were also suppressed by the *cycb1;1* mutation (Figure 2.9*C*). The suppression of *osd1-4*$^{C}$ phenotypes is unlikely due to co-suppression induced by two T-DNA insertions as the expression of *OSD1* is similar in the double and the single *osd1-4*$^{C}$ mutants (Figure 2.9*A*). Thus over-accumulation of CYCB1;1 is likely responsible for the growth and immune phenotypes induced by perturbation of APC/C activities.

**Elevated expression of *OSD1* increases transcript levels of *R* genes to confer enhanced defense responses**

Enhanced disease resistance induced by overexpression of *OSD1* or *UVI4* is likely mediated by *R* genes as indicated by its dependence on *EDS1*, *PAD4*, and temperature. *R*-like genes were also observed to have a higher expression in *OSD1* activation tagging line *osd1-4* (*ebo30*) through low-stringency hybridization on RNA blots (Figure 2.1*D*). To have a more comprehensive analysis of effects by overexpression of *OSD1*, we analyzed transcriptional profiles of Ws, *bon1-2*, *osd1-4*, and *bon1-2 osd1-4* (all in Ws) by RNA-Seq technology (Campbell et al., 2002). Differentially expressed gene lists were further analyzed in Mapman

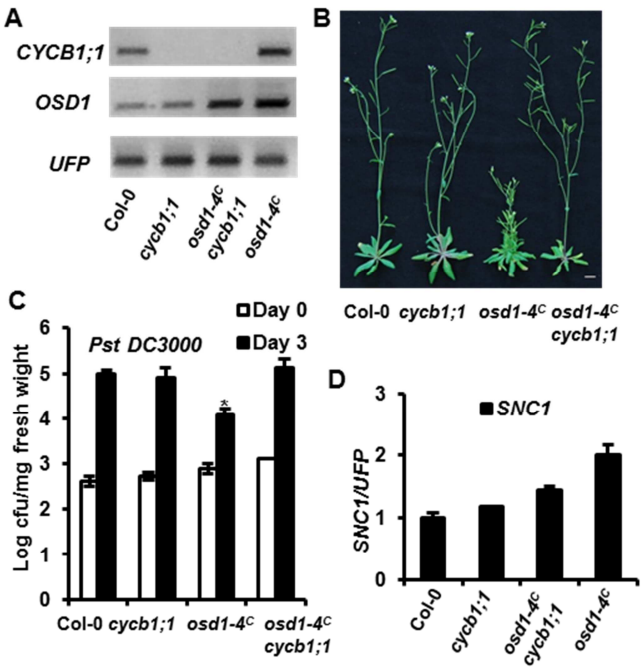


**Figure 2.9 Defense response activation in *osd1-4*$^{C}$ is dependent on *CYCB1;1*. (*A*)** Expression of *CYCB1;1* and *OSD1* in Col-0, *cycb1;1*, *osd1-4*$^{C}$, and *osd1-4*$^{C}$ *cycb1;1* analyzed by RT-PCR (*B*) Growth phenotypes of Col-0, *cycb1;1*, *osd1-4*$^{C}$, and *osd1-4*$^{C}$ *cycb1;1*. (*C*) Growth of *Pst* DC3000 in the above genotypes. The asterisk indicates a statistically significant difference from Col-0 determined by Student's *t* test (P<0.05). (*D*) qRT-PCR analysis of *SNC1* expression in the above genotypes. The error bar indicates standard deviation determined from three measurements.

software (http://mapman.gabipd.org). In *bon1-2*, 418 genes showed altered transcription compared with Ws, and 135 of them are associated with biotic stress (Figure 2.10*A*). In *osd1-4*, 457 genes were differentially expressed compared to Ws, and 121 of them are involved in biotic stress (Figure 2.10*B*). In *bon1-2 osd1-4*, the number of genes with altered transcription increased to 1,045, and 305 of them were categorized as related to biotic stress (Figure 2.10*C*). In *osd1-4*, two *R* genes and two *PR* genes were significantly induced (Table 2.2). In *bon1-2*, three *R* genes and three *PR* genes were significantly induced (Table 2.2). In *bon1-2 osd1-4*, four *R* genes and four PR genes had significantly increased expression (Table 2.2). These observations indicate that *osd1-4* weakly and *bon1-2* moderately upregulate *R* genes and immune responses and the double mutations synergistically upregulate more *R* genes at a higher amplitude and induce a stronger immune response than single mutations.

**Increased *SNC1* transcript is required for enhanced defense responses in *osd1-4*$^C$.**

We tested the contribution of *R* gene upregulation to the defense phenotypes of *OSD1* overexpression. Because *osd1-4* in Ws has a higher expression of the *SNC1* ortholog (though nonfunctional), we analyzed *SNC1* expression in *osd1-4*$^C$ in Col-0 by qRT-PCR (quantitative reverse transcription PCR). A two fold amount of *SNC1* was observed in *osd1-4*$^C$ compared to Col-0, and this increase was largely abolished by the l-o-f mutation of *cycb1;1* (Figure 2.9*D*). When the l-o-f mutation *snc1-11* was introduced into *osd1-4*$^C$, it largely suppressed the small leaf phenotypes of *osd1-4*$^C$ although the double mutant still had a multiple shoot phenotype like the *osd1-4*$^C$ (Figure 2.11*A*). In addition, the *osd1-4*$^C$ *snc1-11* mutant was no longer more resistant to the virulent pathogen *Pst* DC3000 than the wild type or *snc1-11* (Figure 2.11*B*). Again, this suppression is not due to a silencing of *OSD1* expression (Figure 2.12*A*) and the *snc1-11*

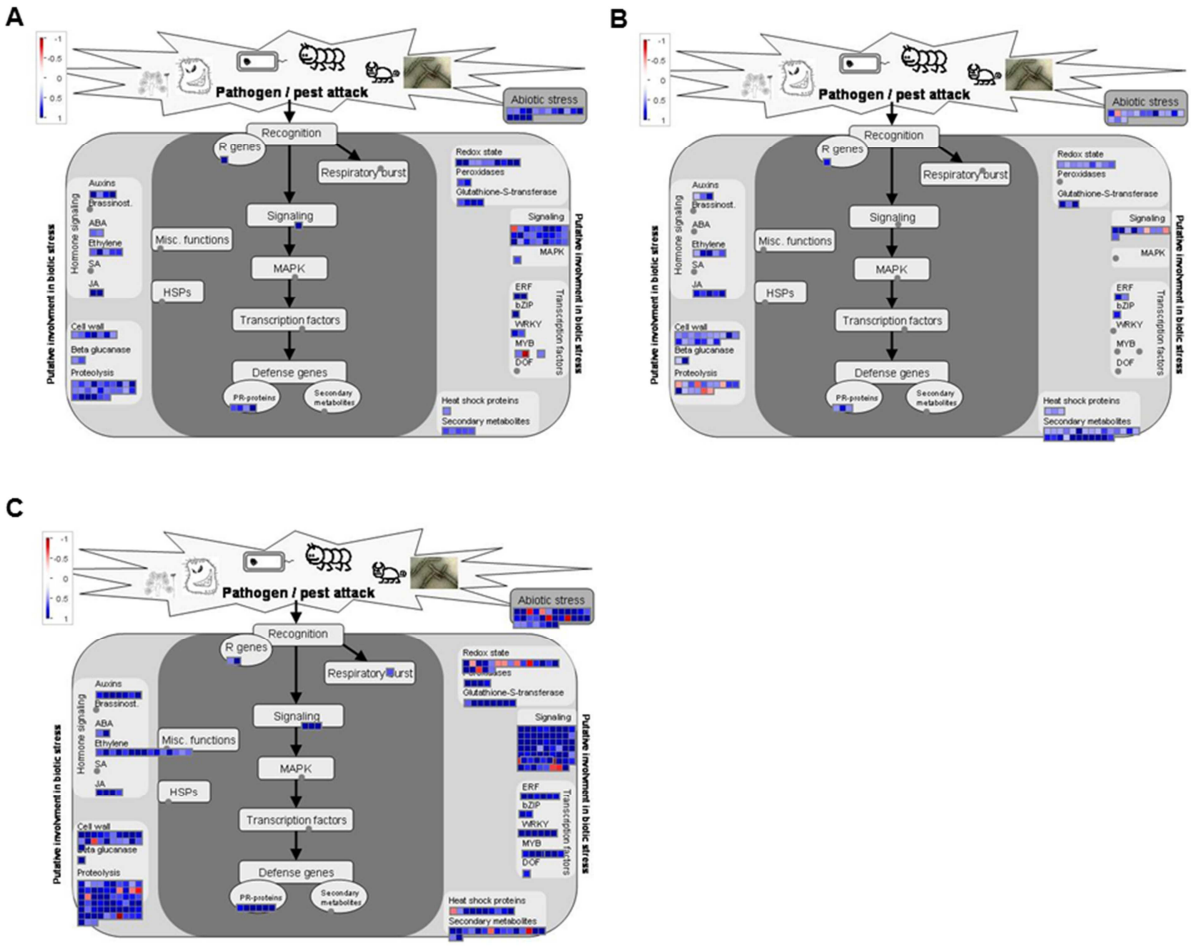


**Figure 2.10 Transcriptome analyses of Ws, *bon1-2*, *osd1-4* and *bon1-2 osd1-4* by RNA-Seq.** The Ws, *bon1-2*, *osd1-4* and *bon1 osd1-4* plants were grown under 14-hr day length at 22°C for three weeks. The above-ground tissues were harvested and total RNA was extracted by following the procedure of Trizol Reagent (Invitrogen). Three biological replicates were performed in all genotypes except for Ws which had two. The program Tophat 2.0 was used to align RNA-Seq reads to Arabidopsis reference genome TAIR10. Differentially expressed genes in different genotypes were identified by the program Cuffdiff. The significance was determined by $p < 0.05$ after Benjamini-Hochberg correction for multiple-testing. Differentially expressed genes in *bon1-2* (*A*), *osd1-4* (B), and *bon1-2 osd1-4* (C) compared to the wild type Ws as analyzed by Mapman software. In *bon1-2*, 128 of the 418 differentially expressed genes are associated with biotic stress. In *osd1-4*, 121 of the 457 differentially expressed genes are associated with biotic stress. In *bon1-2 osd1-4*, 305 of the 1045 differentially expressed genes are associated with biotic stress. All of data were collected from three biological repeats.

**Table 2.2 Differentially expressed *R* and *PR* genes in *bon1-2*, *osd1-4* and *bon1-2 osd1-4* compared to the wild type Ws.** Shown are the gene name, annotation, and their relative expression in *bon1-2*, *osd1-4* and *bon1-2 osd1-4* compared to Ws. Fold changes are in ln value. Significant changes ($p<0.05$) are shaded in gray.

| Gene | Annotation | *bon1-2* vs Ws | | *osd1-4* vs Ws | | *osd1-4 bon1-2* vs Ws | |
|---|---|---|---|---|---|---|---|
| | | Change (ln) | p-value | Change (ln) | p-value | Change (ln) | p-value |
| AT1G57630 | TIR domain family protein | **3.11** | **0.0005** | 1.08 | 0.2738 | **3.90** | **0.0000** |
| AT1G72910 | TIR domain-containing protein | **1.50** | **0.0000** | **0.89** | **0.0000** | **2.52** | **0.0000** |
| AT1G72930 | TIR receptor-like | **1.37** | **0.0000** | **0.79** | **0.0000** | **2.31** | **0.0000** |
| AT3G04210 | Disease resistance protein (TIR-NBS class) | **1.24** | **0.0000** | 0.19 | 0.4297 | **1.65** | **0.0000** |
| AT4G16890 | Disease resistance protein (TIR-NBS-LRR class) | 0.28 | 0.1753 | 0.20 | 0.2254 | **0.58** | **0.0050** |
| AT2G14610 | pathogenesis-related gene 1 | **3.65** | **0.0000** | 0.03 | 0.9608 | **4.65** | **0.0000** |
| AT3G57260 | beta-1,3-glucanase 2 | **4.13** | **0.0000** | **2.38** | **0.0000** | **5.58** | **0.0000** |
| AT3G04720 | pathogenesis-related 4 | **0.65** | **0.0031** | 0.17 | 0.4030 | **1.28** | **0.0000** |
| AT1G75040 | pathogenesis-related gene 5 | **3.13** | **0.0000** | **1.44** | **0.0000** | **4.93** | **0.0000** |

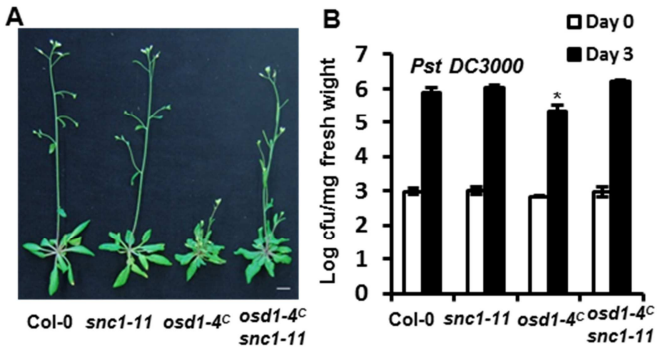


**Figure 2.11 Enhanced disease resistance in *osd1-4$^C$* is dependent on *SNC1*.** (*A*) Growth phenotypes of Col-0, *snc1-11*, *osd1-4$^C$*, and *osd1-4$^C$ snc1-11*. (*B*) Growth of *Pst* DC3000 in the above genotypes. The asterisk indicates a statistically significant difference from Col-0 determined by Student's *t* test ($P<0.05$).

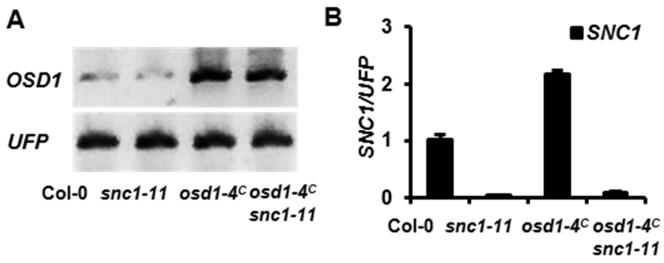


**Figure 2.12 Loss of disease resistance in *snc1-11 osd1-4$^C$* is not due to co-suppression.** (*A*) Expression of *OSD1* in the *snc1-11 osd1-4$^C$* double mutant analyzed by RT-PCR. Expression of *UFP* was used as a control. (*B*) *SNC1* expression in Col-0, *snc1-11*, *osd1-4$^C$*, and *snc1-11 osd1-4$^C$* analyzed by qRT-PCR. The error bar indicates standard deviation determined from three measurements.

mutation abolished the expression of full-length *SNC1* transcript (Figure 2.12*B*). Therefore, enhanced immune response in *osd1-4*$^{C}$ is largely due to an increase of *SNC1* transcript.

A higher *SNC1* transcript was not only observed in *osd1-4*$^{C}$ but also in *apc8-1* and *apc13-2*. Both *apc8-1* and *apc13-2* mutants had approximately 1.5 fold of *SNC1* expression compared to the wild type Col-0, but this increase was lower than that in *osd1-4*$^{C}$ (Figure 2.8 *B* and *C*). The small increase of *SNC1* in *apc8-1* or *apc13-2* was probably not sufficient for an increase of disease resistance or causing growth defects as the *snc1-11* mutation did not alter the growth defects of *apc8-1* or *apc13-2* significantly (Figure 2.8*A*). This suggests that *SNC1* upregulation is likely common in plants with perturbed APC/C although a threshold needs to be reached before it can cause a measurable increase of disease resistance.

**Discussion**

In the course of investigating the regulation of plant disease resistance, we uncovered an intriguing link between cell cycle regulation and defense response regulation. *OSD1* and *UVI4* are negative regulators of APC/C that is responsible for degrading cell cycle proteins (Heyman et al., 2011b; Iwata et al., 2011) (Heyman et al., 2011a; Iwata et al., 2011). The loss of *OSD1* or *UVI4* function leads to various defects in cell cycle progression including omission of meiosis divisions, increased endoreduplication, and possibly increased endomitosis (Hase et al., 2006; d'Erfurth et al., 2009; d'Erfurth et al., 2010; Heyman et al., 2011b; Iwata et al., 2011) Surprisingly, overexpression of either *OSD1* or *UVI4* leads to spontaneous cell death and enhanced disease resistance to a virulent bacterial pathogen (Figure 2.3*B*). This effect is through misregulation of APC/C as a reduction of function of APC/C subunit *APC10* and a l-o-f mutant of APC/C activator *CCS52A1* respectively enhanced and compromised plant defense responses

to the bacterial pathogen (Figure 2.7 *C* and *D*). Furthermore, the enhancement of disease resistance in *OSD1* overexpression mutant is dependent on CYCB1;1, a target of APC/C for degradation (Figure 2.9*C*). Together, these studies indicate that *OSD1*/*UVI4* overexpression down-regulates the APC activity and consequently results in over-accumulation of CYCB1;1 which leads to enhanced defense responses to a bacterial pathogen. Intriguingly, the loss of *OSD1* or *UVI4* function also enhanced disease resistance although to a much less extent (Figure 2.6 *A* and *B*). There is no apparent evidence for a direct role of *OSD1* or *UVI4* in regulating immunity against pathogens. However, it is evident that a perturbation of cell cycle progression by altering *OSD1* and *UVI4* activities could change plant immune responses.

The defense phenotypes in *OSD1* or *UVI4* overexpression are not due to a general dwarfism and/or non-specific stress because they can be largely suppressed by the loss of *PAD4* or *EDS1* whose major function is to transduce *R*-mediated resistance (Figure 2.1*A*, 2*C*, 2*D*). This is corroborated by the transcriptional profile study where biotic response is the major pathway affected by *OSD1* overexpression (Figure 2.10*B*). Several *R* genes were upregulated in the *OSD1* overexpression mutant, and knocking out of one of them, *SNC1*, abolished its disease resistance phenotype (Figure 2.11 *A* and *B*). We propose that misregulated cell cycle progression, for instance by CYCB1;1 over-accumulation, affect the gene expression pattern.

Earlier cell-cycle studies using synchronized suspension cells revealed that different cell cycle phases are associated with slightly different gene expression patterns (Menges et al., 2003), and several *R* genes exhibited peak expression at S or M phases. This differential expression could have physiological consequences. It was reported that cells at different cell cycle phases had different responses to elicitors, and defense gene induction by elicitors were cell cycle dependent (Kadota et al., 2005). *SNC1* was not among the differential *R* genes identified

presumably due to its low expression level or a smaller fluctuation. Nevertheless, we observed an upregulation of *SNC1* in the *osd1-4*$^{C}$ mutant that exhibit enhanced disease resistance as well as in weak mutant alleles of *APC8* and *APC13* that did not exhibit changes in disease resistance. This indicates that upregulation of *SNC1* is the cause rather than the consequence of disease resistance through feedback amplification of *SNC1* by salicylic acid. In addition, the *SNC1* transcript needs to be above a threshold to induce a measurable disease resistance phenotype. As most of the APC/C null mutants are lethal, the partial loss-of-function mutants may have varying degrees of disease resistance depending on the severity of cell cycle perturbation. How cell cycle phases relate to varying expression of genes is not very clear. Cell cycle progression is tied not only with DNA dynamics but also chromatin dynamics (Sanchez Mde et al., 2008) and therefore could have a profound effect on gene expression. Further investigation should reveal general gene regulation during cell cycle phases and the interaction between plants and their pathogens.

## Materials and Methods

### Plant materials, growth, transformation, and pathogen tests

The *ccs52a1-1* (*fzr2-1*) mutant is Salk_083656, the *ccs52b-1* mutant is CS854666, and the *cycb1;1* mutant is CS318535 at Arabidopsis Biological Resource Center. Plant growth, transformation, and pathogen tests were carried out as previously described (Yang and Hua, 2004; Yang et al., 2006a; Zhu et al., 2010). Unless specified otherwise, plants were analyzed for growth phenotypes under constant light conditions and for pathogen growth tests under 12hr light conditions where growth defects in many mutants were reduced.

**Plasmid construction**

The coding region of the *OSD1* cDNA was amplified from pUNI51-At3g57860 (Arabidopsis Biological Research Center) and was cloned first into pSAT6-EGFP-C1 vector and then the binary vector pPZP-RCS2 (Tzfira et al., 2005).

For the promoter-reporter constructs *pOSD1*::*GUS* and *pUVI4*::*GUS*, a 1.5 kb sequence upstream the *OSD1* translation start site and a 1.7 kb sequence 5' to the 19$^{th}$ nucleotide from the translation start site of *UVI4* were cloned into *pGUS2* and *pGUS1* vectors (Diener et al., 2000) respectively.

For the yeast two-hybrid analysis, cDNAs of gene of interest were cloned into pDEST-GADT7 and pDEST-GBKT7 and assays were performed as previously described (Ascencio-Ibanez et al., 2008).

**RNA blot analysis**

RNA blots analysis was carried out as described previously (Yang and Hua, 2004). For *PR1 and OSD1* probes, the full length sequences of the coding regions were used as probes. For low stringency hybridization, an 8 kb genomic fragment of the *SNC1* gene was used as a probe.

**RNA-Seq analysis**

Preparation of cDNA library and RNA-Seq were carried out as previously described (Campbell et al., 2002). The software of MapMan was used to analyze differentially expressed genes associated signaling pathways. The NCBI submission number for the data is SRA059151.

**Quantitative RT-PCR**

qRT-PCR was conducted by following the manufacture's protocol of FastStart universal SYBR Green Master (Roche). Primers for *SNC1* and the reference gene ubiquitin family protein (UFP) were as previous reports (Li et al., 2010; Zhu et al., 2011).

**Acknowledgements**

We thank Drs. Marie Claire Criqui, Atsushi Tanaka, Sheila McCormick, Jane Parker, Xin Li, Cold Spring Harbor Laboratory, Arabidopsis Biological Resource Center for seeds and DNA clones. We thank Dr. Qi Sun for RNAseq analysis and Dr. Thomas Brutnell, Dr. Pinghua Li, Lauren K. Dedow Dr. Shiyan Chen, Dr. Jing Zhou and Dr. Shuhua Yang for technical assistances. We also thank Dr. Wojciech Pawlowski and anonymous reviewers for critical reading of the manuscript. This work was supported by NSF grants IOS-0642289 and IOS-0919914 to J. H.

## References


**Ascencio-Ibanez, J.T., Sozzani, R., Lee, T.J., Chu, T.M., Wolfinger, R.D., Cella, R., and Hanley-Bowdoin, L.** (2008). Global analysis of Arabidopsis gene expression uncovers a complex array of changes impacting pathogen response and cell cycle during geminivirus infection. Plant physiology **148,** 436-454.

**Ausubel, F.M.** (2005). Are innate immune signaling pathways in plants and animals conserved? Nat Immunol **6,** 973-979.

**Campbell, M.A., Fitzgerald, H.A., and Ronald, P.C.** (2002). Engineering pathogen resistance in crop plants. Transgenic research **11,** 599-613.

**Chisholm, S.T., Coaker, G., Day, B., and Staskawicz, B.J.** (2006). Host-microbe interactions: shaping the evolution of the plant immune response. Cell **124,** 803-814.

**Cromer, L., Heyman, J., Touati, S., Harashima, H., Araou, E., Girard, C., Horlow, C., Wassmann, K., Schnittger, A., De Veylder, L., and Mercier, R.** (2012). OSD1 Promotes Meiotic Progression via APC/C Inhibition and Forms a Regulatory Network with TDM and CYCA1;2/TAM. PLoS Genet **8,** e1002865.

**d'Erfurth, I., Jolivet, S., Froger, N., Catrice, O., Novatchkova, M., and Mercier, R.** (2009). Turning meiosis into mitosis. PLoS biology **7,** e1000124.

**d'Erfurth, I., Cromer, L., Jolivet, S., Girard, C., Horlow, C., Sun, Y., To, J.P., Berchowitz, L.E., Copenhaver, G.P., and Mercier, R.** (2010). The cyclin-A CYCA1;2/TAM is required for the meiosis I to meiosis II transition and cooperates with OSD1 for the prophase to first meiotic division transition. PLoS Genet **6,** e1000989.

**Diener, A.C., Li, H., Zhou, W., Whoriskey, W.J., Nes, W.D., and Fink, G.R.** (2000). Sterol methyltransferase 1 controls the level of cholesterol in plants. The Plant cell **12,** 853-870.

**Durrant, W.E., and Dong, X.** (2004). Systemic acquired resistance. Annu Rev Phytopathol **42,** 185-209.

**Hase, Y., Trung, K.H., Matsunaga, T., and Tanaka, A.** (2006). A mutation in the uvi4 gene promotes progression of endo-reduplication and confers increased tolerance towards ultraviolet B light. Plant J **46,** 317-326.

**Heyman, J., Van den Daele, H., De Wit, K., Boudolf, V., Berckmans, B., Verkest, A., Alvim Kamei, C.L., De Jaeger, G., Koncz, C., and De Veylder, L.** (2011a). Arabidopsis ULTRAVIOLET-B-INSENSITIVE4 maintains cell division activity by temporal inhibition of the anaphase-promoting complex/cyclosome. Plant Cell **23,** 4394-4410.

**Heyman, J., Van den Daele, H., De Wit, K., Boudolf, V., Berckmans, B., Verkest, A., Kamei, C.L., De Jaeger, G., Koncz, C., and De Veylder, L.** (2011b). Arabidopsis ULTRAVIOLET-B-INSENSITIVE4 Maintains Cell Division Activity by Temporal Inhibition of the Anaphase-Promoting Complex/Cyclosome. The Plant cell.

**Hua, J., Grisafi, P., Cheng, S.H., and Fink, G.R.** (2001). Plant growth homeostasis is controlled by the Arabidopsis BON1 and BAP1 genes. Genes & development **15,** 2263-2272.

**Inze, D., and De Veylder, L.** (2006). Cell cycle regulation in plant development. Annual review of genetics **40,** 77-105.

**Iwata, E., Ikeda, S., Matsunaga, S., Kurata, M., Yoshioka, Y., Criqui, M.C., Genschik, P., and Ito, M.** (2011). GIGAS CELL1, a Novel Negative Regulator of the Anaphase-Promoting Complex/Cyclosome, Is Required for Proper Mitotic Progression and Cell Fate Determination in Arabidopsis. The Plant cell.

**Iwata, E., Ikeda, S., Abe, N., Kobayashi, A., Kurata, M., Matsunaga, S., Yoshioka, Y., Criqui, M.C., Genschik, P., and Ito, M.** (2012). Roles of GIG1 and UVI4 in genome duplication in Arabidopsis thaliana. Plant Signal Behav **7**.

**Jacobson, M.D., Weil, M., and Raff, M.C.** (1997). Programmed cell death in animal development. Cell **88,** 347-354.

**Jambunathan, N., Siani, J.M., and McNellis, T.W.** (2001). A humidity-sensitive arabidopsis copine mutant exhibits precocious cell death and increased disease resistance. Plant Cell **13,** 2225-2240.

**Jones, J.D., and Dangl, J.L.** (2006). The plant immune system. Nature **444,** 323-329.

**Kadota, Y., Watanabe, T., Fujii, S., Maeda, Y., Ohno, R., Higashi, K., Sano, T., Muto, S., Hasezawa, S., and Kuchitsu, K.** (2005). Cell cycle dependence of elicitor-induced signal transduction in tobacco BY-2 cells. Plant Cell Physiol **46,** 156-165.

**Kasili, R., Walker, J.D., Simmons, L.A., Zhou, J., De Veylder, L., and Larkin, J.C.** (2010). SIAMESE cooperates with the CDH1-like protein CCS52A1 to establish endoreplication in Arabidopsis thaliana trichomes. Genetics **185,** 257-268.

**Lammens, T., Boudolf, V., Kheibarshekan, L., Zalmas, L.P., Gaamouche, T., Maes, S., Vanstraelen, M., Kondorosi, E., La Thangue, N.B., Govaerts, W., Inze, D., and De Veylder, L.** (2008). Atypical E2F activity restrains APC/CCCS52A2 function obligatory for endocycle onset. Proceedings of the National Academy of Sciences of the United States of America **105,** 14721-14726.

**Larson-Rabin, Z., Li, Z., Masson, P.H., and Day, C.D.** (2009a). FZR2/CCS52A1 expression is a determinant of endoreduplication and cell expansion in Arabidopsis. Plant physiology **149,** 874-884.

**Larson-Rabin, Z., Li, Z., Masson, P.H., and Day, C.D.** (2009b). FZR2/CCS52A1 Expression Is a Determinant of Endoreduplication and Cell Expansion in Arabidopsis. Plant Physiology **149,** 874-884.

**Li, Y., Pennington, B.O., and Hua, J.** (2009). Multiple R-like genes are negatively regulated by BON1 and BON3 in arabidopsis. Mol Plant Microbe Interact **22,** 840-848.

**Li, Y., Tessaro, M.J., Li, X., and Zhang, Y.** (2010). Regulation of the expression of plant resistance gene SNC1 by a protein with a conserved BAT2 domain. Plant physiology **153,** 1425-1434.

**Marrocco, K., Thomann, A., Parmentier, Y., Genschik, P., and Criqui, M.C.** (2009). The APC/C E3 ligase remains active in most post-mitotic Arabidopsis cells and is required for proper vasculature development and organization. Development **136,** 1475-1485.

**Marrocco, K., Bergdoll, M., Achard, P., Criqui, M.C., and Genschik, P.** (2010). Selective proteolysis sets the tempo of the cell cycle. Curr Opin Plant Biol **13,** 631-639.

**Menges, M., Hennig, L., Gruissem, W., and Murray, J.A.** (2003). Genome-wide gene expression in an Arabidopsis cell suspension. Plant molecular biology **53,** 423-442.

**Perazza, D., Herzog, M., Hulskamp, M., Brown, S., Dorne, A.M., and Bonneville, J.M.** (1999). Trichome cell growth in Arabidopsis thaliana can be derepressed by mutations in at least five genes. Genetics **152,** 461-476.

**Peters, J.M.** (2006). The anaphase promoting complex/cyclosome: a machine designed to destroy. Nat Rev Mol Cell Biol **7,** 644-656.

**Sanchez Mde, L., Caro, E., Desvoyes, B., Ramirez-Parra, E., and Gutierrez, C.** (2008). Chromatin dynamics during the plant cell cycle. Semin Cell Dev Biol **19,** 537-546.

**Saracco, S.A., Miller, M.J., Kurepa, J., and Vierstra, R.D.** (2007). Genetic analysis of SUMOylation in Arabidopsis: conjugation of SUMO1 and SUMO2 to nuclear proteins is essential. Plant Physiol **145,** 119-134.

**Saze, H., and Kakutani, T.** (2007). Heritable epigenetic mutation of a transposon-flanked Arabidopsis gene due to lack of the chromatin-remodeling factor DDM1. Embo J **26,** 3641-3652.

**Tzfira, T., Tian, G.W., Lacroix, B., Vyas, S., Li, J., Leitner-Dagan, Y., Krichevsky, A., Taylor, T., Vainstein, A., and Citovsky, V.** (2005). pSAT vectors: a modular series of plasmids for autofluorescent protein tagging and expression of multiple genes in plants. Plant molecular biology **57,** 503-516.

**Van Leene, J., Hollunder, J., Eeckhout, D., Persiau, G., Van De Slijke, E., Stals, H., Van Isterdael, G., Verkest, A., Neirynck, S., Buffel, Y., De Bodt, S., Maere, S., Laukens, K., Pharazyn, A., Ferreira, P.C., Eloy, N., Renne, C., Meyer, C., Faure, J.D., Steinbrenner, J., Beynon, J., Larkin, J.C., Van de Peer, Y., Hilson, P., Kuiper, M., De Veylder, L., Van Onckelen, H., Inze, D., Witters, E., and De Jaeger, G.** (2010). Targeted interactomics reveals a complex core cell cycle machinery in Arabidopsis thaliana. Molecular systems biology **6,** 397.

**Vanstraelen, M., Baloban, M., Da Ines, O., Cultrone, A., Lammens, T., Boudolf, V., Brown, S.C., De Veylder, L., Mergaert, P., and Kondorosi, E.** (2009). APC/C-CCS52A complexes control meristem maintenance in the Arabidopsis root. Proceedings of the National Academy of Sciences of the United States of America **106,** 11806-11811.

**Vlot, A.C., Klessig, D.F., and Park, S.W.** (2008). Systemic acquired resistance: the elusive signal(s). Curr Opin Plant Biol **11,** 436-442.

**Wang, Y., Bao, Z., Zhu, Y., and Hua, J.** (2009). Analysis of temperature modulation of plant defense against biotrophic microbes. Mol Plant Microbe Interact **22,** 498-506.

**Weigel, D., Ahn, J.H., Blazquez, M.A., Borevitz, J.O., Christensen, S.K., Fankhauser, C., Ferrandiz, C., Kardailsky, I., Malancharuvil, E.J., Neff, M.M., Nguyen, J.T., Sato,**

**S., Wang, Z.Y., Xia, Y., Dixon, R.A., Harrison, M.J., Lamb, C.J., Yanofsky, M.F., and Chory, J.** (2000). Activation tagging in Arabidopsis. Plant physiology **122,** 1003-1013.

**Wiermer, M., Feys, B.J., and Parker, J.E.** (2005). Plant immunity: the EDS1 regulatory node. Curr Opin Plant Biol **8,** 383-389.

**Yang, H., Li, Y., and Hua, J.** (2006a). The C2 domain protein BAP1 negatively regulates defense responses in Arabidopsis. Plant J **48,** 238-248.

**Yang, S., and Hua, J.** (2004). A haplotype-specific Resistance gene regulated by BONZAI1 mediates temperature-dependent growth control in Arabidopsis. The Plant cell **16,** 1060-1071.

**Yang, S., Yang, H., Grisafi, P., Sanchatjate, S., Fink, G.R., Sun, Q., and Hua, J.** (2006b). The BON/CPN gene family represses cell death and promotes cell growth in Arabidopsis. Plant J **45,** 166-179.

**Zheng, B., Chen, X., and McCormick, S.** (2011). The anaphase-promoting complex is a dual integrator that regulates both MicroRNA-mediated transcriptional regulation of cyclin B1 and degradation of Cyclin B1 during Arabidopsis male gametophyte development. Plant Cell **23,** 1033-1046.

**Zhu, Y., Qian, W., and Hua, J.** (2010). Temperature modulates plant defense responses through NB-LRR proteins. PLoS Pathog **6,** e1000844.

**Zhu, Y., Weng, M., Yang, Y., Zhang, C., Li, Z., Shen, W.H., and Dong, A.** (2011). Arabidopsis homologues of the histone chaperone ASF1 are crucial for chromatin replication and cell proliferation in plant development. Plant J **66,** 443-455.

# CHAPTER 3

## Modulation of cell cycle progression by *OSD1, UVI4* and *CPR5* in Arabidopsis

This chapter is prepared as a manuscript for publication.


### Abstract

Anaphase-promoting complex/cyclosome (APC/C), an E3 ubiquitin ligase containing multiple subunits, plays a pivotal role in cell cycle progression. Two negative regulators, *OSD1* and *UVI4*, inhibit APC/C activity via interaction with its activators, *CCS52A1*, *CCS52A2* and *CCS52B*. Overexpression of *OSD1* or *UVI4* leads to reduced endoreduplication, and the loss of *OSD1* and *UVI4* function each leads to abnormal cell division in meiosis, mitosis and endoreduplication and loss of both functions results in the female gametophyte as well as zygote lethality. Here we report a genetic interaction between *OSD1*/*UVI4* and *CPR5* in the regulation of cell cycle progression and female gametophyte development. *CPR5* was identified as a negative regulator of plant defense responses. Its loss of function mutant exhibits constitutive plant immune responses and reduced endoreduplication. We found that cell cycle defects of *osd1* and *uvi4* single and double mutants can be suppressed by the *cpr5* mutation. The lethality of *osd1 uvi4* double mutant can also be partially suppressed by the loss of *CCS52A1* or *CCS52B* both of which activate the cyclin degradation activities of APC/C. The lack of CYCB1;1 activity might be partially responsible for the lethality of *osd1 uvi4* as overexpression of *CYCB1;1* weakly suppresses the lethality of *osd1 uvi4* and *CYCB1;1* expression is upregulated in *cpr5*. Together, the genetic interactions among *UVI4*, *OSD1, CCS52s* and *CPR5* genes suggests that CPR5 has a direct role in cell cycle regulation and that UVI4/OSD1 and CPR5 may regulate cyclins at protein and transcript level respectively.

## Introduction

Cell division including meiosis and mitosis is a fundamental process in plant growth and development (Inze and De Veylder, 2006). Meiosis ensures the production of plants of the same ploidy after the fusion of gametes, while mitosis is required not only for cell number increase in sporophyte but also for male and female gametophyte development after meiosis (Drews and Yadegari, 2002; Twell, 2011). In a special cell cycle named endoreduplication or endocycle, cells undergo more than one round of replication without cell division to become polyploid (Joubes and Chevalier, 2000). Endoreduplication is critical for developmental processes including cell specification and organ growth as well as physiological responses such as interaction with other organisms (Breuer et al., 2010; Chevalier et al., 2011; De Veylder et al., 2011).

Cell cycle progression is governed by the activity of cyclin-dependent kinase (CDK)-cyclin complex. Eight classes of CDKs including CDKA to CDKG and CDK-like kinases (CKLs) were identified in Arabidopsis, but only CDKA and CDKB were reported to be involved in the regulation of cell cycle progression (Inagaki and Umeda, 2011). During mitotic cell cycle, activities of CDKs are relatively higher at G1/S and G2/M transition phases where a large number of proteins are phosphorylated to promote the onset of DNA replication and mitosis. Cyclins bind to CDKs at specific cell cycle phases to trigger the activation of CDKs. During endocycle, the activity of mitotic CDK-cyclin complex at G2/M transition phase needs to be repressed. The inhibition of CDK-cyclin complex activities is achieved by activation of the anaphase-promoting complex/cyclosome (APC/C) or interaction with cyclin-dependent kinase inhibitors (CKIs or Kip-related proteins).

APC/C, a multiunit E3 ubiquitin-ligase plays critical roles in the cell cycle progression by degrading cell cycle proteins (Peters, 2006; Marrocco et al., 2010). APC/C activity is controlled by two types of activators: *Cell division cycle 20/Fizzy* (*CDC20/FZY*) and *CDC20 homolog/Fizzy-related* (*CDH1/FZR*) which also determine the substrate specificity. Mitotic cell cycle progression requires the function of both *CDC20* and *CDH1*, but the onset and progression of endocycles are only controlled by *CDH1*. Arabidopsis has five *CDC20* homologs (*CDC20.1* to *CDC20.5*) and three *CDH1* homologs (*CCS52A1*, *CCS52A2*, and *CCS52B*). Both *CCS52A1* and *CCS52A2* are reported to regulate the onset of endoreduplication, but the function of *CCS52B* is largely unknown (Lammens et al., 2008; Larson-Rabin et al., 2009; Vanstraelen et al., 2009; Kasili et al., 2010).

Two negative regulators of APC/C in Arabidopsis, *OSD1/GIG1* (*Omission of the Second Division/ gigas cell 1*) and its homolog *UVI4* (*UV Insensitive 4*) were recently identified and functionally characterized in the regulation of cell cycle progression (Heyman et al., 2011; Iwata et al., 2011). The loss of *OSD1* function led to omission of the second meiotic division and a subsequent production of diploid gametes (d'Erfurth et al., 2009). A double mutant of *cycA1;2* and *osd1* had no chromosome segregation during male meiosis, indicating that *CYCA1;2* and *OSD1* promote transitions in both meiotic divisions (d'Erfurth et al., 2010). The mutant *osd1* was recently identified as *gig1* (*gigas cell 1*) because of its gigantic cotyledon epidermal cells with higher ploidy, indicating a role of *OSD1* in endoreduplication or endomitosis in cotyledons (Iwata et al., 2011). The loss of *UVI4* function leads to enhanced resistance to UV-B and increased ploidy level in somatic tissues, indicating that *UVI4* inhibits endocycles (Perazza et al., 1999; Hase et al., 2006). Interactomics experiments by overexpressing core cell cycle genes in Arabidopsis suspension cell culture revealed that both OSD1 and UVI4 interacted with the

APC/C complex (Van Leene et al., 2010). Recent studies further tested these interactions using the yeast two-hybrid system and confirmed the interactions between both UVI4 and OSD1 and APC/C activators CCS52A1, CCS52B, CDC20.1, and CDC20.5 (Heyman et al., 2011; Iwata et al., 2011). Double mutant analysis indicated that *ccs52a1* mutation was epistatic to *uvi4* in the regulation of endoreduplication (Heyman et al., 2011). The ploidy levels in *osd1/gig1* and *uvi4* mutants were even more increased by overexpression of *CDC20.1* or *CCS52B* (Iwata et al., 2011). Increased degradation of CYCA2;3 proteins was observed in the *uvi4* mutant while transient overexpression of *UVI4* or *OSD1* triggered higher accumulation of CYCB1;2 and CYCB1;1 proteins (Heyman et al., 2011; Iwata et al., 2011; Iwata et al., 2012). Moreover, overexpression of *UVI4* and *OSD1* each resulted in enhanced disease resistance through upregulating disease resistance genes in a *CYCB1;1*-dependent manner (Bao et al., 2013). All these demonstrate that *OSD1* and *UVI4* regulate the accumulation of cell cycle proteins by inhibiting the degradation activities of APC/C.

In animal and fungal systems, cell cycle progression is tightly linked to cell survival. Cell damage is assessed by various cell cycle checkpoints that cause cell cycle arrest for DNA repair or lead to cell death (Stevens and La Thangue, 2004). In plants, few examples exist for the association of cell cycle arrest and cell death and the connection between the two processes is not clear. *OSD1*, *UVI4*, and a few APC/C genes appear to affect both cell cycle and cell death/defense. The *CPR5* gene is also implicated in both defense regulation and endoreduplication. Loss-of-function (l-o-f) *cpr5* mutants show increased disease resistance to bacterial pathogens accompanied by high accumulation of salicylic acid and ectopic cell death (Bowling et al., 1997; Boch et al., 1998). The *cpr5* mutant has abnormal trichomes due to reduced endoreduplication and cell death (Kirik et al., 2001). In addition, it has early senescence,

a hyper sensitivity to sucrose (Yoshida et al., 2002), low leaf potassium content (Borghi et al., 2011), abnormal response to ABA (Gao et al., 2011), and abnormal cell wall biosynthesis (Brininstool et al., 2008). *CPR5* could therefore be a component of a general biochemical or cellular process and thus have a broad impact on different processes. However, little is known about its biochemical mode of action besides that it has a transmembrane segment and is localized to both cytoplasm and nucleus (Perazza et al., 2011).

Here we report genetic interactions between *OSD1, UVI4* and *CPR5* genes in the regulation of cell cycle progression. Loss of function mutations *osd1* and *uvi4* promote endoreduplication and lead to lethality of double mutants. The lethality of *osd1 uvi4* could be partially suppressed by mutations in either *CCS52A1* or *CCS52B*. Interestingly, the *cpr5* mutation suppressed many defects of the *osd1* and *uvi4* mutants and the lethality of *osd1 uvi4*, and also triggers induction of *CYCB1;1* expression. All these findings suggest *OSD1, UVI4* and *CPR5* regulate cell cycle progression through altering CDK-cyclin complex activities.

## Results

### Overexpression of *OSD1* and *UVI4* affect endoreduplication in leaves

To investigate the function of *OSD1* in the regulation of cell cycle progression, we analyzed ploidy levels in both loss of function mutants and overexpression transgenic lines of *OSD1* and its homolog *UVI4*. Because loss of *OSD1* function results in whole genome duplication, we selected for ploidy analysis homozygous *osd1-2* plants (a transposon mutant GT21481) in the Landsberg *erecta* (L*er*) background from progenies of heterozygous rather than homozygous *osd1-2* plants. The control was an *uvi4-2* allele in L*er* (Landsberg *erecta*) previously named *pym* (Perazza et al., 1999). In the first pair of leaves of 4- or 6- week old

seedlings, *uvi4-2* had an increase of higher-ploidy cells (32C and 16C) as analyzed by flow cytometry (Figure 3.1A), which is consistent with the previous finding for the *uvi4-1* mutant in Col-0. The *osd1-2* mutant in L*er* also had a significant increase of the number of 16C and 32C cells compared to wild-type L*er* (Figure 3.1A). A very recent study showed that the loss of *OSD1* function triggered endomitosis and the *osd1/gig1* mutants had gigantic cells in cotyledon epidermis (Iwata et al., 2011). Whether the increase of ploidy level in *osd1-2* we observed in the true leaves is due to increased endoreduplication or endomitosis awaits further investigation.

The effect of *OSD1* overexpression on cell cycle progression was also examined in parallel. The *osd1-4* mutant was isolated as an overexpression allele generated from activation tagging mutagenesis, and characterized by strongly enhanced defense responses of *bon1-2* which is a loss-of function mutant of *BONZAI 1*, a negative regulator of plant immunity in the Ws ecotype (Bao et al., 2013). In the *osd1-4* mutant where *OSD1* has a higher expression in the Ws accession (Bao et al., 2013), a reduced ploidy level was observed in leaves compared to the wild type, especially when plants were grown under weaker light illumination (Figure 3.1B). The *osd1-4* plant had significantly more cells with 2C, 4C, and 8C at the expense of cells with 16C and 32C compared to the wild-type Ws plant (Figure 3.1B). The *bon1-2* mutation didn't alter ploidy distribution, and the *bon1 osd1-4* mutant had similar a ploidy level as *osd1-4*. Thus, the level of *OSD1* is critical in controlling ploidy level in leaves, most likely through a regulation of endoreduplication.

Overexpression of a UVI4 and GFP fusion as in *UVI4-OE* confers a dwarf phenotype with multiple shoots in both the wild-type Col-0 and the *uvi4-1* mutant in Col-0 (Hase et al., 2006) (referred to as *uvi4*). *UVI4-OE* had decreased branching trichome number compared to

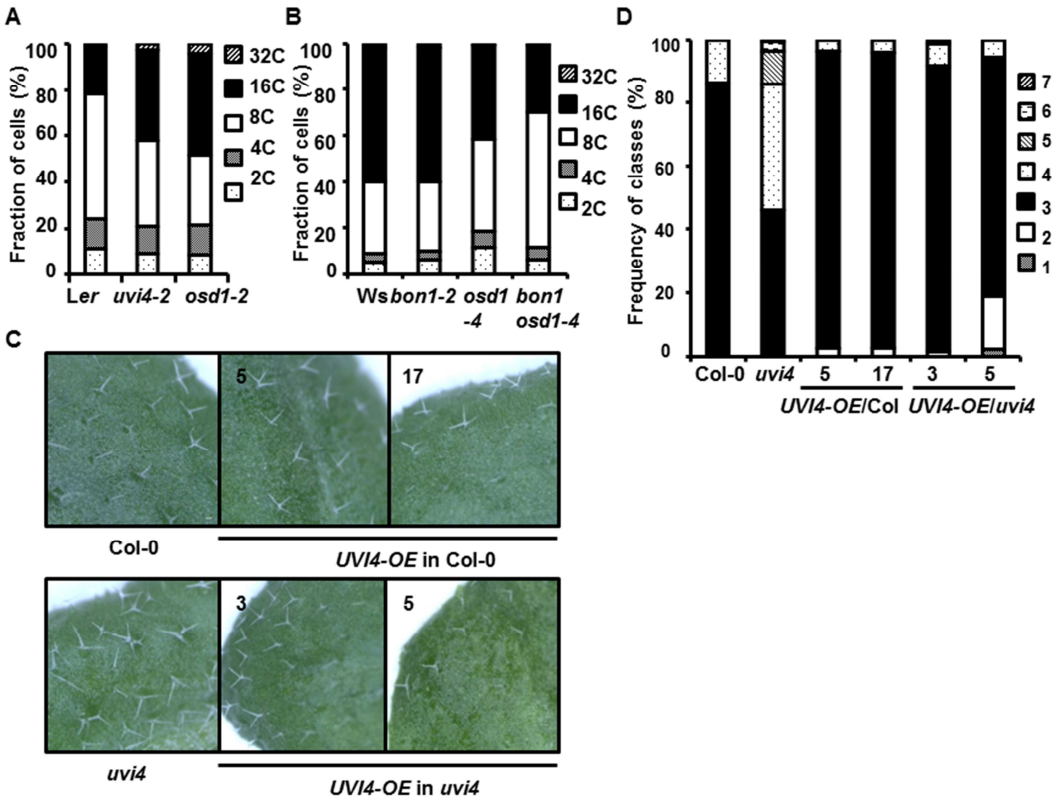


**Figure 3.1 Overexpression of *OSD1* and *UVI4* affect endoreduplication in leaves.** (A) Ploidy levels in the first pair of leaves from the wild-type L*er*, *uvi4-2*, and *osd1-2* grown under 12 hour light/day for 4 weeks. (B) Ploidy levels in the first pair of leaves from Ws, *bon1-2*, *osd1-4* and *bon1 osd1-4* grown under 12 hour light/day for 6 weeks. Averages of three replicas for each sample were shown in (A) and (B). (C) Representative trichome morphologies in Col-0, *uvi4* and *UVI4-OE* lines 5 and 17 in Col-0 and lines 3 and 5 in *uvi4*. (D) Frequencies of each class of trichome numbers in the above genotypes. Approximately 100 to 150 cells were examined for each genotype. The difference between overexpression lines and wild type Col-0 was determined by chi-square test (*UVI4-OE*/Col-0 L5: P=0.013<0.05, L17: P=0.019<0.05; *UVI4-OE*/Col-0 L3: P=0.174>0.05, L5: P=4.29E05<0.05).

Col-0 or *uvi4* (Figure 3.1C). While numbers of trichome branches in wild type and *uvi4* are more than two, around 2.5% of the trichomes in lines 5 and 17 of *UVI4-OE* in Col-0, and 1.5% and 16.9% of the trichomes in lines 3 and 5 of *UVI4-OE* in *uvi4*, respectively, had two branches (Figure 3.1D). The line 5 of *UVI4-OE* in *uvi4* also had 2% trichomes with one branch (Figure 3.1D). These data indicate that overexpression of *UVI4* not only complemented the defects of endoreduplication in the *uvi4* mutant but also further inhibited the progression of endoreduplication in both the wild type and the *uvi4* mutant.

**The *osd1 uvi4* double mutants are defective in female gametophyte and zygote development**

We found that the *osd1 uvi4* double mutant is lethal during both female gameotogenesis and embryogenesis (Figure 3.2), which was also reported recently (Iwata et al., 2011). The *osd1-2*$^{C}$ mutant (refered to as *osd1* from now on) is *osd1-2* mutation from L*er* introgressed into Col-0 using heterozygous mutants, and *uvi4* is also in Col-0. No double mutant seedlings could be identified in a total of 144 progeny plants from a double heterozygote *osd1/OSD1 uvi4/UVI4* (Figure 3.2A). Progeny testing from reciprocal crosses between *osd1/OSD1 uvi4/uvi4* and wild-type Col-0 indicates that approximately 20% (17/83) of *osd1 uvi4* female gametes survived compared to *OSD1 uvi4* gametes while the *osd1 uvi4* male gametes transmitted with only a slightly reduced rate compared to the *OSD1 uvi4* gametes (Figure 3.2B). Indeed, un-developed ovules and arrested embryos were observed in *osd1/OSD1 uvi4/uvi4* siliques (Figure 3.2C). When progenies of the *osd1/OSD1 uvi4/uvi4* plants were analyzed, plants with genotypes of *OSD1/OSD1 uvi4/uvi4* and *osd1/OSD1 uvi4/uvi4* were found but not those of *osd1/osd1 uvi4/uvi4* (Figure 3.2D), indicating that some *osd1 uvi4* female gametes did survive but the *osd1/osd1 uvi4/uvi4* zygote could not survive.

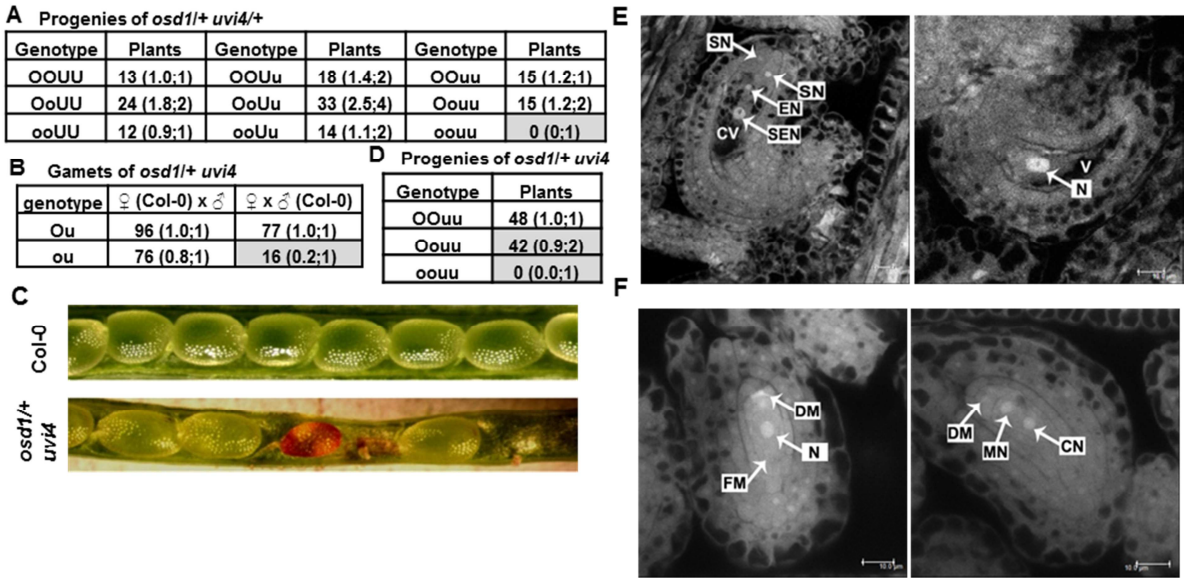


**Figure 3.2 *osd1 uvi4* double mutant is lethal.**
Shown are numbers of plants of each genotype in an analyzed population. The two numbers in parenthesis are the observed ratio of that genotype relative to the top left genotype (left) and the expected ratio when there is no reduced transmission of the gametes or zygotes (right) separated by a semi comma. (A) Analysis of progenies from *osd1/OSD1 UVI4/uvi4*. No *osd1/osd1 uvi4/uvi4* plants (shaded) were found. (B) Analysis of gamete transmission inferred from reciprocal crosses between *osd1/OSD1 uvi4/uvi4* and Col-0. *osd1 uvi4* had a lower transmission rate through female gametes (shaded) but not male gametes. (C) Opened siliques from wild-type Col-0 (upper) and *osd1/OSD1 uvi4/uvi4* (lower) plants. Aborted ovules and embryos can be seen in the mutant silique. (D) Analysis of progenies from *osd1*/*OSD1 uvi4/uvi4*. Notice that both *OSD1/OSD1 uvi4/uvi4* and *osd1/OSD1 uvi4/uvi4* (shaded) were about half of the progenies as expected and there were no *osd1/osd1uvi4/uvi4* (shaded) progenies produced. (E) Confocal laser scanning microscopy of female gametophytes at early developmental stages in the *osd1-2$^{C}$*/+ *uvi4* pistil. All gametes showed either wild-type FG1 (left panel) or FG2 (right panel) features at this stage. FM, functional megaspore. N, uninucleate. DM, degenerating megaspore. MN, micropylar nuleus. CN, chalazal nucleus. (F) Confocal laser scanning microscopy images of the terminal female gametophyte in an *osd1-2$^{C}$/OSD1 uvi4/uvi4* pistil which contained wild-type female gametophyte at FG7 (left panel) and abnormal female gametophyte arrested at FG1 (right panel). SEN, secondary endosperm nucleus; CV, central vacuole; EN, egg nucleus; SN, synergid nucleus; N, nucleus; V, vacuole. Scale bar=10µm.

Using confocal laser scanning microscopy, we analyzed at which stage the female gametophyte development in *osd1 uvi4* is defective. In the pistils of *osd1/OSD1 uvi4/uvi4*, about half of female gametophytes were four-celled, typical of FG7 at terminal development as previously defined (Christensen, 1997) (Figure 3.2E). The other half contained a large nucleus resembling the wild type at the FG1 stage but were likely arrested in development because they had one or more prominent vacuoles which were not present in the wild type at FG1 (Figure 3.2E). No defects were observed in the very early gametophyte development stages when the wild type reached FG1 or FG2 in the *osd1/OSD1 uvi4/uvi4* pistils (Figure 3.2F). Thus, the *osd1 uvi4* female gametophyte fails to develop beyond FG1. The large nucleus with strong DNA staining in the *osd1 uvi4* gamete suggests that it is arrested after DNA replication of the first mitosis.

**The *cpr5* mutation is largely epistatic to *uvi4 and osd1* in regulating endoreduplication**

The fact that overexpression of *OSD1* or *UVI4* confers enhanced disease resistance (Bao et al., 2013) and reduced endoreduplication promoted us to look at genetic interaction between the *OSD1* and *UVI4* genes and the *CPR5* gene that is also involved in these two processes (Bowling et al., 1997; Boch et al., 1998; Kirik et al., 2001; Yoshida et al., 2002). The double l-o-f mutant of *cpr5-2* (Boch et al., 1998) (referred as *cpr5* from now on) and *uvi4* was generated in Col-0 and analyzed for trichome branching resulting from endoreduplication. On the adaxial side of the fourth leaf, wild type Col-0 typically had trichomes with three and four branches, the *cpr5* mutant had fewer branches with mostly one or two, and *uvi4* had more branches mostly with three to five (Figure 3.3A, B). The *cpr5 uvi4* double mutant had trichomes with fewer branches than *cpr5* (Figure 3.3A, B), indicating that *cpr5* is epistatic to *uvi4* in trichome branching phenotype. Flow cytometry analysis was carried out to analyze nuclear DNA content in the first

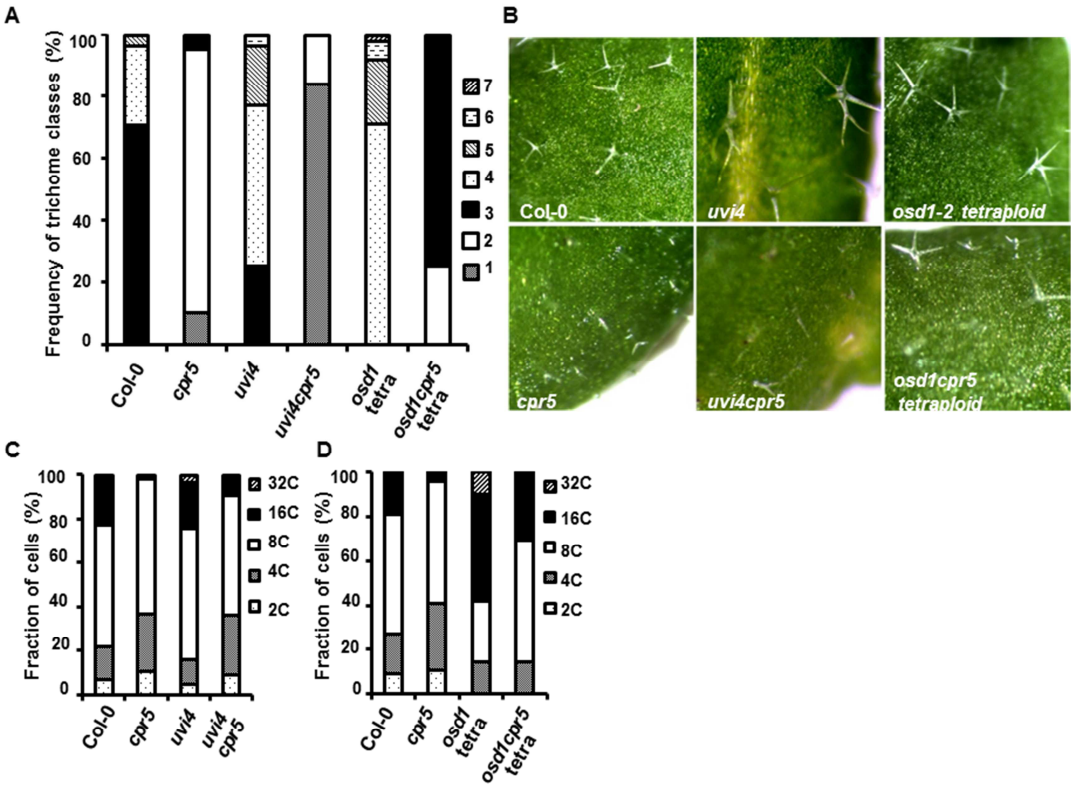


**Figure 3.3 Genetic interactions of *uvi4* and *osd1* with *cpr5*.** (A) Frequency of cells of different branching numbers in Col-0, *cpr5*, *uvi4*, *uvi4 cpr5*, *osd1-2* tetraploid, and *osd1 cpr5* tetraploid plants on the forth leaves. Approximately 100 to 150 cells were examined for each genotype. (B) Shown are representative trichomes from the forth leaves of the above genotypes. (C) DNA ploidy levels of Col-0, *cpr5*, *uvi4*, and *uvi4 cpr5* shown as percentage of cells with 2C to 32C. (D) DNA ploidy levels of Col-0, *cpr5*, *osd1* tetraploid, and *cpr5 osd1* tetraploid shown as percentage of cells with 2C to 32C. Numbers in (C) and (D) are averages of three replicas.

pair of leaves. The *uvi4* mutant contained more cells with higher ploidy while the *cpr5* mutant had more cells with lower ploidy than the wild type (Figure 3.3C). The *cpr5 uvi4* double mutant had cells with a ploidy profile similar to that of *cpr5* (Figure 3.3C), further indicating a suppression of *uvi4* by *cpr5* in endoreduplication.

Genetic interaction between *osd1* and *cpr5* was also analyzed. The *osd1-2* allele in L*er* had increased endoreduplication compared to L*er* in leaves (Figure 3.1A), but it was reported not to have an increase of trichome branching (Hase, Trung et al. 2006). The trichomes of the *osd1-2* tetraploid plants had many more branches than the wild-type diploid plants (Figure 3.3A, B), likely due to genome duplication. The lack of a tetraploid wild-type Col-0 prevented us to analyze the effect of *osd1* on trichome branching in the tetraploid background. Nevertheless, we compared the tetraploid *osd1-2 cpr5* to the tetraploid *osd1-2*. The tetraploid double mutant had trichomes with mostly two and three branches on the adaxial side of the forth leaf, much fewer than those in the *osd1-2* tetraploid (Figure 3.3A, B). Flow cytometry analysis on the first pair of leaves revealed that the tetraploid *osd1-2* had 10% of cells with 32C while the *osd1 cpr5* had only 1% of cells with 32C (Figure 3.3D), indicating that *cpr5* still exhibits endoreduplication defects even in the *osd1-2* mutant background.

**The *cpr5* mutation largely suppressed the lethality of the *uvi4* and *osd1* double mutant**

To determine whether *cpr5* affects gametogenesis, we first carried out reciprocal test crosses between heterozygous *cpr5/CPR5* and the wild type Col-0. F1 progenies were genotyped to determine the transmission of *cpr5* as male and female gametes. The female transmission rate of *cpr5-2* allele was 108% (27/25) compared to the wild type, and the male transmission rate was 169% (61/36) compared to wild type (Figure 3.4A). This data suggested that *cpr5* mutation enhances the transmission of male gametes.

To determine whether *cpr5* can suppress the lethal phenotype of the *osd1 uvi4* double mutant, we crossed *osd1/OSD1 cpr5/cpr5* to *uvi4/uvi4 cpr5/cpr5* and selected *osd1/OSD1 uvi4/UVI4 cpr5/cpr5* plants among the F1 progenies. Out of the 118 F2 plants from this F1, 3 plants were identified as *osd1/osd1 uvi4/uvi4 cpr5/cpr5* (Figure 3.4B, C), indicating that *cpr5* rescued the embryo lethality of *osd1/osd1 uvi4/uvi4* zygotes and possibly reduced the lethality of female gametophyte of *osd1 uvi4*. We further crossed *osd1/OSD1 uvi4/uvi4 cpr5/CPR5*to Col-0 and *uvi4* respectively, and the progeny test was carried out to determine the gamete transmission. The survival rate of *osd1 uvi4* female gametophytes relative to that of *OSD1 uvi4* was about 40% (20/50) and 45% (15/33), while the survival rate of *osd1 uvi4 cpr5* relative to that of *OSD1 uvi4 cpr5* was increased to 73% (29/40) and 108 % (41/38) in crosses to Col-0 and *uvi4* respectively (Figure 3.4D). Thus, *cpr5* suppressed the lethality in the female gamete of *osd1 uvi4*. The difference of apparent rescue extent of the female gametophyte in crosses to the wild type and *uvi4* might result from a different survival rate at the zygote stage.

The *cpr5* mutation also appears to affect the transmission of *osd1*. The *osd1* mutation did not have lower transmission than wild-type *OSD1* (Figure 3.2A). In progenies of *osd1/OSD1 uvi4/UVI4 cpr5/cpr5* plants, plants with the *osd1/OSD1 cpr5/cpr5* genotype were about 50% instead of the expected 200% relative to those with the *OSD1/OSD1 cpr5/cpr5* genotype in combination with any of the *UVI4* genotypes: 12/23 with *UVI4/UVI4*, 18/35 with *uvi4/UVI4*, and 6/11 with *uvi4/uvi4* (Figure 3.4D). This indicates that the *osd1 cpr5* gamete of has a lower transmission rate than *OSD1 cpr5*.

**The *ccs52a1* or *ccs52b* mutation leads to a partial suppression of the lethality of *osd1 uvi4***

Opposite to the function of *OSD1* and *UVI4*, both *CCS52A1* and *CCS52B* positively regulate the activity of APC/C (Larson-Rabin et al., 2009; Iwata et al., 2011). To determine

A Gamets of *cpr5/+*

| genotype | ♀ (Col-0) x ♂ | ♀ x ♂ (Col-0) |
|---|---|---|
| CPR5 | 36 (1.0;1) | 25 (1.0;1) |
| cpr5 | 61 (1.7;1) | 27 (1.1;1) |

B Progenies of *osd1/+ uvi4/+ cpr5*

| Genotype | plants | Genotype | plants | Genotype | plants |
|---|---|---|---|---|---|
| OOUUcc | 23 (1;1) | OOUucc | 35 (1.5;2) | OOuucc | 11 (0.5;1) |
| OoUUcc | 12 (0.5;2) | OoUucc | 18 (0.8;4) | Oouucc | 6 (0.3;2) |
| ooUUcc | 3 (0.1;1) | ooUucc | 7 (0.3;2) | oouucc | 3 (0.1;1) |

C

Col-0 *uvi4* *osd1-2$^{C}$* *cpr5* *cpr5 uvi4* *cpr5 osd1* *cpr5 uvi4 osd1*

D Gamets of *osd1/+ uvi4 cpr5/+*

| Genotype | ♀ (Col) x ♂ | ♀ x ♂ (Col) | ♀ (*uvi4*) x ♂ | ♀ x ♂ (*uvi4*) |
|---|---|---|---|---|
| OuC | 39 (1.0;1) | 50 (1.0;1) | 32 (1.0;1) | 33 (1.0;1) |
| Ouc | 33 (0.8;1) | 40 (0.8;1) | 29 (0.9;1) | 38 (1.2;1) |
| ouC | 47 (1.2;1) | 20 (0.4;1) | 27 (0.8;1) | 15 (0.4;1) |
| ouc | 37 (0.9;1) | 29 (0.6;1) | 32 (1.0;1) | 41 (1.2;1) |

**Figure 3.4 *cpr5* suppressed the *osd1 uvi4* double mutant phenotype.**

Shown are numbers of plants of each genotype in an analyzed population. The two numbers in parentheses are the observed ratios of that genotype relative to the top left genotype (left) and the expected ratios when there is no reduced transmission of the gametes or zygotes (right) separated by a semicolon.

(A) Analysis of gamete transmission inferred from of reciprocal crosses between *CPR5/cpr5* and Col-0. The *cpr5* had a higher transmission rate as male gamete (shaded) but not female gamete. (B) Analysis of progenies from *osd1/OSD1 uvi4/UVI4 cpr5/cpr5*. Notice the presence of *osd1/osd1 uvi4/uvi4 cpr5/cpr5* (shaded) while there was no *osd1/osd1 uvi4/uvi4* in progenies of *osd1/OSD1 UVI4/uvi4* (Figure 3.2A). Also notice that plants with *osd1/OSD1 cpr5/cpr5* genotypes irrespective of the *uvi4* genotypes (darker shaded) were fewer than expected, suggesting a lower transmission of *osd1 cpr5* than *OSD1 cpr5*. (C) Morphology of Col-0, *uvi4*, *osd1-2$^{C}$*, *cpr5*, *cpr5 uvi4*, *cpr5 osd1*and *cpr5 uvi4 osd1* grown for 6 weeks under 12h-light / 12h-dark condition. (D) Analysis of gamete transmission inferred from of reciprocal crosses between *osd1/OSD1 uvi4/uvi4 CPR5/cpr5* and Col-0 or *uvi4*. Notice a lower transmission (20 versus 50 with Col-0 and 15 versus 33 with *uvi4*) of *osd1uvi4CPR5* (shaded) compared to *OSD1uvi4CPR5* as female gametes but an increased transmission rate (29 versus 40 with Col-0 and 41 versus 38 with *uvi4*) of *osd1uvi4cpr5* (darker shaded) compared to that of *osd1uvi4CPR5*.

whether the lethality of *osd1 uvi4* can be rescued by mutations in *CCS52A1* or *CCS52B*, we crossed loss-of-function mutation of *CCS52A1* (SALK_083656) and *CCS52B* (CS854666) respectively with *uvi4/uvi4 osd1/OSD1*. In their F2 progenies, plants with genotypes *osd1/OSD1 uvi4/uvi4 ccs52a1*/*ccs52a1* and *osd1/OSD1 uvi4/uvi4 ccs52b*/*ccs52b* were isolated and their progenies were analyzed. We found that *ccs52a1* mutation can partially suppress the lethality of *osd1uvi4*. From 96 progenies of *osd1/OSD1 uvi4/uvi4 ccs52a1*/*ccs52a1*, two plants were homozygous triple mutants, 41 plants were *OSD1/OSD1 uvi4/uvi4 ccs52a1*/*ccs52a1*, and 53 were *osd1/OSD1 uvi4/uvi4 ccs52a1*/*ccs52a1* (Figure 3.5A, D). These data indicate that the *ccs52a1* mutation partially suppresses lethality of female gametophyte and zygote defects of *uvi4 osd1*.

In progenies of *osd1/OSD1 uvi4/uvi4 ccs52b*/*ccs52b*, 1 out of 58 plants was identified as *osd1/osd1 uvi4/uvi4 ccs52b/ccs52b*, 19 plants were *OSD1/OSD1 ccs52b/ccs52b uvi4/uvi4* and 38 were *osd1/OSD1 uvi4/uvi4 ccs52b/ccs52b* (Figure 3.5B). This is in contrast to the absence of *osd1/osd1 uvi4/uvi4* with wild-type *CCS52B* (Figure 3.2D). The 1:2 ratio of *OSD1/OSD1 uvi4/uvi4 ccs52b/ccs52b* to *osd1/OSD1 uvi4/uvi4 ccs52b/ccs52b* indicates that female gametophyte lethality is completely suppressed by *ccs52b* mutation. To further investigate the function of *CCS52B* in the lethality of *osd1 uvi4*, we analyzed progenies of *osd1/OSD1 uvi4/uvi4 CCS52B/ccs52b*. 2 out of 49 progenies from *osd1/OSD1 uvi4/uvi4 CCS52B/ccs52b* were identified as triple homozygous mutants, one plant was *osd1/osd1 uvi4/uvi4 CCS52B/ccs52b* and one was *osd1/osd1 uvi4/uvi4 CCS52B/CCS52B* (Figure 3.5C, E, F). The unexpected occurrence of *uvi4 osd1* double mutant with wild-type *CCS52B* suggests that either extra mutations exist in *ccs52b* mutant or *uvi4*, *osd1* and *ccs52b* mutations affect megagametogenesis through the

**A** Progenies of *osd1/+ uvi4ccs52a1*

| Genotype | Plants |
|---|---|
| OOuua2a2 | 41(1.0;1) |
| Oouua2a2 | 53(1.3;2) |
| oouua2a2 | 2(0.05;1) |

**B** Progenies of *osd1/+ uvi4ccs52b*

| Genotype | Plants |
|---|---|
| Oouubb | 19(1.0;1) |
| Oouubb | 38(2.0;2) |
| oouubb | 1(0.05;1) |

**C** Progenies of *osd1/+ uvi4ccs52b/+*

| Genotype | Plants | Genotype | Plants | Genotype | Plants |
|---|---|---|---|---|---|
| OOuuBB | 4 (1.0; 1) | OOuuBb | 13(3.25;2) | OOuubb | 2(0.5;1) |
| OouuBB | 7(1.75;2) | OouuBb | 15(3.75;4) | Oouubb | 4(1.0; 2) |
| oouuBB | 1(0.25;1) | oouuBb | 1(0.25;2) | oouubb | 2(0.5;1) |

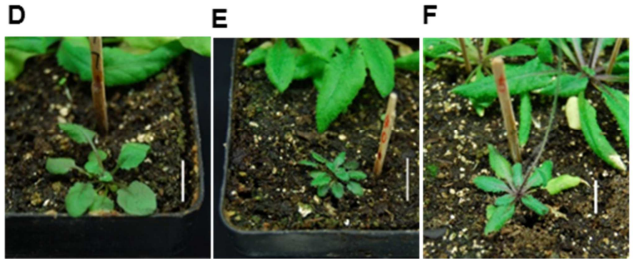


**Figure 3.5 *CCS52A1* and *CCS52B* partially mediate the lethality of *osd1 uvi4*.** (A) Analysis of progenies from *osd1/OSD1 uvi4/uvi4 ccs52a1/ccs52a1*. 2 *osd1/osd1 uvi4/uvi4 ccs52a1/ccs52a1* plants (shaded) were found. (B) Analysis of progenies from *osd1/OSD1 uvi4/uvi4 ccs52b/ccs52b*. One *osd1/osd1 uvi4/uvi4 ccs52b/ccs52b* plant (shaded) was found. (C) Analysis of progenies from *osd1/OSD1 uvi4/uvi4 ccs52b/CCS52B*. 2 *osd1/osd1 uvi4/uvi4 ccs52b/ccs52b* plants (shaded) were found. Notice the presence of one *osd1/osd1 uvi4/uvi4 ccs52b/CCS52B* plant (shaded) and one *osd1/osd1 uvi4/uvi4 CCS52B/CCS52B* (shaded). (D) Morphology of *osd1/osd1 uvi4/uvi4 ccs52a1/ccs52a1*. (E) Morphology of *osd1/osd1 uvi4/uvi4 ccs52b/ccs52b*. (F) Morphology of *osd1/osd1 uvi4/uvi4 CCS52B/CCS52B* isolated from *osd1/OSD1 uvi4/uvi4 ccs52b/CCS52B*.

sporophytic tissue surrounding the female gametophyte. Taken together, the lethality of *uvi4 osd1* was partially dependent on the activities of *CCS52A1* and *CCS52B.*

**Overexpression of *CYCB1;1* potentially partially suppress the lethality of *osd1 uvi4* double mutant.**

Overexpression of *OSD1* and *UVI4* each leads to a significant increase of CYCB1;1, (Iwata et al., 2011; Iwata et al., 2012). To test whether or the female gametophyte lethality of *osd1 uvi4* is due to over-degradation of CYCB1;1. CYCB1;1 fused with GFP at C-terminal were overexpressed by a duplicate 35S promoter in *osd1/OSD1 uvi4/uvi4* (Tzfira et al., 2005), and 15 transgenic lines were isolated. Progenies from three independent lines L3, L34 and L37 were analyzed at T2 stage for *osd1* segregation. One seedling that was an *osd1 uvi4* homozygote containing the *CYCB1;1-GFP* transgene was identified from a pool of 72 plants of L34 (Figure 3.6A). In contrast, no such seedlings were isolated from progenies of *osd1/OSD1 uvi4/uvi4* grown in soil (Figure 3.2D), suggesting that *CYCB1;1* overexpression might have a weak suppression on the lethality of *osd1 uvi4*. However, this seedling was much smaller than *uvi4* or *osd1/OSD1 uvi4/uvi4* mutants containing *CYCB1;1-GFP* (Figure 3.6A). We subsequently analyzed approximately 24 T2 progenies each of 12 other transgenic lines, but did not find any *osd1 uvi4* homozygous seedlings. Segregation ratios between *OSD1/OSD1 uvi4/uvi4* and *osd1/OSD1 uvi4/uvi4* in five representative independent transgenic lines were larger than 1:1 (Figure 3.6B). All these data suggest that overexpression of *CYCB1;1* might occasionally suppress the female gametophyte lethality of *osd1 uvi4*. However, a larger T2 pool of L34 is needed to determine the role of CYCB1;1. Alternatively, a variation of CYCB1;1 that resists the regulation by APC/C at the protein level can be tested.

A


*CYCB1;1-OE/osd1 uvi4*

B Progenies of *osd1/+ uvi4 with 35S::CYCB1;1:GFP*

| Genotypes | Plants in different transgenic lines | | | | |
|---|---|---|---|---|---|
| | L3 | L34 | L37 | L53 | L8 |
| OOuu | 39 | 46 | 31 | 15 | 16 |
| Oouu | 32 | 25 | 25 | 9 | 8 |
| oouu | 0 | 1 | 0 | 0 | 0 |

**Figure 3.6 Overexpression of *CYCB1;1* potentially partially suppresses the lethality of *osd1 uvi4*.** (A) Morphology of *35S::CYCB1;1:GFP* transgenic plants in *osd1/OSD1 uvi4/uvi4* (1), *uvi4* (2) and *osd1 uvi4* (3). (B) Analysis of progenies from *osd1/OSD1 uvi4/uvi4* containing *35S::CYCB1;1:GFP*. Notice the presence of one *osd1/osd1 uvi4/uvi4 plants* (shaded) in line 34 (L34) while there was no *osd1/osd1 uvi4/uvi4* plant in progenies of other lines (L37, L53, L3 and L8).

### *CYCB1;1* expression is altered in *cpr5* and *UVI4* and *OSD1* overexpression lines

Endoreduplication is inhibited by overexpression of *UVI4* and *OSD1* as well as loss of *CPR5* function. We investigated whether progression of cell cycle is similarly altered in *osd1-4* (overexpression allele) and *cpr5* by analyzing cyclins specific to different phases of the cell cycle. These include G1-phase *AtCYCD3;3*, S-phase histone *H3.1*, G2-phase *AtCYCA2;1* and G2 to M transition *AtCYCB1;1* (Zhu et al., 2011). Only *AtCYCB1;1* was found to have altered expression in these plants compared to wild-type Ws and Col-0 using semi-quantitative PCR (Figure 3.7A). The alteration in these genotypes was confirmed with quantitative real-time RT-PCR (Figure 3.7B). The *CYCB1;1* expression had a three-fold increase in *cpr5*, and a slight increase in *osd1-4* compared to the wild type. This suggests that there is a delay in G2 to M transition in the *cpr5* and *osd1-4*. Therefore, *cpr5* and *osd1-4* likely affects cell cycle genes at the transcript level directly or indirectly.

To determine whether elevated *CYCB1;1* expression results in the phenotype of *cpr5* , we introduced *cycb1;1* loss of function mutation into *cpr5*. The *cpr5 cycb1;1* plant exhibited the same morphology as *cpr5*, and did not have alternation of $H_2O_2$ accumulation compared to *cpr5* by DAB staining (Figure 3.7C, D). This is in contrast to early observation that *cycb1;1* suppressed dwarf morphology and defense responses of *osd1-4*$^{C}$ (Bao et al., 2013). These data suggest *CPR5* may have more downstream targets besides *CYCB1;1* in the regulation of cell cycle progression and disease responses.

### The *krp6* mutation enhances *cpr5* phenotype and does not suppress the lethality of *osd1 uvi4*

To further understand how *cpr5* affected cell cycle progression, we analyzed transcription profile of *cpr5* by RNA-seq technology (Campbell et al., 2002) and found that 403 genes

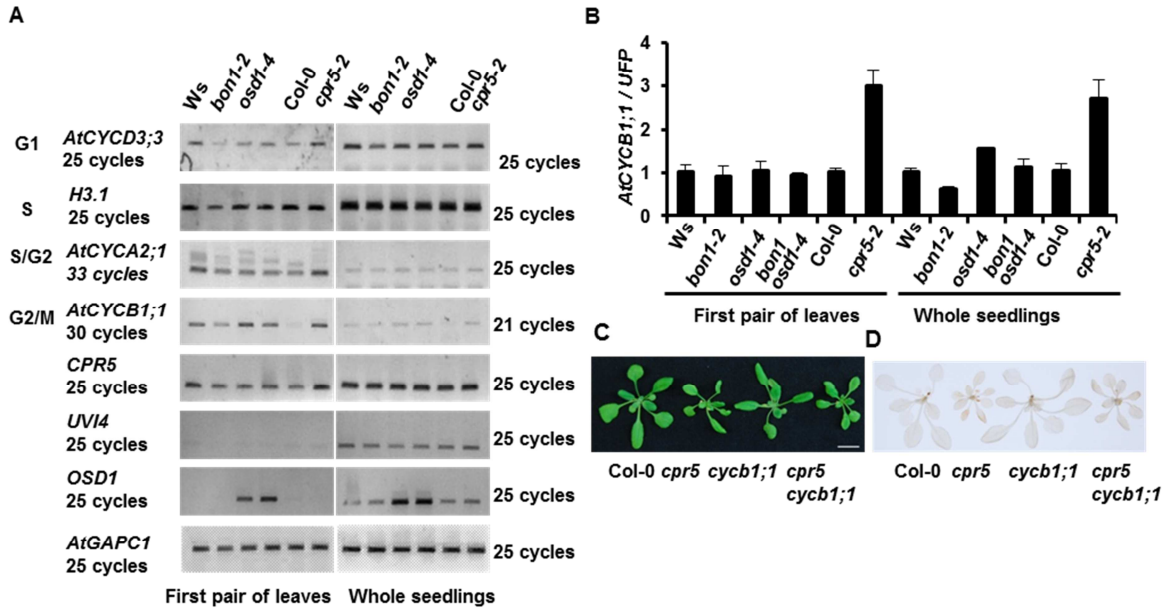


**Figure 3.7 Expression of cell cycle genes, *CPR5*, *UVI4* and *OSD1* in *bon1 osd1-4* and *cpr5* mutants.** (A) Analysis of cell cycle marker genes, *CPR5*, *UVI4*, and *OSD1* in the first pair of leaves and the whole seedlings by RT-PCR. *AtGAPC1* was used as a control. (B) Expression levels of *AtCYCB1;1* analyzed by quantitative real time RT-PCR. (C) Morphology of Col-0, *cpr5*, *cycb1;1* and *cpr5 cycb1;1*. (D) $H_2O_2$ accumulation in the above genotypes analyzed by DAB staining.

exhibited differential expression. Further analysis of these genes in Mapman software (http://mapman.gabipd.org) indicates that 159 genes might be involved in biotic stress (Figure 3.8). Four genes were annotated as being involved in female gametophyte development. Among these, cyclin dependent kinase inhibitor, *Kip-related protein 6* (*KRP6*, At3g19150) had a significant increase in *cpr5* compared to Col-0. As over-accumulation of KRP6 had defects on both male and female gametogenesis (Kim et al., 2008; Liu et al., 2008), we tested the genetic interaction between *krp6* and *cpr5*. *cpr5* mutant did not exhibit any defects on gametophyte development but rather increased the male gamete transmission (Figure 3.4A). The loss of function mutant of *KRP6* was crossed into *cpr5* and the *krp6 cpr5* double mutant was isolated. The *krp6* mutant did not exhibit any morphological defects compared to wild-type Col-0, but *cpr5 krp6* double mutant was even smaller than *cpr5* and had a darker DAB staining than *cpr5* (Figure 3.9A, B). Therefore, *cpr5* and *krp6* had additive effects.

The interaction between CDKA;1 and KRP6 suggests that *KRP6* may inhibit activities of CDK-cyclin complex (De Veylder et al., 2001). Overexpression of *KRP6* leads to defects in both male and female gametogenesis (Liu et al., 2008). To determine whether *krp6* mutation affects the lethality of *osd1 uvi4*, we introduced *krp6* mutation into *osd1 uvi4*. In F2 progenies, *osd1/OSD1 uvi4/uvi4 krp6/krp6* was isolated for further genetic analysis. 57 out of 108 plants in F3 progenies was *OSD1/OSD1 uvi4/uvi4 krp6/krp6*, 51 plants were *osd1/OSD1 uvi4/uvi4 krp6/krp6* and none of *osd1/osd1uvi4/uvi4 krp6/krp6* was isolated (Figure 3.9C). Approximate 1:1 ratio between *OSD1/OSD1 uvi4/uvi4 krp6/krp6* and *osd1/OSD1 uvi4/uvi4 krp6/krp6* suggest that *KRP6* is not required for the lethality of *osd1 uvi4*.

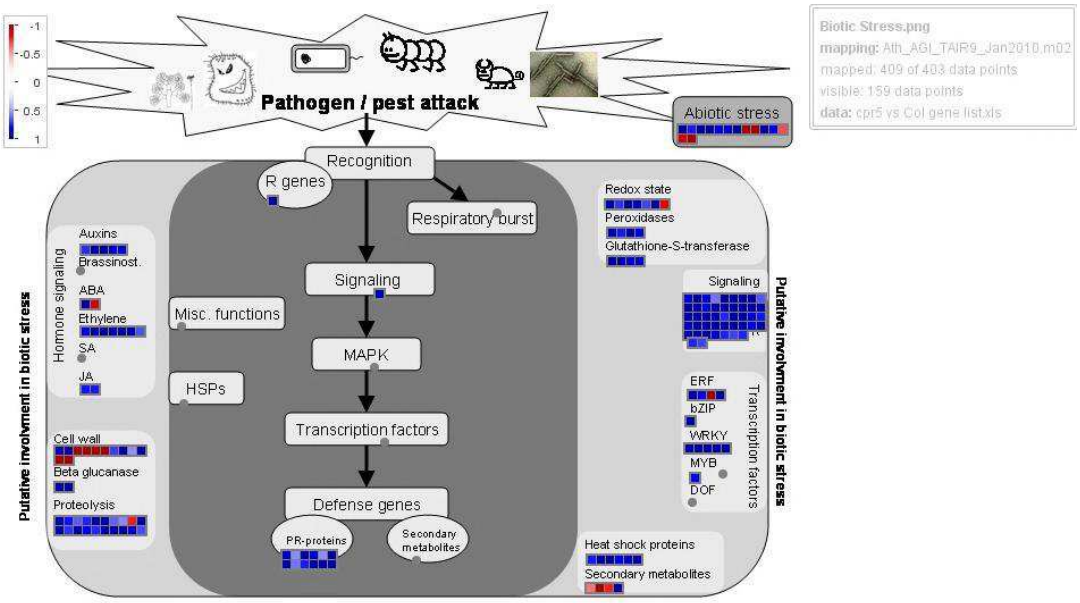


**Figure 3.8 Transcriptome analyses of Col-0 and *cpr5-2* by RNA-Seq.** The Col-0 and *cpr5-2* plants were grown under 14-hr day length at 22°C for three weeks. Total RNAs were extracted from the above-ground tissues following the procedure of Trizol Reagent (Invitrogen). The programs Tophat 2.0 and Cuffdiff were used to align RNA-Seq reads to Arabidopsis reference genome TAIR10 and identify differentially expressed genes in *cpr5-2*. The significant expression change was determined by $p < 0.05$ after Benjamini-Hochberg correction for multiple-testing. Differentially expressed genes in *cpr5-2* compared to the wild-type Col-0 were analyzed by Mapman software. In *cpr5-2*, 159 of the 403 differentially expressed genes are associated with biotic stress. All of data were collected from two biological repeats.

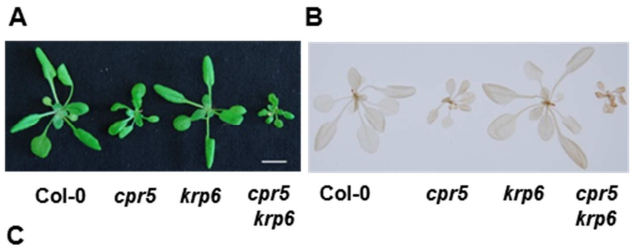


C

| Genotypes | Plants |
|---|---|
| OOuukk | 57 |
| Oouukk | 51 |
| oouukk | 0 |

**Figure 3.9 *KRP6* does not mediate the *cpr5* phenotype or the lethality of *osd1 uvi4*.** (A) Morphology of Col-0, *cpr5*, *krp6* and *cpr5 krp6*. (B) $H_2O_2$ accumulation in the above genotypes analyzed by DAB staining. (C) Analysis of progenies from *osd1/OSD1 uvi4/uvi4 krp6/krp6*. No *osd1/osd1 uvi4/uvi4 krp6/krp6* plants (shaded) were found.

**Discussion**

*OSD1* and *UVI4* are negative regulators of APC/C that is responsible for degrading cell cycle proteins. The loss of function of *OSD1* and *UVI4* leads to various defects in cell cycle progression including omission of meiotic divisions, increased endoreduplication and possibly endomitosis, and female gametophyte lethality of the double mutant. Overexpression of either *OSD1* or *UVI4* leads to reduced endoreduplication (this study), spontaneous cell death and enhanced disease resistance to a bacterial pathogen (Bao et al., 2013).

In this study, we investigated whether and which of the APC activators, *CCS52A1* and *CCS52B*, mediates the gametophyte defects in *osd1 uvi4*. An earlier study shows that *CCS52A1* mediates the *UVI4* function, and the loss of *ccs52a1* mutation is epistatic to *uvi4* in endoreduplication (Heyman et al., 2011). The loss of function of *CCS52A2* resulted in severe defects in both shoot and root apical meristems (Lammens et al., 2008; Vanstraelen et al., 2009; Liu et al., 2012), which prevented us from analyzing *CCS52A2* interaction with *uvi4* and *osd1*. We show here that loss of function of *CCS52A1* and *CCS52B* each partially rescued the lethality of *osd1 uvi4* (Figure 3.5), indicating that *OSD1* and *UVI4* function through *CCS52* genes in female gametophyte development and zygote development. The *ccs52b* mutation completely suppressed the lethality of *osd1 uvi4* female gametophytes.

Intriguingly, some *osd1 uvi4* double mutant plants without the *ccs52b* mutation were isolated from progenies of *osd1/OSD1 uvi4/uvi4 ccs52b/CCS52B.* These *osd1 uvi4* plants grew better than their sibling *osd1 uvi4 ccs52b* plants (Figure 3.5E, F). One explanation for this phenomenon is that the *ccs52b* mutant that we used contains another mutation that suppresses the female gametophyte lethality of *osd1 uvi4*. Another possibility is that the female gametophyte lethality of *osd1 uvi4* is due to defects in the sporophytic tissue surrounding the female

gametophyte that has been shown to play important roles in megagametogenesis (Yadegari and Drews, 2004). The use of another loss of function *ccs52b* allele will resolve this issue. Overall, defects on cell cycle progression in *uvi4* and *osd1* might be largely due to the activation of APC/C.

The similarity of *UVI4* and *OSD1* overexpression phenotype with that of the loss of function mutant *cpr5* promoted us to investigate their potential interaction. Genetic data provided here demonstrate that *CPR5* has a direct function in cell cycle regulation and *OSD1*/*UVI4* and *CPR5* genes function antagonistically to regulate endoreduplication, female gametophyte formation and zygote development. The *cpr5* mutation suppressed multiple defects in *uvi4* and *osd1* single and double mutants, including the endoreduplication phenotype of *uvi4*, embryo lethality of *osd1/osd1 uvi4/uvi4* double mutants, and the low viability of *osd1 uvi4* female gametophytes.

*CPR5* might act downstream of *OSD1* and *UVI4* or in parallel with *CCS52A1* and *CCS52B* to affect cell cycle progression. *UVI4* was shown to regulates the abundance of cyclin *CYCA2;3* protein likely through *CCS52A1* (Heyman et al., 2011) and overexpression of *OSD1*/*GIG1* increased the protein level of cyclin *CYCB1;2* and *CYCB1;1* (Iwata et al., 2011; Iwata et al., 2012). This indicates that cell cycle defects, likely through cyclin level change, in *uvi4* and *osd1* are compensated by the *cpr5* defect.

Opposite endoreduplication defects in *uvi4* and *osd1* versus in *cpr5* suggest alterations at G2/M during the mitotic cell cycle progression. The expression of *CYCB1;1* is tightly associated with the mitotic cell division, and had a peak expression at G2 /M (Colon-Carmona et al., 1999; Schnittger et al., 2002). *OSD1* overexpression phenotype was largely suppressed by loss of *CYCB1;1* function (Bao et al., 2013). Overexpression of *CYCB1;1* might have a weak

suppression effect on the lethality of *osd1 uvi4*, which needs to be further studied (Figure 3.6) . Moreover, *CYCB1;1* expression was dramatically increased in *cpr5* mutant, suggesting that *cpr5* mutation leads to a promoted CDK-CYCB1;1 complex activity which may explain the reduced endoreduplication and increased male transmission of *cpr5*. However, no suppression of the *cpr5* defects were observed for the loss of *cycb1;1* (Figure 3.7C, D). This indicates that *CYCB1;1* might not play a major role in *CPR5* function. All these data suggest that genetic interactions among *OSD1*, *UVI4* and *CPR5* in the regulation of cell cycle progression may be due to the alteration of CDK-cyclin complex activities.

Another candidate cell cycle gene subject to *CPR5* regulation is *KRP6*. Transcriptome analysis revealed that a cyclin dependent kinase inhibitor, *KRP6* had elevated expression in *cpr5*. *KRP6* has an essential function in meiosis and thus the formation of gametophytes (Kim et al., 2008; Liu et al., 2008). We found that *krp6* mutation enhanced *cpr5* phenotype, and did not suppress the lethality of *osd1 uvi4* (Figure 3.9). All these data suggest that elevated expression of *KRP6* might result from a compensatory mechanism by perturbed cell cycle progression in *cpr5*. There are 7 KRPs in Arabidopsis and they all interact with CDKA;1 except KRP5 in vitro despite low sequence similarity with each other (De Veylder et al., 2001; Verkest et al., 2005). The reduction of another *KRP* in *cpr5* might trigger the activation of *KRP6* to compensate the function, and knocking out *KRP6* exacerbates the *cpr5* defects. This hypothesis can be tested by further overexpression of *KRP6* or other *KRP* genes in *cpr5*.

In conclusion, we propose a working model to explain *UVI4* and *OSD1*-mediated cell cycle progression and female gametophyte development (Figure 3.10). In *uvi4* and *osd1* loss of function mutants, the inhibition on APC/C activator *CCS52* genes is relieved. The over-activation of APC/C leads to over-degradation of cyclins and thus low activities of CDK-cyclin

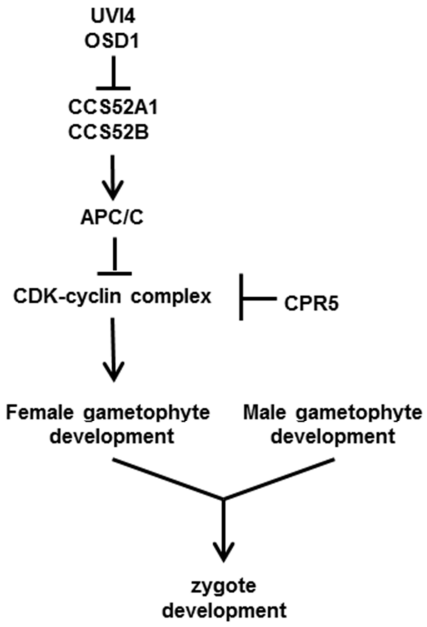


**Figure 3.10 A working model of the *OSD1, UVI4* and *CPR5* gene function in the regulation of cell cycle progression.** *UVI4* and *OSD1* negatively regulate APC/C activities through the interaction with *CCS52A1* and *CCS52B*. Without *OSD1* and *UVI4*, the activated APC/C mediates more degradation of cyclins and results in the reduction of activities of CDK-cyclin complex which consequently affect the female gametophyte development. *cpr5* mutation triggers up-regulation of *CYCB1;1* and enhanced activities of CDK-cyclin complex might largely compensate the loss from the degradation by APC/C resulting in normal female gametophyte development.

complex which consequently triggers endoreduplication and arrests female gametophyte development. The *cpr5* mutation enhances activities of CDK-cyclin complex by upregulating *CYCB1;1* RNA expression and therefore compensates the low activity of APC/C in *osd1* or *uvi4* mutants. Therefore, genetic interactions among *OSD1*, *UVI4* and *CPR5* in the regulation of cell cycle progression indicate fine regulation of CDK-cyclin complex.

## Materials and Methods

### Plant materials, growth and transformation

Seeds of SALK_083656, CS854666, SALK_001978 and CS874737 were obtained from Arabidopsis Biological Research Center (ABRC). Plant growth and transformation were performed as previously described (Yang and Hua, 2004; Yang et al., 2006; Zhu et al., 2010).

### Plasmid construction

The coding region of *CYCB1;1* gene was amplified and cloned first into pDONR222 and then moved into pSAT6-DEST-EGFP-N1 vector (Tzfira et al., 2005) .

### Ploidy measurement

The first and second true leaves from two plants of 4 to 6-week old were collected and chopped in "Aru" buffer containing 97.5% $MgSO_4$ (0.246% $MgSO_4 \cdot 7H_2O$, 0.37% KCl and 0.12% Hepes), 0.1% DTT and 2.5% Triton X-100 (Arumuganathan and Earle, 1991). 10 µl of PI (propidium iodide) stock solution (5 mg/ml) and 5 µl RNase stock solution (10 mg/ml) were added into each sample of approximately 600 µl. Beckman-Coulter Epics XL-MCL flow cytometer was used to measure ploidy with rice and maize leaf samples as controls. Three replicas were analyzed for each sample.

**Confocal microscopy**

The development of ovules was analyzed by using Leica TCS SP2 confocal microscope according to protocols previously described (Christensen, 1997; Shi et al., 2005).

**Acknowledgements**

We thank Arabidopsis Biological Resource Center for DNA clones, Cold Spring Harbor Laboratory for the *osd1-2* (GT21481) mutant, Dr. Jean-Marc Bonneville for the *pym* seeds and Dr. Atsushi Tanaka for the *uvi4* seeds. We thank Dr. Shiyan Chen for help on the qRT-PCR analysis and Dr. Shuhua Yang for participation of T-DNA tagging of *bon1-2*. This work was supported by NSF grants IOS-0642289 and IOS-0919914 to J. H.

## Reference


**Arumuganathan, K., and Earle, E.D.** (1991). Estimation of nuclear DNA content of plants by flow cytometry. Plant Molecular Biology Reporter **9,** 229-233.

**Bao, Z., Yang, H., and Hua, J.** (2013). Perturbation of cell cycle regulation triggers plant immune response via activation of disease resistance genes. Proceedings of the National Academy of Sciences of the United States of America **110,** 2407-2412.

**Boch, J., Verbsky, M.L., Robertson, T.L., Larkin, J.C., and Kunkel, B.N.** (1998). Analysis of resistance gene-mediated defense responses in Arabidopsis thaliana plants carrying a mutation in CPR5. Mol Plant Microbe In **11,** 1196-1206.

**Borghi, M., Rus, A., and Salt, D.E.** (2011). Loss-of-function of Constitutive Expresser of Pathogenesis Related Genes5 affects potassium homeostasis in Arabidopsis thaliana. PLoS One **6,** e26360.

**Bowling, S.A., Clarke, J.D., Liu, Y., Klessig, D.F., and Dong, X.** (1997). The cpr5 mutant of Arabidopsis expresses both NPR1-dependent and NPR1-independent resistance. Plant Cell **9,** 1573-1584.

**Breuer, C., Ishida, T., and Sugimoto, K.** (2010). Developmental control of endocycles and cell growth in plants. Curr Opin Plant Biol **13,** 654-660.

**Brininstool, G., Kasili, R., Simmons, L.A., Kirik, V., Hulskamp, M., and Larkin, J.C.** (2008). Constitutive Expressor Of Pathogenesis-related Genes5 affects cell wall biogenesis and trichome development. BMC Plant Biol **8,** 58.

**Campbell, M.A., Fitzgerald, H.A., and Ronald, P.C.** (2002). Engineering pathogen resistance in crop plants. Transgenic research **11,** 599-613.

**Chevalier, C., Nafati, M., Mathieu-Rivet, E., Bourdon, M., Frangne, N., Cheniclet, C., Renaudin, J.P., Gevaudant, F., and Hernould, M.** (2011). Elucidating the functional role of endoreduplication in tomato fruit development. Ann Bot **107,** 1159-1169.

**Christensen, C.A.** (1997). Megagametogenesis in Arabidopsis wild type and the *Gf* mutant. Sex Plant Reprod **10,** 49–64

**Colon-Carmona, A., You, R., Haimovitch-Gal, T., and Doerner, P.** (1999). Technical advance: spatio-temporal analysis of mitotic activity with a labile cyclin-GUS fusion protein. Plant J **20,** 503-508.

**d'Erfurth, I., Jolivet, S., Froger, N., Catrice, O., Novatchkova, M., and Mercier, R.** (2009). Turning meiosis into mitosis. PLoS biology **7,** e1000124.

**d'Erfurth, I., Cromer, L., Jolivet, S., Girard, C., Horlow, C., Sun, Y., To, J.P., Berchowitz, L.E., Copenhaver, G.P., and Mercier, R.** (2010). The cyclin-A CYCA1;2/TAM is required for the meiosis I to meiosis II transition and cooperates with OSD1 for the prophase to first meiotic division transition. PLoS Genet **6,** e1000989.

**De Veylder, L., Larkin, J.C., and Schnittger, A.** (2011). Molecular control and function of endoreplication in development and physiology. Trends in plant science **16,** 624-634.

**De Veylder, L., Beeckman, T., Beemster, G.T., Krols, L., Terras, F., Landrieu, I., van der Schueren, E., Maes, S., Naudts, M., and Inze, D.** (2001). Functional analysis of cyclin-dependent kinase inhibitors of Arabidopsis. The Plant cell **13,** 1653-1668.

**Drews, G.N., and Yadegari, R.** (2002). Development and function of the angiosperm female gametophyte. Annu Rev Genet **36,** 99-124.

**Gao, G., Zhang, S., Wang, C., Yang, X., Wang, Y., Su, X., Du, J., and Yang, C.** (2011). Arabidopsis CPR5 independently regulates seed germination and postgermination arrest of development through LOX pathway and ABA signaling. PLoS One **6,** e19406.

**Hase, Y., Trung, K.H., Matsunaga, T., and Tanaka, A.** (2006). A mutation in the uvi4 gene promotes progression of endo-reduplication and confers increased tolerance towards ultraviolet B light. Plant J **46,** 317-326.

**Heyman, J., Van den Daele, H., De Wit, K., Boudolf, V., Berckmans, B., Verkest, A., Kamei, C.L., De Jaeger, G., Koncz, C., and De Veylder, L.** (2011). Arabidopsis ULTRAVIOLET-B-INSENSITIVE4 Maintains Cell Division Activity by Temporal Inhibition of the Anaphase-Promoting Complex/Cyclosome. The Plant cell.

**Inagaki, S., and Umeda, M.** (2011). Cell-cycle control and plant development. International review of cell and molecular biology **291,** 227-261.

**Inze, D., and De Veylder, L.** (2006). Cell cycle regulation in plant development. Annual review of genetics **40,** 77-105.

**Iwata, E., Ikeda, S., Matsunaga, S., Kurata, M., Yoshioka, Y., Criqui, M.C., Genschik, P., and Ito, M.** (2011). GIGAS CELL1, a Novel Negative Regulator of the Anaphase-Promoting Complex/Cyclosome, Is Required for Proper Mitotic Progression and Cell Fate Determination in Arabidopsis. The Plant cell.

**Iwata, E., Ikeda, S., Abe, N., Kobayashi, A., Kurata, M., Matsunaga, S., Yoshioka, Y., Criqui, M.C., Genschik, P., and Ito, M.** (2012). Roles of GIG1 and UVI4 in genome duplication in Arabidopsis thaliana. Plant signaling & behavior **7,** 1079-1081.

**Joubes, J., and Chevalier, C.** (2000). Endoreduplication in higher plants. Plant Mol Biol **43,** 735-745.

**Kasili, R., Walker, J.D., Simmons, L.A., Zhou, J., De Veylder, L., and Larkin, J.C.** (2010). SIAMESE cooperates with the CDH1-like protein CCS52A1 to establish endoreplication in Arabidopsis thaliana trichomes. Genetics **185,** 257-268.

**Kim, H.J., Oh, S.A., Brownfield, L., Hong, S.H., Ryu, H., Hwang, I., Twell, D., and Nam, H.G.** (2008). Control of plant germline proliferation by SCF(FBL17) degradation of cell cycle inhibitors. Nature **455,** 1134-1137.

**Kirik, V., Bouyer, D., Schobinger, U., Bechtold, N., Herzog, M., Bonneville, J.M., and Hulskamp, M.** (2001). CPR5 is involved in cell proliferation and cell death control and encodes a novel transmembrane protein. Curr Biol **11,** 1891-1895.

**Lammens, T., Boudolf, V., Kheibarshekan, L., Zalmas, L.P., Gaamouche, T., Maes, S., Vanstraelen, M., Kondorosi, E., La Thangue, N.B., Govaerts, W., Inze, D., and De Veylder, L.** (2008). Atypical E2F activity restrains APC/CCCS52A2 function obligatory for endocycle onset. Proceedings of the National Academy of Sciences of the United States of America **105,** 14721-14726.

**Larson-Rabin, Z., Li, Z., Masson, P.H., and Day, C.D.** (2009). FZR2/CCS52A1 expression is a determinant of endoreduplication and cell expansion in Arabidopsis. Plant physiology **149,** 874-884.

**Liu, J., Zhang, Y., Qin, G., Tsuge, T., Sakaguchi, N., Luo, G., Sun, K., Shi, D., Aki, S., Zheng, N., Aoyama, T., Oka, A., Yang, W., Umeda, M., Xie, Q., Gu, H., and Qu, L.J.** (2008). Targeted degradation of the cyclin-dependent kinase inhibitor ICK4/KRP6 by

RING-type E3 ligases is essential for mitotic cell cycle progression during Arabidopsis gametogenesis. The Plant cell **20,** 1538-1554.

**Liu, Y., Ye, W., Li, B., Zhou, X., Cui, Y., Running, M.P., and Liu, K.** (2012). CCS52A2/FZR1, a cell cycle regulator, is an essential factor for shoot apical meristem maintenance in Arabidopsis thaliana. BMC Plant Biol **12,** 135.

**Marrocco, K., Bergdoll, M., Achard, P., Criqui, M.C., and Genschik, P.** (2010). Selective proteolysis sets the tempo of the cell cycle. Curr Opin Plant Biol **13,** 631-639.

**Perazza, D., Herzog, M., Hulskamp, M., Brown, S., Dorne, A.M., and Bonneville, J.M.** (1999). Trichome cell growth in Arabidopsis thaliana can be derepressed by mutations in at least five genes. Genetics **152,** 461-476.

**Perazza, D., Laporte, F., Balague, C., Chevalier, F., Remo, S., Bourge, M., Larkin, J., Herzog, M., and Vachon, G.** (2011). GeBP/GPL transcription factors regulate a subset of CPR5-dependent processes. Plant physiology **157,** 1232-1242.

**Peters, J.M.** (2006). The anaphase promoting complex/cyclosome: a machine designed to destroy. Nat Rev Mol Cell Biol **7,** 644-656.

**Schnittger, A., Schobinger, U., Stierhof, Y.D., and Hulskamp, M.** (2002). Ectopic B-type cyclin expression induces mitotic cycles in endoreduplicating Arabidopsis trichomes. Curr Biol **12,** 415-420.

**Shi, D.Q., Liu, J., Xiang, Y.H., Ye, D., Sundaresan, V., and Yang, W.C.** (2005). SLOW WALKER1, essential for gametogenesis in Arabidopsis, encodes a WD40 protein involved in 18S ribosomal RNA biogenesis. The Plant cell **17,** 2340-2354.

**Stevens, C., and La Thangue, N.B.** (2004). The emerging role of E2F-1 in the DNA damage response and checkpoint control. DNA Repair (Amst) **3,** 1071-1079.

**Twell, D.** (2011). Male gametogenesis and germline specification in flowering plants. Sexual Plant Reproduction **24,** 149-160.

**Tzfira, T., Tian, G.W., Lacroix, B., Vyas, S., Li, J., Leitner-Dagan, Y., Krichevsky, A., Taylor, T., Vainstein, A., and Citovsky, V.** (2005). pSAT vectors: a modular series of plasmids for autofluorescent protein tagging and expression of multiple genes in plants. Plant molecular biology **57,** 503-516.

**Van Leene, J., Hollunder, J., Eeckhout, D., Persiau, G., Van De Slijke, E., Stals, H., Van Isterdael, G., Verkest, A., Neirynck, S., Buffel, Y., De Bodt, S., Maere, S., Laukens, K., Pharazyn, A., Ferreira, P.C., Eloy, N., Renne, C., Meyer, C., Faure, J.D., Steinbrenner, J., Beynon, J., Larkin, J.C., Van de Peer, Y., Hilson, P., Kuiper, M., De Veylder, L., Van Onckelen, H., Inze, D., Witters, E., and De Jaeger, G.** (2010). Targeted interactomics reveals a complex core cell cycle machinery in Arabidopsis thaliana. Molecular systems biology **6,** 397.

**Vanstraelen, M., Baloban, M., Da Ines, O., Cultrone, A., Lammens, T., Boudolf, V., Brown, S.C., De Veylder, L., Mergaert, P., and Kondorosi, E.** (2009). APC/C-CCS52A complexes control meristem maintenance in the Arabidopsis root. Proceedings of the National Academy of Sciences of the United States of America **106,** 11806-11811.

**Verkest, A., Weinl, C., Inze, D., De Veylder, L., and Schnittger, A.** (2005). Switching the cell cycle. Kip-related proteins in plant cell cycle control. Plant physiology **139,** 1099-1106.

**Yadegari, R., and Drews, G.N.** (2004). Female gametophyte development. The Plant cell **16 Suppl,** S133-141.

**Yang, H., Li, Y., and Hua, J.** (2006). The C2 domain protein BAP1 negatively regulates defense responses in Arabidopsis. Plant J **48,** 238-248.

**Yang, S., and Hua, J.** (2004). A haplotype-specific Resistance gene regulated by BONZAI1 mediates temperature-dependent growth control in Arabidopsis. The Plant cell **16,** 1060-1071.

**Yoshida, S., Ito, M., Nishida, I., and Watanabe, A.** (2002). Identification of a novel gene HYS1/CPR5 that has a repressive role in the induction of leaf senescence and pathogen-defence responses in Arabidopsis thaliana. Plant J **29,** 427-437.

**Zhu, Y., Qian, W., and Hua, J.** (2010). Temperature modulates plant defense responses through NB-LRR proteins. PLoS Pathog **6,** e1000844.

**Zhu, Y., Weng, M., Yang, Y., Zhang, C., Li, Z., Shen, W.H., and Dong, A.** (2011). Arabidopsis homologues of the histone chaperone ASF1 are crucial for chromatin replication and cell proliferation in plant development. Plant J **66,** 443-455.

# CHAPTER 4

## *MOS1* modulates defense responses, floral transition and cell cycle progression via *SNC1*, *FLC* and *CYCD3;1*, respectively

This chapter is prepared as a manuscript for publication.


### Abstract

Accurate and appropriate cell cycle progression is critical for plant growth and development, floral transition and even plant immune responses to pathogens. During the course of studying the negative regulation of plant immunity by *BON1*, we identified a suppressor of *bon1-1* (*sbo3*) as a mutant allele of the *MOS1* (*MODIFIER OF snc1*, *1*) gene. We found that *MOS1* regulates not only plant defense responses but also flowering time and endoreduplication. The change in expression of *SNC1*, *FLC*, *CYCD3;1* is likely responsible for the defense inhibition, late flowering and enhanced endoreduplication in *mos1* respectively. Furthermore, the late flowering and enhanced endoreduplication phenotypes in *mos1* are dependent on *SUF4*, a positive regulator of *FLC*. Interestingly, the MOS1 protein interacts with SUF4 and MAD2, a component in the spindle check point complex. The interaction of MOS1 and MAD2 with SUF4 may inhibit the function of SUF4 to promote flowering and inhibit endoreduplication. MOS1 function is antagonized by another spindle check point component MAD1 that also interacts with SUF4 and MAD2. Together, these findings reveal that MOS1 functions through repressing SUF4 to regulate flowering time and endocycle and suggest an involvement of cell cycle control in flowering time regulation.

## Introduction

Plants have a complex network to sense endogenous signals and environmental cues in order to catch the proper flowering time which is critical for the reproduction of plants. In the past decades, four major pathways to control floral transition were identified: photoperiod pathways, autonomous pathway, vernalization pathway and gibberellin (GA) pathway (Kim et al., 2009). Both the autonomous and vernalization pathways regulate the flowering time through repressive regulation of *FLC* expression (Kim et al., 2009; Crevillen and Dean, 2011). *FRIGIDA* (*FRI*) activates *FLC* expression, and this interaction differentiates early and late flowering accessions of Arabidopsis (Clarke and Dean, 1994; Shindo et al., 2005). *FLC* is a central regulator of flowering time and it behaves as a strong repressor of floral transition in both the autonomous pathway and the vernalization pathway (Michaels and Amasino, 1999). FRI interacts with FRIGIDA LIKE1 (FRL1), FRIGIDA ESSENTIAL1 (FES1), SUF4 (Suppressor of FRIGIDA 4) and FLC EXPRESSOR (FLX) to form a transcription activator complex to regulate *FLC* expression (Choi et al., 2011). SUF4, a C2H2-type zinc-finger protein, acts as a transcriptional activator by binding to a cis-element of *FLC* promoter to stimulate *FLC* expression (Kim et al., 2006; Choi et al., 2011). *FRI* and *SUF4* are not required for the reactivation of *FLC* expression in early embryos, but are required for the maintenance of *FLC* expression at late embryogenesis stage (Kim et al., 2009). SUF4 recruits EARLY FLOWERING IN SHORT DAYS (EFS) and PAF1 (RNA polymerase II associated factor 1)-like complex to the *FLC* locus and induces histone H3 lysine 4 (H3K4) trimethylation at *FLC* to activate *FLC* expression (Kim and Michaels, 2006).

In yeast and animal cells, spindle assembly checkpoint (SAC) acts as a safeguard to ensure the accurate progression of mitosis and meiosis. SAC proteins include Mitotic Arrest

Deficient (MAD) 1, 2 and 3 and Budding Unperturbed by Benzimidazole (Bub) 1, 2 and 3 (Li and Murray, 1991). MAD1 is localized predominantly at unattached kinetochore and recruits MAD2 to form a MAD1-MAD2 complex. MAD2 has two distinct conformations, open and closed. Closed MAD2 is bound to MAD1 and serves as a template for the conversion of the open form into the closed form (De Antoni et al., 2005). Closed MAD2 binds to CDC20 and the formation of MAD2-CDC20 complex promotes the binding of BUB3 and MAD3 to form mitotic checkpoint complex (MCC) (Kulukian et al., 2009; Kim et al., 2012). *CDC20/Fizzy* is one type of activator of APC/C (Anaphase promoting complex /cyclosome) which is a multiunit ubiquitin E3 ligase that targets cyclins for degradation. Another type of activators of APC/C is *CCS52/CDH1/Fizzy-related* (*FZR*). Homologs of SAC components and APC/C activators are identified in Arabidopsis. The Arabidopsis *MAD2* is reported to regulate the root elongation and the growth of root meristem (Gudmundsdottir and Ashworth, 2004). Arabidopsis contains five *CDC20* homologs (*CDC20.1*-*CDC20.5*) and three *CCS52* homologs (*CCS52A1*, *CCS52A2* and *CCS52B*). Two *CDC20* homologs, *CDC20.1* and *CDC20.2* have functions in the regulation of plant male fertility and meristem size and interact with one APC/C subunit *APC10* (Kevei et al., 2011). Two negative regulators of APC/C have been identified in Arabidopsis. These two proteins, UV-B-insensitive 4 (UVI4) and *Omission of Second Division 1* (OSD1) interact with APC/C activators to inhibit APC/C activity (Heyman et al., 2011; Iwata et al., 2011).

Interestingly, these cell cycle regulators are found to influence plant defense responses against pathogens. The loss of *UVI4* and *OSD1* led to a weak activation of defense responses (Bao et al., 2013). Overexpression of *UVI4* and *OSD1* triggered enhanced disease resistance, which is due to upregulation of a mitotic cyclin *CYCB1;1* and subsequently an upregulation of resistance (*R*) genes, including *SNC1* (Bao et al., 2013) .

The plant immune system has at least two branches of defense namely PTI (pattern-triggered immunity) and ETI (effector-triggered immunity) in response to general microbe associated molecular pattern (MAMP) and specific effectors respectively. ETI is usually associated with elevated reactive oxygen species (ROS) production, programed cell death and activation of defense related genes such as pathogenesis-related (*PR*) genes. ETI is mediated by R genes (Jones and Dangl, 2006; Vlot et al., 2009; Dodds and Rathjen, 2010) with the major group of *R* genes encoding nucleotide binding site (NBS) - leucine-rich repeat (LRR) proteins.

Defense responses need to be repressed when there is no pathogen infection, as constitutive activation of defense responses can result in severe growth and development defects (Heil and Baldwin, 2002). In Arabidopsis, *BON1* and its homologs *BON2* and *BON3* are negative regulators of plant immune responses (Hua et al., 2001; Yang et al., 2006b; Li et al., 2009). A loss-of-function ( l-o-f) *bon1-1* allele has a dwarf phenotype and constitutive defense responses due to upregulation of a Col-0 accession specific *R* gene *SNC1* (*suppressor of npr1, constitutive 1*) (Hua et al., 2001; Jambunathan et al., 2001; Yang and Hua, 2004). *SNC1* encodes a TIR-NBS-LRR protein and its gain of function mutant *snc1-1* exhibited enhanced disease resistance and dwarf morphological phenotype (Zhang et al., 2003). To understand how *BON1* regulates *SNC1*-mediated defense responses, we isolated a *suppressor of bon1-1* (*sbo*) *3* as *MOS1* (*MODIFIER OF snc1, 1*). We found that *MOS1* regulates plant defense responses, flowering time and endoreduplication through *SNC1, FLC* and potentially *CYCD3;1* respectively. Further, MOS1 and MAD1 antagonistically regulate floral transition and endoreduplication through the interaction with MAD2 and SUF4.

## Results

### The *sbo3* mutation suppresses the *bon1-1* phenotype

To better understand how *BON1* negatively regulates plant defense responses, we carried out a suppressor screen of *bon1-1* via fast neutron mutagenesis. The *bon1-1* (referred as *bon1*) plants were dwarf and had curly leaves due to the constitutive activation of *SNC1*-mediated defense responses. Mutants that had close to wild-type morphology and reduced autoimmune responses compared to *bon1* were named *suppressor of bon1* (*sbo*). One such mutant *sbo3 bon1* resembles the wild type in morphology (Figure 4.1A). The *sbo3* mutation also suppressed disease resistance in *bon1*. The growth of virulent bacterial pathogen *Pseudomonas syringae* pv. *tomato* (*Pst*) DC3000 was 10-fold more in *sbo3 bon1* than in *bon1*, (Figure 4.1B). Consistent with this defense phenotype, RNA blot analysis showed that the expression of *PR1* was dramatically reduced in *sbo3 bon1* compared to *bon1* (Figure 4.1C). The defense phenotype in *bon1* is due to upregulation of *SNC1*. RNA blot analysis showed that *SNC1* upregulation was suppressed by *sbo3* (Figure 4.1C). Therefore, *sbo3* mutation suppressed all known *bon1* phenotypes by reducing the expression of *SNC1*.

### The *SBO3* gene is identified as *MOS1*

The *sbo3* mutation is a single recessive nuclear mutation. When *sbo3 bon1* was backcrossed to *bon1*, the F1 progeny exhibited a *bon1* morphology and the F2 population segregated approximately a quarter plants with a suppressor or wild type morphological phenotype (9 out of 28). To identify the *sbo3* mutation, we crossed *sbo3 bon1* in the Columbia background (Col) to *bon1-2* in Wassilewskija (Ws) (Hua et al., 2001; Yang and Hua, 2004) and *bon1-2 SNC1* with *SNC1* allele from Col-0 introgressed in *bon1-2*, respectively. Linkage analysis on F2 progenies indicated that the *sbo3* mutation was located on chromosome 4

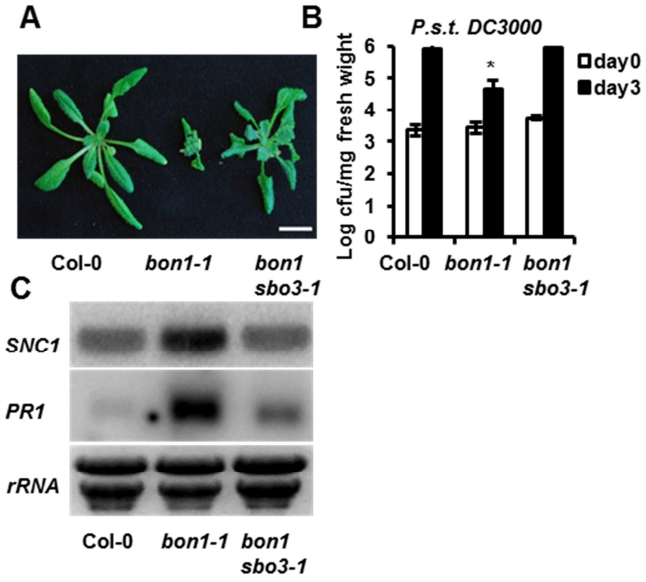


**Figure 4.1 Suppression of *bon1* phenotype by the *sbo3* mutant.** (A) Morphology of Col-0, *bon1-1* and *bon1 sbo3* plants grown at 22°C for 3 weeks. (B) Growth of virulent bacterial pathogen *Pseudomonas syringae* pv. *tomato* (*Pst*) DC3000 in Col-0, *bon1-1,* and *bon1 sbo3* at day 0 and day 3 after inoculation. The asterisk indicates a statistically significant difference from Col-0 determined by Student's *t* test ($P < 0.05$). (C) Expression of *SNC1* and *PR1* genes in Col-0, *bon1-1* and *bon1 sbo3* were analyzed by RNA blotting. *rRNA*s were used as loading controls.

between the ciw11 and JH27 markers. 1450 F2 plants were analyzed and the *sbo3* mutation was narrowed to the region between JHdcaps41 and JH22 on chromosome 4. At that time, *modifier of snc1, 1* (*mos1*) was identified at the same region and reported to suppress the *snc1-1* phenotype (Li et al., 2010). As *MOS1* is very close to *SBO3*, we sequenced *MOS1* gene in *sbo3 bon1* and found an 80bp deletion in the fourth exon of MOS1.

We confirmed that *SBO3* is *MOS1* by three assays. First we crossed *bon1* to another *mos1* mutant *mos1-4* (Salk_126709) which has a T-DNA inserted in the last exon of *MOS1*. Double mutant of *bon1 mos1-4* was identified and it exhibited a *bon1* suppressor phenotype (Figure 4.2B). In addition, F1 progenies of the cross between *bon1 sbo3* and *bon1 mos1-4* exhibited a *bon1* suppressor phenotype (Figure 4.2D), indicating that *sbo3* and *mos1* are the same *bon1* suppressor. In addition, the wild-type *MOS1* gene complemented the *sbo3* mutation. A 10 kb genomic fragment of *MOS1* gene including a 2.6 kb promoter coding region and a 1.5 kb 3'UTR region was transformed into *bon1 sbo3*, and all of the 17 transgenic lines obtained exhibited a *bon1*-like phenotype (Figure 4.2E). We thus conclude that *MOS1* is *SBO3* and referred *sbo3* as *mos1-6*.

**The *sbo3/mos1-6* mutant is a stronger allele than *mos1-4***

The single mutant *mos1-6* was isolated from F2 populations of cross between *bon1 mos1-6* and wild-type Col-0 plants. The *mos1-6* mutant has an 80bp deletion in the fourth exon, which is a stronger allele than *mos1-4* mutant containing a T-DNA insertion in the last exon (Figure 4.2B). Neither *mos1-6* nor *mos1-4* exhibited morphological differences from Col-0 (Figure 4.3A). RNA blot analysis indicated that both *SNC1* and *PR1* expression were reduced in *bon1 mos1-6* and *bon1 mos1-4* double mutants. *SNC1* expression was slightly lower in the *mos1* single

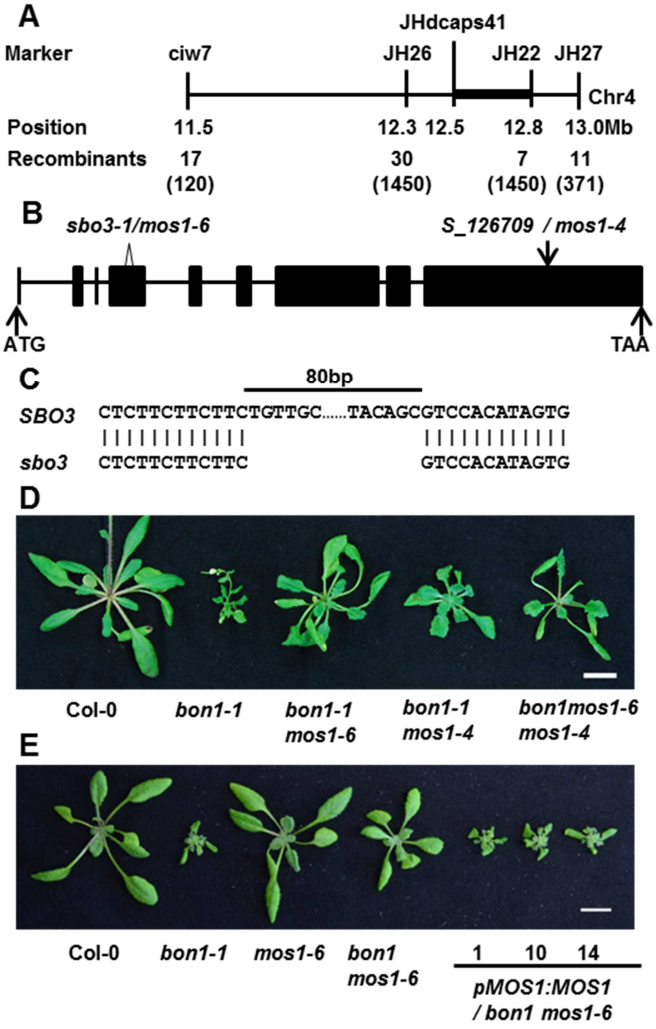


**Figure 4.2 The *SBO3* gene is *MOS1*. (A) Diagram of map-based cloning of the *SBO3* gene.** Shown are molecular markers used for mapping, their positions on chromosome 4 (Chr4), and the number of recombinants at each molecular marker. (B) Gene structure and mutations of *MOS1*. A deletion mutation in *mos1-6* and a T-DNA insertion in *mos1-4* are indicated. (C) The DNA sequence of 80 bp deletion in *mos1-6*. (D) *mos1-4* mutation suppresses *bon1-1* phenotype. Shown are 4-week-old plants. (E) Complementation of *bon1 mos1-6* by the *MOS1* transgene. Shown are three independent *pMOS1::MOS1* transgenic lines in *bon1 mos1-6* compared with Col-0, *bon1-1*, *mos1-6* and *bon1 mos1-6* plants grown at 22°C for 3 weeks.

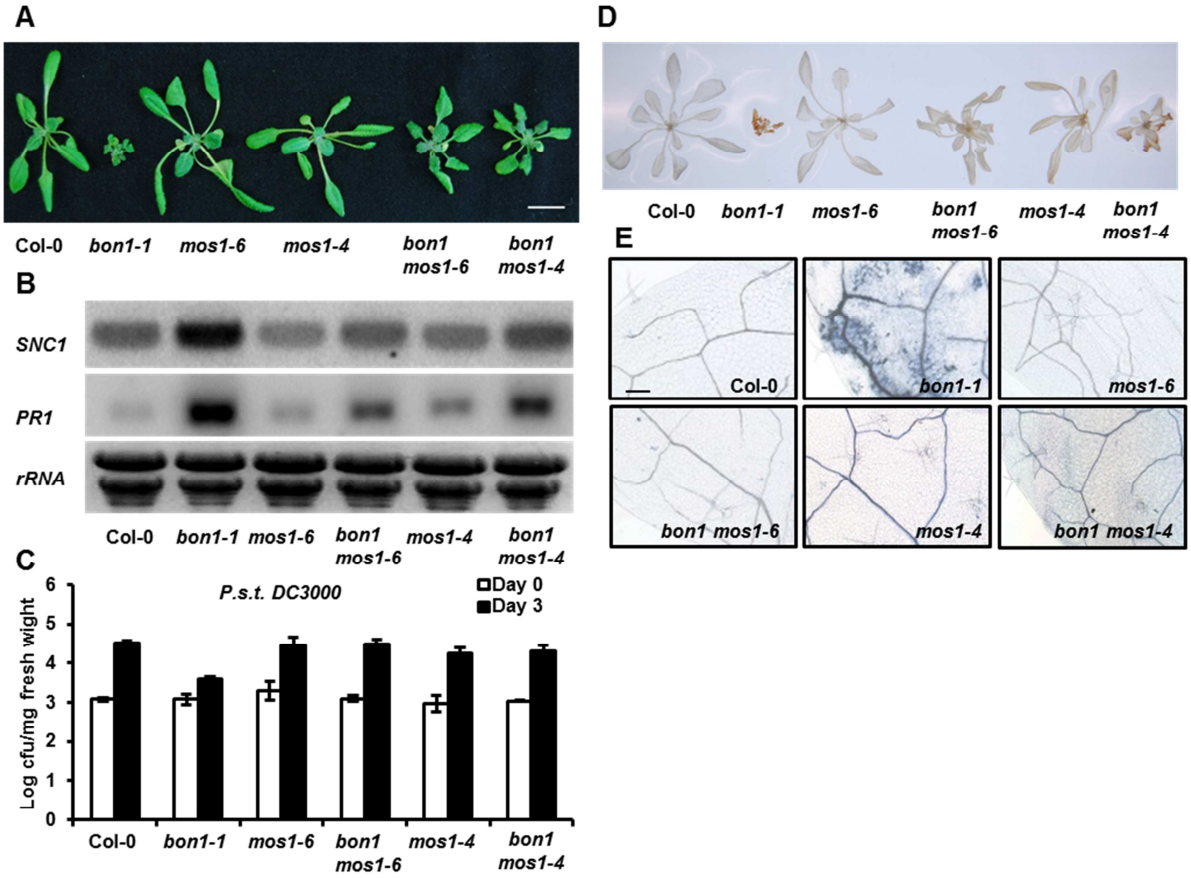


**Figure 4.3 The *mos1* mutations suppress defense responses in *bon1-1*.** (A) Morphology of Col-0, *bon1-1*, *mos1-6*, *mos1-4*, *bon1 mos1-6* and *bon1 mos1-4*. No significant morphological defects were observed in mos1-6 and mos1-4. (B) *mos1* mutations repress the transcription of *SNC1*. (C) Growth of virulent bacterial pathogen *Pseudomonas syringae* pv. *tomato* (*Pst*) DC3000 in Col-0, *bon1-1*, *mos1-6*, *bon1 mos1-6* , *mos1-4* and *bon1 mos1-4* at day 0 and day 3 after inoculation. (D) $H_2O_2$ accumulation in the above genotypes analyzed by DAB staining. (E) Cell death phenotype in the above genotypes analyzed by Trypan blue staining.

mutants compared to Col-0 (Figure 4.3B), which was as same as reported (Li et al., 2010). To determine whether *mos1* mutations abolished other defense phenotypes in *bon1-1*, we analyzed $H_2O_2$ production and cell death in leaves by DAB (3,3'-Diaminobenzidine) staining and trypan blue staining, respectively. Reduced DAB staining was observed in both *bon1 mos1-6* and *bon1 mos1-4* compared to *bon1*, but the extent of reduction in *bon1 mos1-6* was higher than *bon1 mos1-4* (Figure 4.3D). This result indicated that elevation of $H_2O_2$ production in *bon1-1* was largely repressed by *mos1* mutations and the suppression effects of *mos1-6* is stronger than *mos1-4*. No obvious trypan blue staining was observed in either *bon1 mos1-6* or *bon1 mos1-4* (Figure 4.3E). These indicate that cell death and ROS accumulation in *bon1-1* were significantly suppressed by *mos1* mutations and that *mos1-6* is a stronger allele than *mos1-4*.

**The *mos1* mutation results in a *FLC*-dependent late flowering phenotype.**

The *mos1-4* mutant was reported to have a late flowering phenotype (Li et al., 2010), and we found a similar but stronger late flowering phenotype in *mos1-6* under the constant light condition (Figure 4.4A). Under the 16-hour-light / day condition, *mos1-6* had 2 more rosette leaves than Col-0 at bolting, while *mos1-4* had the same number of leaves as the wild type (Figure 4.4C).

Because *FLC* is a central regulator of flowering time, we examined the role of *FLC* in the late flowering phenotype in *mos1* mutants. As vernalization (growth at 4°C for 6 weeks) has been shown to reduce *FLC* expression and promotes flowering, we tested the effect of vernalization on *mos1* plants. Under constant light, non-vernalized *mos1-6* exhibited a delayed floral transition, while six-week 4ºC-treated *mos1-6* had a similar bolting time to the wild-type Col-0 (Figure 4.4A, B). Under 16h light / day condition, *mos1-6* had 8 rosette leaves after vernalization which is greatly reduced from the 14 rosette leaves without vernalization (Figure

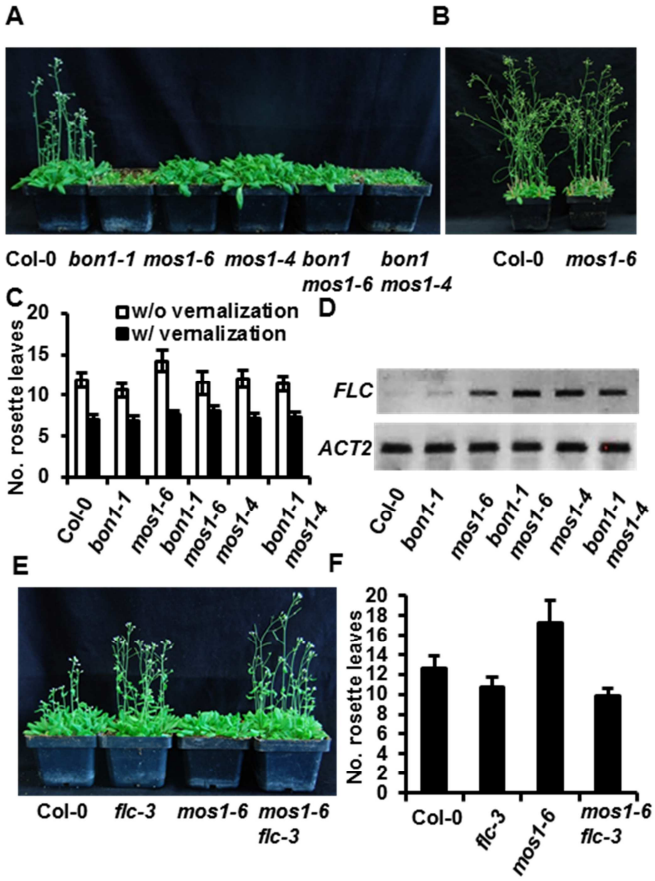


**Figure 4.4 The *mos1* mutations result in a late flowering phenotype.** (A) Morphology of Col-0, *bon1-1*, *mos1-6*, *mos1-4*, *bon1 mos1-6* and *bon mos1-4 grown for 4 weeks* under constant light. (B) Morphology of Col-0 and mos1-6 grown for 4 weeks under constant light after 6-week 4°C treatment. (C) Comparison of flowering time in Col-0, *bon1-1*, *mos1-6*, *mos1-4*, *bon1 mos1-6* and *bon mos1-4* grown under constant light with or without 4°C treatment. (n>20) (D) RT-PCR analysis of FLC expression in 3-week old plants. (E) Late flowering phenotype in *mos1-6* is abolished by *flc-3* mutation. (F) Comparison of flowering time in Col-0 (n=23), *flc-3* (n=25), *mos1-6* (n=25) and *mos1-6 flc-3* (n=25) grown under constant light. The asterisk indicates a statistically significant difference from Col-0 determined by Student's *t* test ($P < 0.05$).

4.4C). This strongly suggests that FLC upregulation is responsible for the late flowering phenotype in *mos1*. Indeed *FLC* expression was dramatically increased in *mos1* and *mos1 bon1* mutants including *mos1-6*, *mos1-4*, *bon1 mos1-6* and *bon1 mos1-4* as analyzed by RT (reverse transcription) -PCR (Figure 4.4D).

We further demonstrated that *FLC* expression change was the cause of late flowering phenotype by introducing *flc-3* into *mos1-6*. The *flc-3* mutant was reported to have an early flowering phenotype under short day condition but not long day condition (Michaels and Amasino, 2001). The double mutant *mos1-6 flc-3*, unlike *mos1-6*, did not exhibit a late flowering phenotype (Figure 4.4E). At bolting, the *mos1-6 flc-3* had 10 rosette leaves which were similar to the 11 rosette leaves in *flc-3* (Figure 4.4F). All of these data indicate that the late flowering phenotype in *mos1* is due to upregulation of *FLC*.

**MOS1 interacts with MAD2 and SUF4**

To further understand the biochemical process MOS1 is involved in, we looked for MOS1 interacting proteins. MOS1 was identified as a MAD2 co-immunoprecipitated protein when *MAD2* was overexpressed in Arabidopsis cell suspension culture (Van Leene et al., 2010). We analyzed the direct physical interaction between MOS1 and MAD2 by the yeast GAL4 two-hybrid assay. Yeast cells containing both *MOS1* and *MAD2* exhibited growth on selection media while cells with either *MOS1* or *MAD2* showed no growth, indicating a physical interaction between the two proteins (Figure 4.5A). The yeast MAD2 protein is known to interact with the yeast MAD1 and BUB3.1, two other components in the SAC complex in yeast, and these interactions have also been observed for Arabidopsis proteins in Arabidopsis suspension cells and *Nicotiana benthamiana* (Gudmundsdottir and Ashworth, 2004; Caillaud et al., 2009; Van Leene et al., 2010). We therefore tested the interaction of MOS1 with MAD1 and BUB3.1 by the

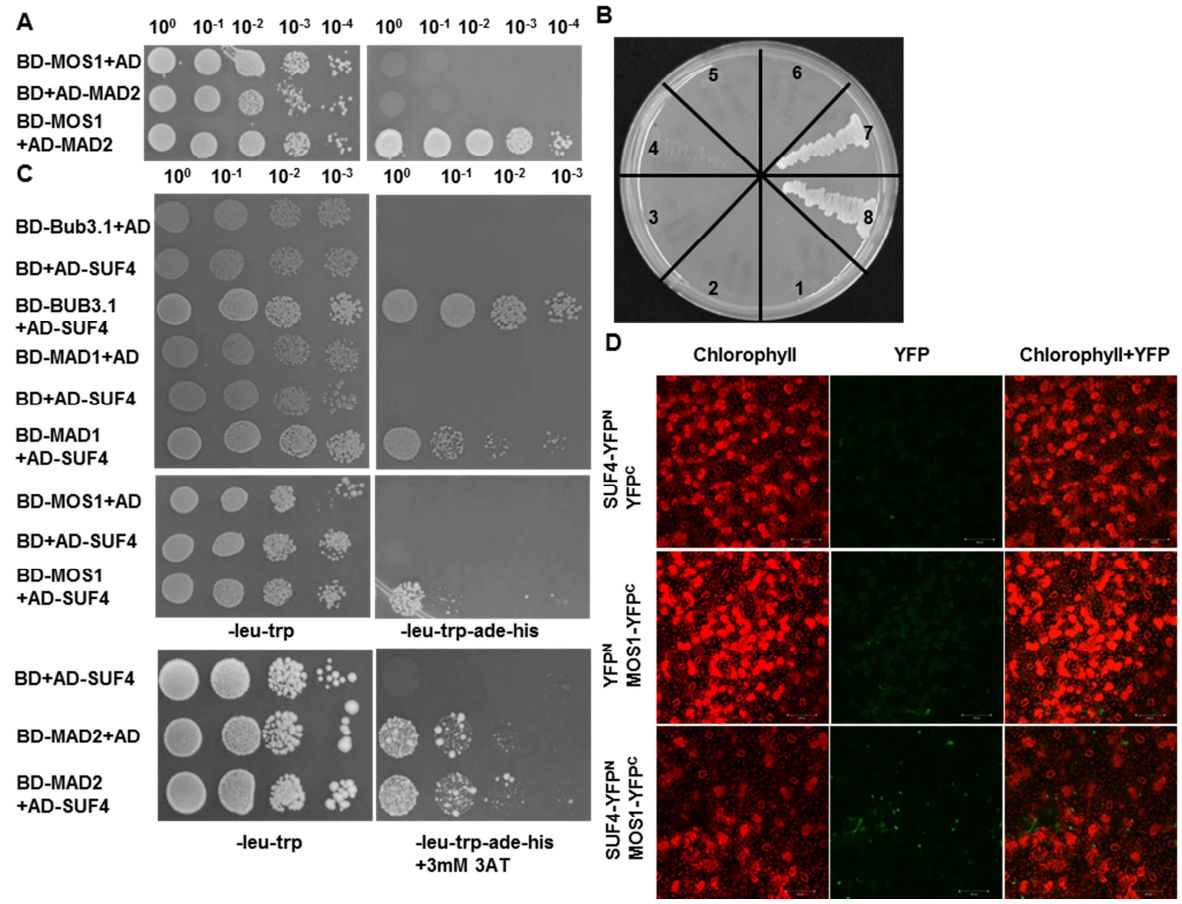


**Figure 4.5 MOS1 interacts with SAC components and SUF4.** (A) Interaction between MOS1 and MAD2 analyzed by Y2H. Shown are serial dilutions of yeast strains containing different combinations of constructs on the selection plate SC-Ade-His-Leu-Trp. AD: activation domain of GAL4. BD: DNA binding domain of GAL4. (B) Interaction between MOS1 and MAD1 and BUB3.1. (1-3), BD-MOS1 and AD-MAD1 (4-6), BD-MOS1 and AD-BUB3.1 (7-8), BD-BUB3.1 and AD-SUF4. (C) Interactions of SUF4 with BUB3.1, MAD1, MOS1 and MAD2 analyzed by the yeast two-hybrid assay. Shown are serial dilutions of yeast strains containing different combinations of constructs on the selection plate SC-Ade-His-Leu-Trp. (D) Confocal microscopy images from BIFC assay in *N. benthamina*. SUF4 protein fused with $YFP^N$ and MOS1 protein fused with $YFP^C$ were transiently expressed in N. benthamiana. Images were taken at 60 h after infiltration. Green signals are from YFP and red signals are from chlorophyll. Scale bar=100µm.

yeast two-hybrid assay. Unlike with MAD2, MOS1 interaction was not detected with MAD1 or BUB3.1 (Figure 4.5B).

Interestingly, BUB3 was identified as a SUF4 interacting protein (Van Leene et al., 2010). As *SUF4* was involved in the activation of *FLC* expression, we tested the SUF4 interaction with MOS1, MAD1, MAD2 and BUB3 by the yeast two-hybrid assay. BUB3.1, MAD1 and MOS1 had strong, moderate and weak interactions with SUF4, respectively (Figure 4.5C). The MAD2 fusion protein itself had auto-activity, but nevertheless also exhibited a very weak interaction with SUF4 (Figure 4.5C).

To confirm the physical interaction between MOS1 and SUF4 in planta, we did bimolecular fluorescence complementation (BiFC) analysis using transient expression in *Nicotiana benthamiana* (Schutze et al., 2009). SUF4 was fused with the N terminal part of YFP (SUF4-$YFP^N$) and MOS1 was fused with the C terminal part of YFP (MOS1-$YFP^C$). When both fusions were expressed in *N. benthamiana* leaves by Agrobacteria mediated infiltration, fluorescence signals were observed and the signals resided in the nucleus. No signals were detected when SUF4-$YFP^N$ was co-expressed with $YFP^C$ or MOS1-$YFP^C$ was coexpressed with $YFP^N$ (Figure 4.5D), indicating that MOS1 could interact with SUF4 in plants.

**The *MOS1* gene is expressed ubiquitously and the MOS1 protein is localized in the nucleus**

We determined the expression pattern of *MOS1* using a reporter gene *GUS* (*β-glucuronidase*) under the control of the native promoter and the first exon of *MOS1*. This GUS reporter was found to be expressed ubiquitously, including in shoot apical meristem and inflorescence meristem, root, hypocotyl, cotyledons and leaves (Figure 4.6A). Prior reports showed *MOS1* expression only in shoot meristems (Li et al., 2010; Li et al., 2011), which might

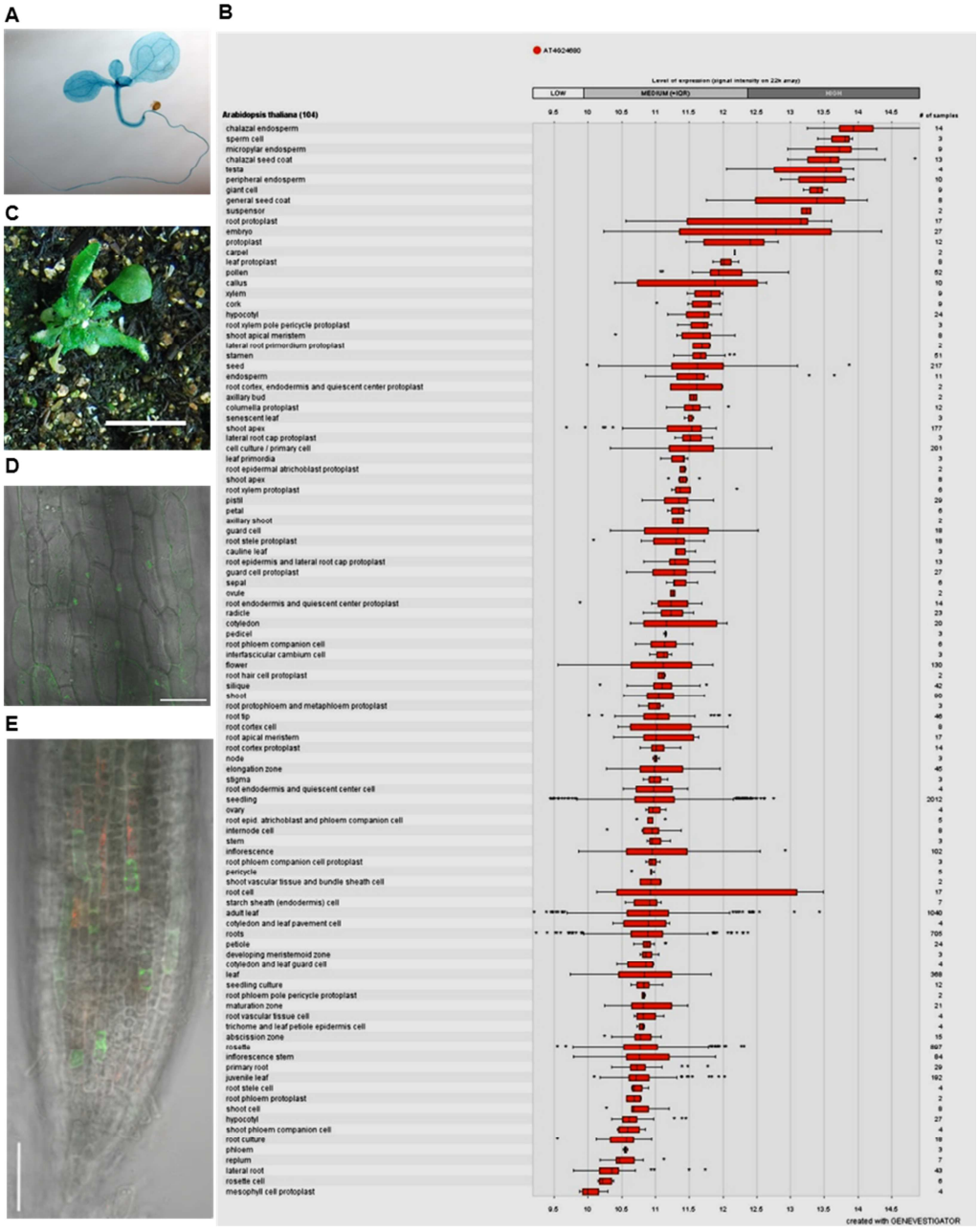


**Figure 4.6 Expression pattern and protein localization of *MOS1*.** (A) GUS staining of transgenic lines of *pMOS1::GUS* at 9 days after germination. (B) Tissue-specific expression pattern. Shown are data collected from the Genevestigator website. (C-D) Subcellular localization of MOS1 in the root hair zone (C) and root tip (D). Shown is the root of *p35S::GFP:MOS1* transgenic plant in *bon1 mos1-6*. Green signals are from GFP and red signals are from propidium iodide staining to mark cell boundaries. Scale bar=50μm.

have resulted from a shorter regulatory sequences used in the reporter construct than in this study. The ubiquitous expression of *MOS1* is consistent with the microarray data collected from Genevestigator website (www.genevestigator.com/gv/) (Figure 4.6B).

The MOS1 was reported to localize in the nucleus by using a C-terminal truncated form without the BAT2 domain (Li et al., 2010; Li et al., 2011). We determined the subcellular localization of MOS1 by a MOS1:GFP fusion expressed under the control of the cauliflower mosaic virus (CaMV) 35S promoter. This fusion is functional as it complemented the *mos1-6* mutant in *bon1* (Figure 4.6C). In *bon1 sbo3* transgenic plants with MOS1:GFP fusion, very weak GFP signals could be detected in root cells of young seedlings where auto-fluorescence is low compared with in other tissues, and these signals appeared to be nuclear. In the transgenic root, MOS1:GFP was not observed in all root cells. Instead, it was found in zones where root hair is developing but not in the root tip or elongation zone (Figure 4.6D, E). These analyses suggest that *MOS1* is transcribed in all tissue types and its protein might have a short life span in most cells.

**_SUF4_ mediates flowering phenotype of _mos1-6_**

To determine whether the regulation of flowering time by *MOS1* is dependent on *SUF4*, we introduced a *SUF4* l-o-f mutation into *mos1-6*. While this single mutant *suf4-2* had a same flowering time as the wild-type Col-0, the *suf4*-2 mutation abolished late flowering phenotype of *mos1-6* (Figure 4.7A). At bolting, *mos1-6* had 4 more leaves than the wild type, while *mos1 suf4* had 13 rosette leaves similar to *suf4-2* and Col-0 (Figure 4.7B). This suppression is correlated with a reduction of *FLC* expression in *mos1 suf4*. Consistent with an earlier report (Kim et al., 2006), *FLC* had a much reduced expression in *suf4* than in Col-0, as no expression could be detected at 25 cycles in RT-PCR analysis. High expression of *FLC* in *mos1* was reduced by *suf4*,

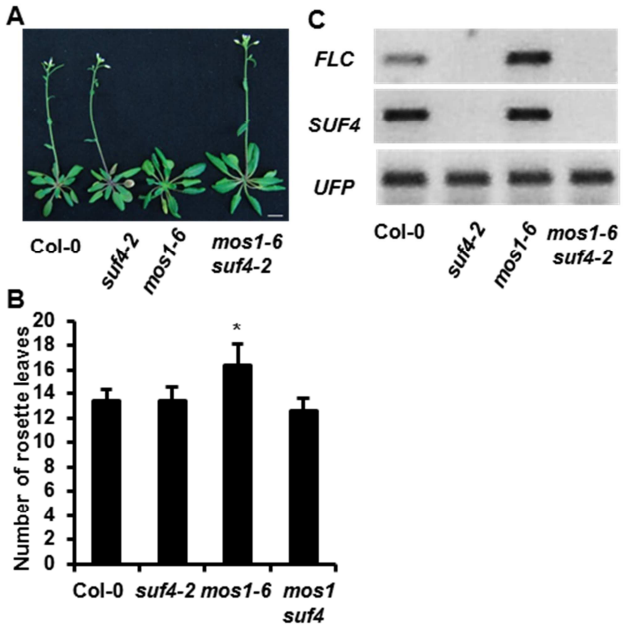


**Figure 4.7 Late flowering phenotype in *mos1* is dependent on *SUF4*.** (A) *suf4-2* mutation suppresses the late flowering phenotype of *mos1-6*. (B) RT-PCR analysis indicates that no *FLC* is detected in *suf4-2*. (C) Comparison of flowering time in Col-0, *suf4-2*, *mos1-6* and *mos1 suf4* grown under constant light (n=15). The asterisk indicates a statistically significant difference from Col-0 as determined by a Student's *t* test ($P < 0.05$).

and no *FLC* expression was detected in *mos1-6 suf4-2* as in *suf4-2* at 25 cycles of RT-PCR (Figure 4.7C). Therefore, *MOS1*-regulated flowering time and *FLC* expression was dependent on the function of *SUF4*.

### *MOS1* and *SUF4* affect endoreduplication

The interaction between MOS1 and MAD2 prompted us to investigate the effect of *mos1* mutations on cell cycle progression. We measured the ploidy distribution in the first pair of leaves at 4-week old by using flow cytometer and found an increase of ploidy levels in *mos1* mutants. In *mos1-6*, *bon1 mos1-6*, *mos1-4* and *bon1 mos1-4*, the portion of 16C increased to 30%, 33%, 28% and 28% respectively from 22% in Col-0 (Figure 4.8A). The *mos1-6*, *bon1 mos1-6*, *mos1-4* and *bon1 mos1-4* mutants also contained 32C cells at 2%, 3%, 1% and 2% respectively compared to 1% in Col-0 (Figure 4.8A). Correspondingly, the portion of cells with 2C, 4C and 8C changed from 8%, 21% and 48% in Col-0 to 9%, 21% and 38% in *mos1-6*, 7%, 20% and 37% in *bon1 mos1-6*, 10%, 21% and 40% in *mos1-4* and 9%, 20% and 42% in *bon1 mos1-4* (Figure 4.8A). Again, *mos1-6* mutation had stronger effect on the ploidy levels than *mos1-4*. Thus, *mos1* mutation resulted in the promotion of endoreduplication with *mos1-6* having a stronger effect than *mos1-4*.

To determine whether the enhanced endoreduplication in *mos1-6* is dependent on *SUF4*, we measured the ploidy distribution in the first pair of leaves of 4-week-old plants in Col-0, *suf4-2*, *mos1-6* and *mos1 suf4*. The *suf4-2* mutant has a slightly reduced ploidy level than Col-0, containing 5% more 8C and 6% less 16C than Col-0. The *mos1 suf4* mutant had reduced ploidy level than *mos-6*, containing 13% more 8C, 7% less 16 C and 4% less 32C than *mos1-6* (Figure 4.8B). This data indicates that *suf4-2* mutant largely suppressed endoreduplication phenotype in

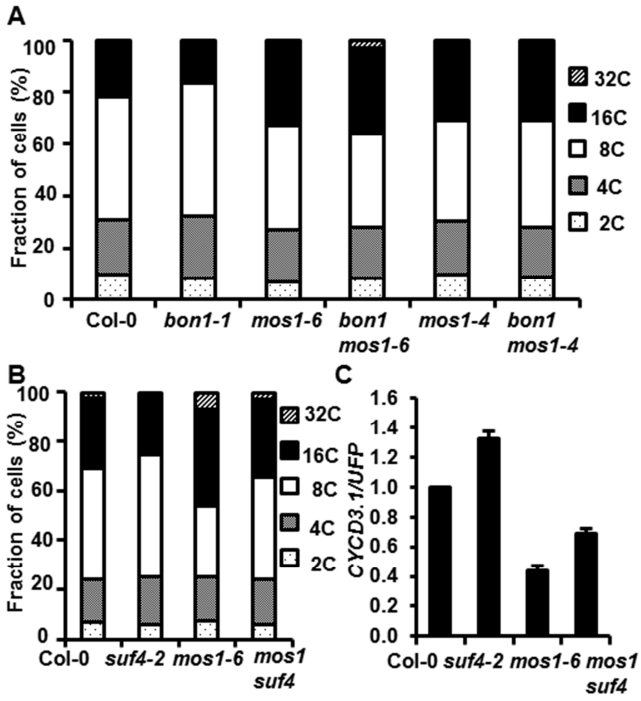


**Figure 4.8 *MOS1* and *SUF4* affect endoreduplication.** (A) Ploidy levels in the first pair of leaves from the wild-type Col-0, *bon1-1*, *mos1-6*, *bon1 mos1-6*, *mos1-4* and *bon1 mos1-4* grown under constant light for 4 weeks. Each sample for measurement was collected from two individual plants. The ploidy distribution was calculated from more than 5000 nuclei. Data are average of three replicas. (B) Ploidy levels in the first pair of leaves from the wild-type Col-0, *suf4-2*, *mos1-6* and *mos1 suf4* grown under constant light for 4 weeks. (C) qRT-PCR analysis of *CYCD3;1* expression in indicated genotypes. The error bars indicate standard deviation determined from three measurements.

**Table 4.1 Differentially expressed *SNC1*, *CYCD3;1* and flowering time genes in *bon1-1*, *mos1-6* and *bon1-1 mos1-6 com*pared to wild-type Col-0.**

Shown are the gene symbols, annotation, and their relative expression in *bon1-1*, *mos1-6* and *bon1-1 mos1-6* compared to Col-0. Fold changes are in ln value. Significant changes ($p<0.05$) are shaded in gray.

| Gene | Annotation | *bon1-1* vs Col-0 | | *mos1-6* vs Col-0 | | *bon1-1 mos1-6* vs Col-0 | |
|---|---|---|---|---|---|---|---|
| | | Change (ln) | p-value | Change (ln) | p-value | Change (ln) | p-value |
| AT5G10140 | K-box region and MADS-box transcription factor family protein, FLC | -0.61 | 0.1128 | 2.41 | 0.0000 | 2.40 | 0.0000 |
| AT3G02380 | CONSTANS-like 2 | 0.11 | 0.4657 | -0.66 | 0.0005 | -0.27 | 0.0705 |
| AT2G45660 | AGAMOUS-like 20, SOC | 0.36 | 0.0155 | -0.84 | 0.0000 | -0.60 | 0.0002 |
| AT1G65480 | PEBP (phosphatidylethanolamine-binding protein) family protein, FT | 0.09 | 0.7784 | -2.09 | 0.0003 | -1.19 | 0.0038 |
| AT4G16890 | disease resistance protein (TIR-NBS-LRR class), putative | 0.73 | 0.0000 | -0.26 | 0.1552 | 0.04 | 0.8044 |
| AT4G34160 | CYCLIN D3;1 | 0.06 | 0.7136 | -0.87 | 0.0000 | -0.95 | 0.0000 |

*mos1-6*. Therefore, function of *MOS1* in endoreduplication, as in flowering time, is also dependent on *SUF4*.

Transcriptome analysis revealed that a cyclin gene *CYCD3;1* was down-regulated in *mos1-6* (Table 4.1). Decreased or elevated *CYCD3;1* expression were reported to promote or reduce endoreduplication, respectively (Schnittger et al., 2002; Dewitte et al., 2007). To assess the role of *CYCD3;1* expression in the promoted endoreduplication in *mos1-6*, we analyzed *CYCD3;1* expression by quantitative real-time RT-PCR (qRT-PCR) in Col-0, *suf4-2*, *mos1-6* and *mos1 suf4* (Figure 4.8C). In *suf4-2* single mutant, *CYCD3;1* expression was up-regulated compared to Col-0, and *mos1 suf4* had an increase of *CYCD3;1* expression compared to *mos1-6* although the expression level was lower than in Col-0 (Figure 4.8C). These data suggest that the expression of *CYCD3;1* is correlated with endoreduplication and *MOS1* and *SUF4* likely modulate endoreduplication through regulating *CYCD3;1* expression.

**_MOS1_ and the _SAC_ gene _MAD1_ antagonistically regulate flowering time**

The association of MOS1 and SAC with SUF4 and MOS1 prompted us to analyze their effects in flowering time. We isolated l-o-f mutants of *MAD1* (*mad1-1*, Salk_039008) and introduced this mutation into *mos1-6*. The *mad1-1* mutant exhibited a slightly earlier flowering than Col-0, with 2 fewer rosette leaves less than Col-0 at bolting (Figure 4.9A). The *mos1-6* mutant was late flowering, with 19 leaves at bolting. *mos1 mad1* bolted slightly earlier than *mos1-6* but much late than *mad1-1*. It had and 3 fewer rosette leaves less than *mos1-6* and 4 more leaves than *mad1-1* at bolting (Figure 4.9B). This suggests that *mad1* and *mos1* have additive effects on flowering time. RT-PCR analysis showed a slight reduction of *FLC* transcription in *mad1-1*, but no obvious change was detected in *mos1 mad1* double mutants

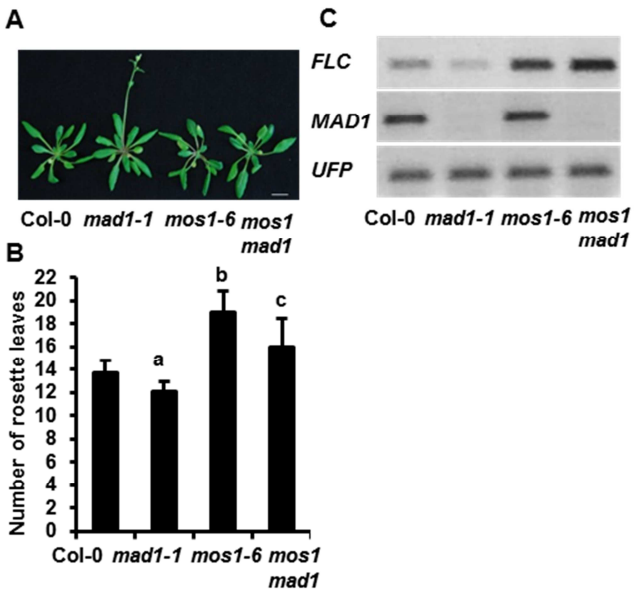


**Figure 4.9 *MOS1* and *MAD1* antagonistically regulate flowering time.** (A) Morphology of Col-0, *mad1-1*, *mos1-6* and *mos1 mad1* grown for 6 weeks under constant light. (B) Comparison of flowering time in Col-0 (n=23), *mad1-1* (n=18), *mos1-6* (13) and *mos1 mad1* (n=18) grown under constant light. The error bar indicates standard deviation. The letters a, b and c indicate statistically significant differences at different extents from Col-0 determined by Student's *t* test ($P < 0.05$). (E) RT-PCR analysis of *FLC* expression in 3-week old plants of Col-0, *mad1-1*, *mos1-6* and *mos1 mad1*.

compared to *mos1-6* (Figure 4.9C). In sum, *MAD1* is partially required to repress the floral transition, and it functions in parallel to *MOS1* in the regulation of floral transition.

**_MOS1_ antagonizes _MAD1_ to affect endoreduplication**

To understand whether the promoted endoreduplication in *mos1-6* is dependent on *MAD1*, we measured the ploidy distribution in the first pair of leaves of 4-week-old plants in Col-0, *mad1-1*, *mos1-6* and *mos1 mad1*. *mad1-1* had a similar ploidy profile to the wild type, but the increase of ploidy level in *mos1-6* is suppressed by *mad1-1*. *mos1 mad1* had 10% more 8C, 16% less 16C and 3% less 32C than *mos1-6* (Figure 4.10A). Because *CYCD3;1* is implicated in ploidy control in *mos1-6*, we analyzed the expression of *CYCD3;1* in *mad1-1* and *mos1 mad1* mutants. In *mad1-1* mutant, *CYCD3;1* expression was slightly up-regulated compared to the wild type but the change was not statistically significant. However, *mos1 mad1* double mutant had a significant increase of *CYCD3;1* expression compared to *mos1-6* , although the expression level was lower than in Col-0 (Figure 4.10B). These data suggest that *MOS1* antagonizes *MAD1* to affect endoreduplication.

**_MOS1_ largely mediates defense responses in _mad1_ and _bon1_ mutants**

The *mad1-1* single mutant does not exhibit obvious morphological defects. To determine whether *MAD1* is involved in defense responses induced in *bon1-1*, we introduced *mad1-1* mutation into *bon1-1* and *bon1 mos1-6*. The *bon1 mad1* exhibited a stronger growth defect than *bon1*, and the *mad1 bon1 mos1* had a weaker phenotype than *bon1 mad1* (Figure 4.11A, B). This indicates that *bon1* and *mad1* have synergistic interaction and that *mos1* can largely suppress growth defects of *bon1 mad1*. To answer whether the growth variations were due to the change of *SNC1* expression, we analyzed *SNC1* expression by qRT-PCR in different genotypes. *SNC1* had 1.5-fold increase in both *bon1-1* and *bon1 mad1* but had 0.26-, 0.32- and 0.11-fold reduction

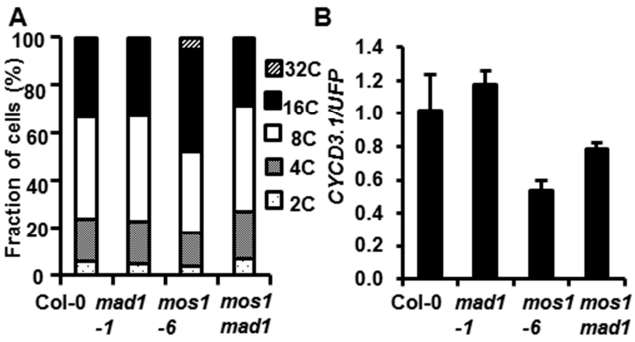


**Figure 4.10 *MOS1* and *MAD1* antagonistically affect endoreduplication.** (A) Ploidy levels in the first pair of leaves from wild-type Col-0, *mad1-1*, *mos1-6* and *mos1 mad1* grown under constant light for 4 weeks. Each sample for measurement was collected from two plants. The ploidy distribution was calculated from more than 5000 nuclei. Data are average of three replicas. (B) qRT-PCR analysis of *CYCD3;1* expression in indicated genotypes. The error bars indicate standard deviations determined from three measurements.

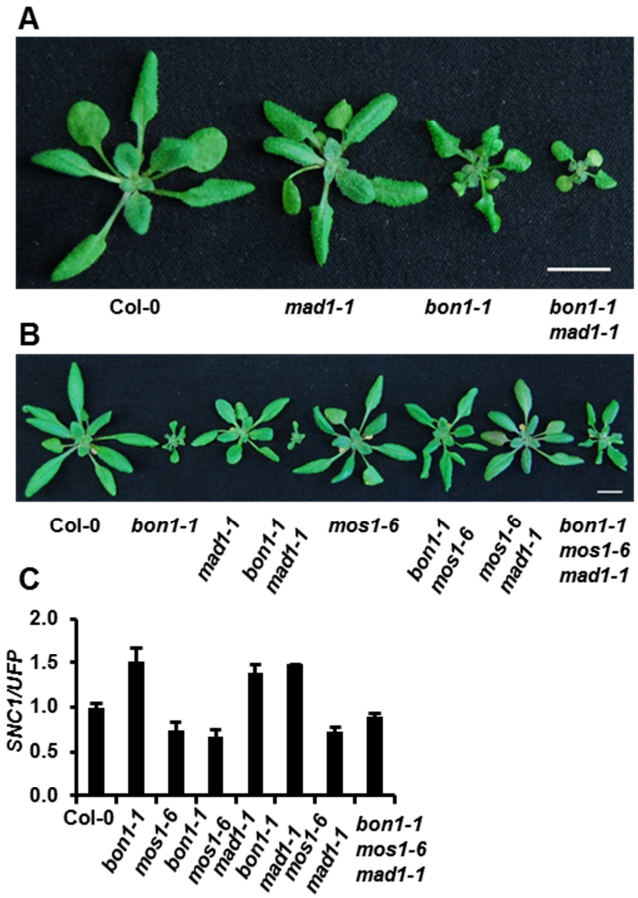


**Figure 4.11 The *mos1* mutation largely suppresses defense phenotypes in *bon1* and *mad1*.** (A) Morphology of Col-0, *mad1-1*, *bon1-1* and *bon1 mad1-1* grown for 3 weeks under constant light. (B) Morphology of Col-0, *bon1-1*, *mad1-1*, *bon1-1 mad1-1*, *mos1-6*, *bon1 mos1-6*, *mos1-6 mad1-1* and *bon1 mos1-6 mad1-1* grown for 3 weeks under constant light. (C) qRT-PCR analysis of *SNC1* expression in indicated genotypes. The error bar indicates standard deviation determined from three measurements.

in *mos1-6*, *bon1 mos1* and *bon1 mos1 mad1* compared to Col-0 (Figure 4.11C). Therefore *mos1* can reduce *SNC1* expression in all these genetic backgrounds, which likely accounts for the suppression of growth defects in *bon1 mad1* mutant. Interestingly, *SNC1* had 1.4-fold increase in *mad1-1* single mutant, although *mad1-1* did not exhibit severe growth defects. All these data suggest that *MOS1* mediates the growth inhibition co-regulated by *BON1* and *MAD1*.

***MAD2* and *BUB3* are involved in flowering time control and endoreduplication**

To determine whether *MAD2* affects the function of *MOS1*, we introduced the l-o-f *mad2-2* mutation, previously reported to have defects in root elongation and meristem growth (Gudmundsdottir and Ashworth, 2004), into *mos1-6*. The *mad2* single mutant showed a slightly late flowering time compared to the wild-type Col-0. The *mos1 mad2* double mutant showed a similar flowering time as *mos1-6* (Figure 4.12A). At bolting, *mad2-2* had 15 rosette leaves compared to 14 rosette leaves in Col-0, and *mos1 mad2* double mutant had 17 rosette leaves compared to 18 rosette leaves in *mos1-6* (Figure 4.12B). Statistical analysis indicated that *mad2-2* was significantly different from Col-0 in rosette leaf number at bolting but *mos1 mad2* were not significantly different with *mos1-6*. RT-PCR analysis indicated that *FLC* expression was similar between Col-0 and *mad2-2* and between *mos1-6* and *mos1 mad2* (Figure 4.12C). All these data suggest that *MAD2* has a weak effect on the regulation of flowering time.

We further measured the ploidy distribution in the first pair of leaves of 4-week-old plants in Col-0, *mad2-2*, *mos1-6* and *mos1 mad2*. The *mad2-2* mutant had 4% more 16C and 1% more 32C than Col-0. The *mad2 mos1* mutant had 14% more 8C, 10% less 16C and 6% less 32C than *mos1-6* (Figure 4.12D). These data indicate that *mad2-2* mutation, although inducing a slightly higher ploidy, largely suppressed the high ploidy defects in *mos1-6*. All these data suggest that the promoted endoreduplication in *mos1-6* was largely dependent on *MAD2*.

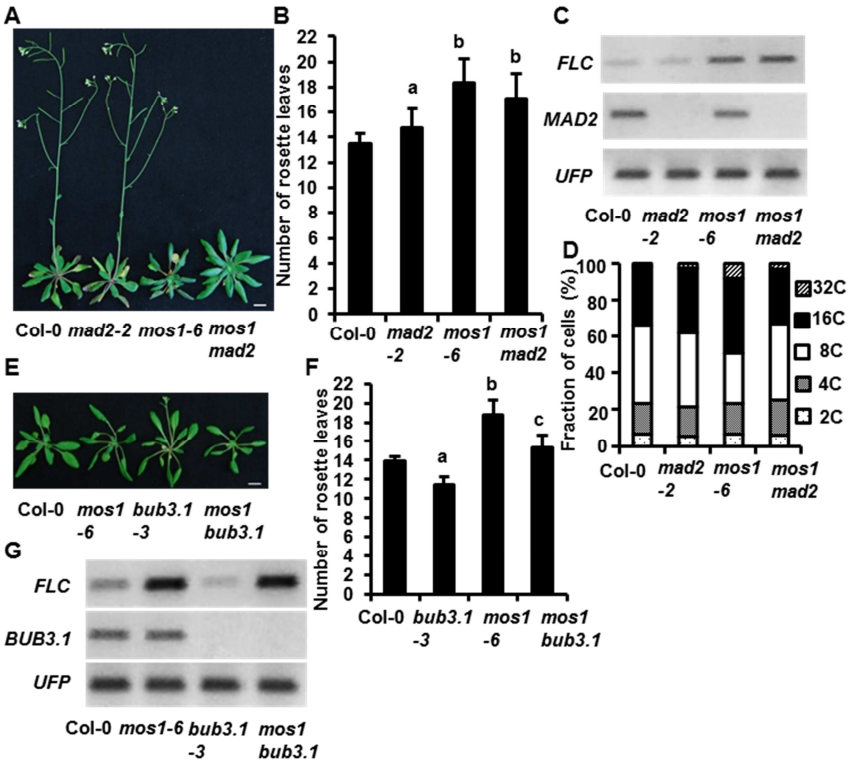


**Figure 4.12 Involvement of *MAD2* and *BUB3* in flowering time control and endoreduplication.** (A) Morphology of Col-0, *mad2-2*, *mos1-6* and *mos1 mad2* plants grown for 6 weeks under constant light. (B) Comparison of flowering time in the above genotypes (n=20) grown under constant light. The error bar indicates standard deviation. The letters a, b and c indicate statistically significant differences from Col-0 determined by Student's *t* test ($P < 0.05$). (C) RT-PCR analysis of *FLC* expression in 3-week old plants of the indicated genotypes. (D) Ploidy levels in the first pair of leaves from the wild-type Col-0, *mad2-2*, *mos1-6* and *mos1 mad2* grown under constant light for 4 weeks. Each sample for measurement was collected from two individual plants. The ploidy distribution was calculated from more than 5000 nuclei. Data are average of three replicas. (E) Morphology of Col-0, *bub3.1-3*, *mos1-6* and *mos1 bub3.1* grown for 6 weeks under constant light. (F) Comparison of flowering time in Col-0 (n=17), *bub3.1-3* (n=17), *mos1-6* (n=21) and *mos1 bub3.1* (n=19) grown under constant light. The error bar indicates standard deviation. The letters a, b and c indicate statistically significant differences from Col-0 determined by Student's *t* test ($P < 0.05$). (G) RT-PCR analysis of *FLC* expression in 3-week old plants of Col-0, *mos1-6*, *bub3.1-3* and *mos1 bub3.1*.

We then isolated l-o-f mutants of *BUB3.1* (*bub3.1-3*, CS100981) and introduced the mutation into *mos1-6*. The *bub3.1-3* exhibited slightly earlier flowering than Col-0 and the *bub3 mos1* flowered in-between *mos1* and *bub3* (Figure 4.12E). At bolting, *bub3.1-3* had 2 fewer rosette leaves than Col-0, and *mos1 bub3.1* had 3 fewer rosette leaves than *mos1-6* and 4 more leaves than *bub3.1-3* (Figure 4.12F). A slight reduction of *FLC* transcription was observed in *bub3.1-3* by RT-PCR, but no obvious change was detected in *mos1 bub3.1* double mutants compared to *mos1-6* (Figure 4.12G). Overall, no epistatic interaction was observed between *bub3.1* and *mos1*, and *BUB3.1* and *MOS1* may function in parallel in the regulation of floral transition.

**Discussion**

Here we characterize a transcriptional regulator *MOS1* that modulates multiple processes including defense responses, floral transition and endoreduplication. Altered expression of *SNC1*, *FLC* and possibly *CYCD3;1* in *mos1* are responsible for the reduced defense, later flowering and increased endoreduplication, respectively. We further demonstrated that SUF4 interacts with MOS1 and mediates the flowering time and endoreduplication control through *SUF4*. In addition, a potential involvement of mitotic checkpoint in floral transition and endoreduplication was revealed through their interaction with MOS1 and SUF4.

***MOS1* functions through *SUF4* to regulate floral transition and endoreduplication**

This study establishes *MOS1* as a repressor of *FLC*, a central repressor of floral transition. The *mos1* mutations triggered a late flowering phenotype which is *FLC*-dependent (Figure 4.5). SUF4 is a C2H2 transcription factor that binds to the *FLC* promoter region and recruits PAF1-

complex and EFS to the *FLC* locus to activate *FLC* transcription (Kim et al., 2006; Kim and Michaels, 2006). SUF4 also interacts with FRI to form a large complex by recruiting chromatin remodeling factors to trigger the activation of *FLC* expression (Choi et al., 2011) and interacts with LUMINIDEPENDENS (LD) to repress the *FLC* expression in the absence of *FRI* (Kim et al., 2006). Multiple interacting proteins of SUF4 supported different layers of regulation on *FLC* activation. We found that MOS1 has a direct physical interaction with SUF4 (Figure 4.5C, D), and it represses *FLC* expression in a *SUF4*-dependent manner (Figure 4.7). Thus MOS1 normally inhibits SUF4 activity and keeps *FLC* expression low. In the *mos1* mutant, SUF4 has a higher activity and induces higher *FLC* transcription and consequent later flowering.

A similar interaction between *MOS1* and *SUF4* might function in endoreduplication control. The *mos1* mutation triggers promotion of endoreduplication in a *SUF4*-dependent manner, and the loss of function of *SUF4* leads to a slight reduction of endoreduplication (Figure 4.8). Our study suggest that *CYCD3;1* might mediate their effects on endoreduplication. Endoreduplication is associated with the repression of mitotic CDK-cyclin complex activities during G2 to M transition phase and the activation of DNA replication (Inagaki and Umeda, 2011). *CYCA3;2, CYCA2;3* and *CYCD3;1* were reported as negative regulators of endoreduplication (Inze and De Veylder, 2006). Decreased or elevated *CYCD3;1* expression were reported to promote and reduce endoreduplication, respectively (Schnittger et al., 2002; Dewitte et al., 2007). Expression of *CYCD3;1* in *mos1* and *suf4* mutants are correlated with the endocycle phenotypes. In *mos1* mutant, *CYCD3;1* was down-regulated (Table 4.1), which is partially reverted by the *suf4* mutation. A slight increase of *CYCD3;1* expression was observed in *suf4* single mutant (Figure 4.8C), suggesting that *SUF4* repress the expression of *CYCD3.1* directly or indirectly. Reduced *CYCD3;1* expression in *mos1* again suggests that *MOS1* normally

represses the function of *SUF4*. The correlation between *CYCD3;1* expression and endoreduplication phenotype in *suf4* and *mos1 suf4* further supported that the interaction between MOS1 and SUF4 was critical for *MOS1* function.

**SAC components affect flowering time and endoreduplication**

MAD1 is one important component of the Spindle assembly checkpoint (SAC) which contains 5 other proteins, MAD2, 3 and BUB1, 2, 3. The SAC mechanism has been well studied in yeast and mammalians but not in plants. Functional SAC is required to delay cell cycle progression until all kinetochores have been correctly attached to the spindle (Li and Murray, 1991). Orthologs of SAC components were identified in Arabidopsis and they do interact with each other (as tested in yeasts) and attach to the kinetochore (Yu et al., 1999; Gudmundsdottir and Ashworth, 2004; Caillaud et al., 2009). Their biological functions have not been well characterized except for the promotion of root elongation and the growth of root meristem by *MAD2* in Arabidopsis (Gudmundsdottir and Ashworth, 2004). Here, we identified a role of *MAD1*, *MAD2*, and *BUB3.1* in regulation flowering time and endoreduplication. Most prominently, *MAD1* appears to have a close link with *MOS1* function and antagonizes *MOS1* function in flowering time control, endoreduplication and defense responses. The *mad1-1* mutant exhibited a slightly early flowering phenotype and had a weak down-regulation of *FLC* expression (Figure 4.9). The *mad1-1* mutation partially suppressed late flowering phenotype (Figure 4.9), largely restored the cell cycle progression of *mos1-6* (Figure 4.10) and partially repressed the *mos1* phenotype in *bon1* through modulating *SNC1* expression (Figure 4.11). All the data indicate that *MAD1* antagonistically affects *MOS1* function. *SUF4* was required for *MOS1* function and the interaction between *MAD1* and *SUF4* suggests that a competition may

occur between *MOS1* and *MAD1* in binding with *SUF4* in the regulation of floral transition and endoreduplication.

MAD2 is found to interact with MOS1 and SUF4 in yeast two-hybrid assays (Figure 4.5A, C), but the biological significance of these interactions is not clear. Loss of function mutant *mad2-2* exhibited slightly late flowering without a change of *FLC* expression, but this mutation did not affect the flowering phenotype of *mos1-6* (Figure 4.12A, B, C), suggesting that *MOS1* may play a more direct role than *MAD2* in the regulation of flowering time. The *mad2-2* mutation induces a slightly promoted endoreduplication, but largely suppressed the endoreduplication phenotype of *mos1-6* (Figure 4.12D). This indicates a role of *MAD2* in mediating the function of *MOS1* in endoreduplication.

Our study indicates that *BUB3.1* and *MOS1* antagonistically regulate the floral transition. Loss of function mutant of *BUB3.1* exhibited slightly early flowering and had a weak reduction of *FLC* expression (Figure 4.12 E, F, G), and *bub3.1-3* mutation partially suppressed the late flowering phenotype of *mos1-6* (Figure 4.12 F). No interaction between *BUB3.1* and *MOS1* was observed, but *BUB3.1* strongly interacted with *SUF4* (Figure 4.5C). All the data suggested that the antagonism between *MOS1* and *BUB3.1* on flowering time control might be due to their physical interaction with *SUF4*.

**Model for the regulation of flowering time and endoreduplication by MOS1, SUF4, and SAC components**

We propose a working model for the function of *MOS1* and SAC in the regulation of floral transition and endoreduplication (Figure 4.13). MOS1 and MAD2 interact with each other, facilitate the floral transition and repress the endoreduplication. The interaction between MOS1-MAD2 complex and SUF4 inhibit the SUF4 transcriptional activity, and consequently represses

*FLC* expression to trigger the floral transition and activates *CYCD3;1* expression to repress the endoreduplication. SUF4 is known to bind directly to the promoter of *FLC*, and it remains to be determined if SUF4 binds to the promoter of *CYCD3;1*. If so, it remains to be determined how the SUF4 binding leads to transcriptional activation in one target gene but repression in another. MAD1 also interacts with MAD2 and it has an antagonistic interaction with MOS1 in the regulation of floral transition and endoreduplication. It is possible that the interaction between MAD1-MAD2 complex and SUF4 competes with the MOS1-MAD2 interaction with SUF4 and therefore protects the SUF4 activity from inhibited and consequently activates *FLC* expression and represses *CYCD3;1* expression.

## Materials and methods

### Plant materials, growth, transformation, and pathogen tests

Seeds of *mos1-4* (Salk_126709), *ddm1-10* (CS9604 or SALK_093009), *mad1-1* (SALK_039008), *mad2-2* (SAIL_191_G06) *Bub3.1-3* (CS100981) and *suf4-2* (SALK_093449) were obtained from Arabidopsis Biological Research Center (ABRC). Plant growth, transformation, and pathogen tests were carried out as previously described (Yang and Hua, 2004; Yang et al., 2006a; Zhu et al., 2010).

### Map-based cloning

The *sbo3 bon1* double mutant was crossed with *bon1-2 SNC1* which had functional *SNC1* allele from Col-0 introgressed into *bon1-2*. Bulked segregation analyses with around 50 wild type-like plants identified the linkage to the marker ciw11 on Chromosome 4. Further SNP markers were generated by using the information from the website (http://msqt.weigelworld.org/), and 1450 wild type-like plants were used for fine mapping.

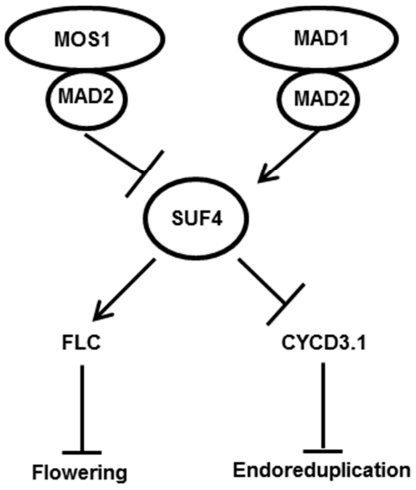


**Figure 4.13 A working model for *MOS1* in the regulation of floral transition and endoreduplication.** MOS1 and MAD2 interact with each other, facilitate the floral transition and repress the endoreduplication. The MOS1-MAD2 complex inhibits the SUF4 activity, and consequently represses *FLC* expression and directly or indirectly activates *CYCD3;1* expression. MOS1 function is antagonized by MAD1 that also interacts with MAD2 . The interaction of the MAD1-MAD2 complex with SUF4 competes with MOS1-MAD2 and thus keeps SUF4 from being inhibited.

**Plasmid construction**

A 2.6kb upstream of the ATG start codon plus 30bp after the ATG was cloned into a gateway entry vector pDONR222 by BP reaction and moved to the destination vector pGUS1-GW by LR reaction. The construct used to complement the *mos1-6* mutation was generated by amplifying the 10kb of genomic fragment including the promoter 2.6kb upstream of the ATG start codon, the coding region and the 3' UTR 1.5kb downstream of the TAA stop codon. The whole fragment was firstly cloned into pDONR222 by BP reaction and moved to the destination vector pGUS1-GW by LR reaction. To generate *p35S::MOS1:GFP* construct, the genomic piece of *MOS1* was amplified by PCR with forward primer (5'-GGGGACAAGTTTGTACAAAAAA GCAGGCTTCATGACCTCTAGCACGACAGGA-3') and reverse primer (5'-GGGGACCACT TTGTACAAGAAAGCTGGGTTGTTTCTATCACCAGTGAATCC-3'). *MOS1* genomic DNA was cloned into PDONR222 by BP reaction and transferred into pGWB405 destination vector (Nakagawa et al., 2007).

**Y2H and BiFC**

For the yeast two-hybrid analysis, cDNAs of gene of interest were cloned into pDEST-GADT7 and pDEST-GBKT7 and assays were performed as previously described (Ascencio-Ibanez et al., 2008). For BiFC analysis, SUF4 cDNA was cloned into pSPYNE-35S GW destination vector and MOS1 cDNA was cloned into pSPYCE-35S GW destination vector by LR reactions and assays were performed as previously described (Schutze et al., 2009).

**RNA blot analysis**

RNA blots analysis was carried out as described previously (Yang and Hua, 2004). For *PR1* and *SNC1* probe, the full length sequence and the first exon of the coding regions were used as probes, respectively.

**Quantitative RT-PCR**

qRT-PCR was conducted by following the manufacture's protocol of FastStart universal SYBR Green Master (Roche). Primers for *SNC1* and the reference gene ubiquitin family protein (UFP) were as previous reports (Li et al., 2010; Zhu et al., 2011). The Primers for amplification of *CYCD3;1* are CYCD3;1qRT-F (5'-CAACTACCAGTGGACCGCAT-3') and CYCD3;1qRT-R (5'-TCAATCACGCAGCTTGGACT-3').

**Transcriptome analysis**

Preparation of cDNA library and RNA-Seq were carried out as previously described (Zhong et al., 2011). Differentially expressed genes associated signaling pathways were further characterized by Mapman software.

**Ploidy measurement**

The first and second true leaves from two plants of 4 to 6-week old were collected and chopped in "Aru" buffer containing 97.5% $MgSO_4$ (0.246% $MgSO_4 \cdot 7H_2O$, 0.37% KCl and 0.12% Hepes), 0.1% DTT and 2.5% Triton X-100 (Arumuganathan and Earle, 1991). 10 µl of PI (propidium iodide) stock solution (5 mg/ml) and 5 µl RNase stock solution (10 mg/ml) were added into each sample of approximately 600 µl. BD Accuri C6 flow cytometer was used to measure ploidy. Three replicas were analyzed for each sample.

**Acknowledgements**

We thank Arabidopsis Biological Resource Center for DNA clones. We thank Dr. Shiyan Chen and Dr. Xiaohong Wang for help on the qRT-PCR analysis. We thank Xian Qu and Dr. Adrienne Roeder for confocal microscopy. This work was supported by NSF grants IOS-0642289 and IOS-0919914 to J. H.

## Reference


**Arumuganathan, K., and Earle, E.D.** (1991). Estimation of nuclear DNA content of plants by flow cytometry. Plant Molecular Biology Reporter **9,** 229-233.

**Ascencio-Ibanez, J.T., Sozzani, R., Lee, T.J., Chu, T.M., Wolfinger, R.D., Cella, R., and Hanley-Bowdoin, L.** (2008). Global analysis of Arabidopsis gene expression uncovers a complex array of changes impacting pathogen response and cell cycle during geminivirus infection. Plant physiology **148,** 436-454.

**Bao, Z., Yang, H., and Hua, J.** (2013). Perturbation of cell cycle regulation triggers plant immune response via activation of disease resistance genes. Proceedings of the National Academy of Sciences of the United States of America **110,** 2407-2412.

**Caillaud, M.C., Paganelli, L., Lecomte, P., Deslandes, L., Quentin, M., Pecrix, Y., Le Bris, M., Marfaing, N., Abad, P., and Favery, B.** (2009). Spindle assembly checkpoint protein dynamics reveal conserved and unsuspected roles in plant cell division. PLoS One **4,** e6757.

**Choi, K., Kim, J., Hwang, H.J., Kim, S., Park, C., Kim, S.Y., and Lee, I.** (2011). The FRIGIDA complex activates transcription of FLC, a strong flowering repressor in Arabidopsis, by recruiting chromatin modification factors. The Plant cell **23,** 289-303.

**Clarke, J.H., and Dean, C.** (1994). Mapping FRI, a locus controlling flowering time and vernalization response in Arabidopsis thaliana. Molecular & general genetics : MGG **242,** 81-89.

**Crevillen, P., and Dean, C.** (2011). Regulation of the floral repressor gene FLC: the complexity of transcription in a chromatin context. Current opinion in plant biology **14,** 38-44.

**De Antoni, A., Pearson, C.G., Cimini, D., Canman, J.C., Sala, V., Nezi, L., Mapelli, M., Sironi, L., Faretta, M., Salmon, E.D., and Musacchio, A.** (2005). The Mad1/Mad2 complex as a template for Mad2 activation in the spindle assembly checkpoint. Current biology : CB **15,** 214-225.

**Dewitte, W., Scofield, S., Alcasabas, A.A., Maughan, S.C., Menges, M., Braun, N., Collins, C., Nieuwland, J., Prinsen, E., Sundaresan, V., and Murray, J.A.** (2007). Arabidopsis CYCD3 D-type cyclins link cell proliferation and endocycles and are rate-limiting for cytokinin responses. Proceedings of the National Academy of Sciences of the United States of America **104,** 14537-14542.

**Dodds, P.N., and Rathjen, J.P.** (2010). Plant immunity: towards an integrated view of plant-pathogen interactions. Nature reviews **11,** 539-548.

**Gudmundsdottir, K., and Ashworth, A.** (2004). BRCA2 in meiosis: turning over a new leaf. Trends in cell biology **14,** 401-404.

**Heil, M., and Baldwin, I.T.** (2002). Fitness costs of induced resistance: emerging experimental support for a slippery concept. Trends in plant science **7,** 61-67.

**Heyman, J., Van den Daele, H., De Wit, K., Boudolf, V., Berckmans, B., Verkest, A., Kamei, C.L., De Jaeger, G., Koncz, C., and De Veylder, L.** (2011). Arabidopsis ULTRAVIOLET-B-INSENSITIVE4 Maintains Cell Division Activity by Temporal Inhibition of the Anaphase-Promoting Complex/Cyclosome. The Plant cell.

**Hua, J., Grisafi, P., Cheng, S.H., and Fink, G.R.** (2001). Plant growth homeostasis is controlled by the Arabidopsis BON1 and BAP1 genes. Genes & development **15,** 2263-2272.

**Inagaki, S., and Umeda, M.** (2011). Cell-cycle control and plant development. International review of cell and molecular biology **291,** 227-261.

**Inze, D., and De Veylder, L.** (2006). Cell cycle regulation in plant development. Annual review of genetics **40,** 77-105.

**Iwata, E., Ikeda, S., Matsunaga, S., Kurata, M., Yoshioka, Y., Criqui, M.C., Genschik, P., and Ito, M.** (2011). GIGAS CELL1, a Novel Negative Regulator of the Anaphase-Promoting Complex/Cyclosome, Is Required for Proper Mitotic Progression and Cell Fate Determination in Arabidopsis. The Plant cell.

**Jambunathan, N., Siani, J.M., and McNellis, T.W.** (2001). A humidity-sensitive Arabidopsis copine mutant exhibits precocious cell death and increased disease resistance. Plant Cell **13,** 2225-2240.

**Jones, J.D., and Dangl, J.L.** (2006). The plant immune system. Nature **444,** 323-329.

**Kevei, Z., Baloban, M., Da Ines, O., Tiricz, H., Kroll, A., Regulski, K., Mergaert, P., and Kondorosi, E.** (2011). Conserved CDC20 cell cycle functions are carried out by two of the five isoforms in Arabidopsis thaliana. PloS one **6,** e20618.

**Kim, D.H., Doyle, M.R., Sung, S., and Amasino, R.M.** (2009). Vernalization: winter and the timing of flowering in plants. Annual review of cell and developmental biology **25,** 277-299.

**Kim, S., Choi, K., Park, C., Hwang, H.J., and Lee, I.** (2006). SUPPRESSOR OF FRIGIDA4, encoding a C2H2-Type zinc finger protein, represses flowering by transcriptional activation of Arabidopsis FLOWERING LOCUS C. The Plant cell **18,** 2985-2998.

**Kim, S., Sun, H., Tomchick, D.R., Yu, H., and Luo, X.** (2012). Structure of human Mad1 C-terminal domain reveals its involvement in kinetochore targeting. Proceedings of the National Academy of Sciences of the United States of America **109,** 6549-6554.

**Kim, S.Y., and Michaels, S.D.** (2006). SUPPRESSOR OF FRI 4 encodes a nuclear-localized protein that is required for delayed flowering in winter-annual Arabidopsis. Development **133,** 4699-4707.

**Kulukian, A., Han, J.S., and Cleveland, D.W.** (2009). Unattached kinetochores catalyze production of an anaphase inhibitor that requires a Mad2 template to prime Cdc20 for BubR1 binding. Developmental cell **16,** 105-117.

**Li, R., and Murray, A.W.** (1991). Feedback control of mitosis in budding yeast. Cell **66,** 519-531.

**Li, Y., Pennington, B.O., and Hua, J.** (2009). Multiple R-like genes are negatively regulated by BON1 and BON3 in arabidopsis. Mol Plant Microbe Interact **22,** 840-848.

**Li, Y., Tessaro, M.J., Li, X., and Zhang, Y.** (2010). Regulation of the expression of plant resistance gene SNC1 by a protein with a conserved BAT2 domain. Plant physiology **153,** 1425-1434.

**Li, Y., Dong, O.X., Johnson, K., and Zhang, Y.** (2011). MOS1 epigenetically regulates the expression of plant Resistance gene SNC1. Plant signaling & behavior **6,** 434-436.

**Michaels, S.D., and Amasino, R.M.** (1999). FLOWERING LOCUS C encodes a novel MADS domain protein that acts as a repressor of flowering. The Plant cell **11,** 949-956.

**Michaels, S.D., and Amasino, R.M.** (2001). Loss of FLOWERING LOCUS C activity eliminates the late-flowering phenotype of FRIGIDA and autonomous pathway mutations but not responsiveness to vernalization. The Plant cell **13,** 935-941.

**Nakagawa, T., Suzuki, T., Murata, S., Nakamura, S., Hino, T., Maeo, K., Tabata, R., Kawai, T., Tanaka, K., Niwa, Y., Watanabe, Y., Nakamura, K., Kimura, T., and Ishiguro, S.** (2007). Improved Gateway binary vectors: high-performance vectors for creation of fusion constructs in transgenic analysis of plants. Bioscience, biotechnology, and biochemistry **71,** 2095-2100.

**Schnittger, A., Schobinger, U., Bouyer, D., Weinl, C., Stierhof, Y.D., and Hulskamp, M.** (2002). Ectopic D-type cyclin expression induces not only DNA replication but also cell division in Arabidopsis trichomes. Proceedings of the National Academy of Sciences of the United States of America **99,** 6410-6415.

**Schutze, K., Harter, K., and Chaban, C.** (2009). Bimolecular fluorescence complementation (BiFC) to study protein-protein interactions in living plant cells. Methods Mol Biol **479,** 189-202.

**Shindo, C., Aranzana, M.J., Lister, C., Baxter, C., Nicholls, C., Nordborg, M., and Dean, C.** (2005). Role of FRIGIDA and FLOWERING LOCUS C in determining variation in flowering time of Arabidopsis. Plant physiology **138,** 1163-1173.

**Van Leene, J., Hollunder, J., Eeckhout, D., Persiau, G., Van De Slijke, E., Stals, H., Van Isterdael, G., Verkest, A., Neirynck, S., Buffel, Y., De Bodt, S., Maere, S., Laukens, K., Pharazyn, A., Ferreira, P.C., Eloy, N., Renne, C., Meyer, C., Faure, J.D., Steinbrenner, J., Beynon, J., Larkin, J.C., Van de Peer, Y., Hilson, P., Kuiper, M., De Veylder, L., Van Onckelen, H., Inze, D., Witters, E., and De Jaeger, G.** (2010). Targeted interactomics reveals a complex core cell cycle machinery in Arabidopsis thaliana. Molecular systems biology **6,** 397.

**Vlot, A.C., Dempsey, D.A., and Klessig, D.F.** (2009). Salicylic Acid, a multifaceted hormone to combat disease. Annual review of phytopathology **47,** 177-206.

**Yang, H., Li, Y., and Hua, J.** (2006a). The C2 domain protein BAP1 negatively regulates defense responses in Arabidopsis. Plant J **48,** 238-248.

**Yang, S., and Hua, J.** (2004). A haplotype-specific Resistance gene regulated by BONZAI1 mediates temperature-dependent growth control in Arabidopsis. The Plant cell **16,** 1060-1071.

**Yang, S., Yang, H., Grisafi, P., Sanchatjate, S., Fink, G.R., Sun, Q., and Hua, J.** (2006b). The BON/CPN gene family represses cell death and promotes cell growth in Arabidopsis. Plant J **45,** 166-179.

**Yu, H.G., Muszynski, M.G., and Kelly Dawe, R.** (1999). The maize homologue of the cell cycle checkpoint protein MAD2 reveals kinetochore substructure and contrasting mitotic and meiotic localization patterns. The Journal of cell biology **145,** 425-435.

**Zhang, Y., Goritschnig, S., Dong, X., and Li, X.** (2003). A gain-of-function mutation in a plant disease resistance gene leads to constitutive activation of downstream signal transduction pathways in suppressor of npr1-1, constitutive 1. The Plant cell **15,** 2636-2646.

**Zhong, S., Joung, J.G., Zheng, Y., Chen, Y.R., Liu, B., Shao, Y., Xiang, J.Z., Fei, Z., and Giovannoni, J.J.** (2011). High-throughput illumina strand-specific RNA sequencing library preparation. Cold Spring Harbor protocols **2011,** 940-949.

**Zhu, Y., Qian, W., and Hua, J.** (2010). Temperature modulates plant defense responses through NB-LRR proteins. PLoS Pathog **6,** e1000844.

**Zhu, Y., Weng, M., Yang, Y., Zhang, C., Li, Z., Shen, W.H., and Dong, A.** (2011). Arabidopsis homologues of the histone chaperone ASF1 are crucial for chromatin replication and cell proliferation in plant development. Plant J **66,** 443-455.

# CHAPTER 5

## Summary and future directions

Plant immune responses are usually activated only under the attack of plant pathogens. Constitutive activation of plant immune responses leads to severe growth and development defects (Heil and Baldwin, 2002). In Arabidopsis, *BON1* (*BONZAI1*) and its homologs *BON2* and *BON3* negatively regulate plant defense responses (Hua et al., 2001; Yang and Hua, 2004; Li et al., 2009). The *bon1-1* mutant in Col-0 has enhanced disease resistance and dwarf morphology due to upregulation of an *R* gene, *SNC1* (*suppressor of npr1-1, constitutive 1*) (Yang and Hua, 2004). Another *bon1-2* allele in Ws does not have enhanced defense responses or morphological defects due to the absence of functional *SNC1* allele in Ws. To understand how *BON1* affects plant defense responses, I took two approaches. One is functional analyses of an enhancer of *bon1-2, ebo30*, and the other is the isolation and analyses of a suppressor of *bon1-1, sbo3*.

In the *ebo30* study, I found a connection between cell cycle progression and plant immunity, suggesting that perturbed cell cycle progression could activate expression of *R* genes and plant immune responses. Dr. Huijun Yang isolated *ebo30* as *osd1-4,* an activation allele of *OSD1* (*Omission of Second Division 1*). The *bon1-2 osd1-4* mutant had enhanced disease resistance and exhibited dwarf morphology similar to *bon1-1*. OSD1 and its homolog UVI4 (UV-B-insensitive 4) are two negative regulators of APC/C, a multisubunit ubiquitin E3 ligase which plays critical roles in the regulation of cell cycle progression (Heyman et al., 2011a; Iwata et al., 2011). Further studies revealed that overexpression of *OSD1* and *UVI4* each leads to enhanced disease resistance to a bacterial pathogen, which is associated with a higher expression of disease resistance (*R*) genes. Moreover, knockdown mutant of *APC10*, a subunit of APC/C,

exhibited a similar phenotype to that of overexpression of *OSD1* or *UVI4*, indicating that altered APC/C function induces immune responses. Enhanced immune response induced by *OSD1* overexpression is dependent on *CYCB1;1* which is a degradation target of APC/C. It is also associated with upregulation of *R* genes and is dependent on the *R* gene *SNC1*.

The immediate questions are how cell cycle progression affects expression of *R* genes such as *SNC1* and what other components are involved in the connection between cell cycle regulation and plant immunity. One possibility is that activation of gene expression is associated with cell cycle phase (Menges et al., 2002, 2003). The altered *SNC1* expression in *OSD1* overexpression plants might be due to the extension or compression of a particular cell cycle phase. This can be tested by identifying *SNC1* expression pattern associated with cell cycle phases by using synchronized Arabidopsis suspension cells. To answer the second question, Dr. Huijun Yang and I already isolated three suppressors of *bon1 osd1-4*, with each suppressing a different aspect of the morphological defects of *bon1 osd1-4*, including general dwarfness, later shoots, and curly leaves. To clone these genes, I generated F2 populations by backcrossing with *bon1 osd1-4*. In each population, I collected more than 50 seedlings which are similar to *bon1 osd1-4* and more than 50 wild type-like seedlings. They can be potentially used for identifying suppressor mutations through next generation sequencing.

Further study of the role of *OSD1* revealed a close link among *UVI4*, *OSD1* and *CPR5* genes in the regulation of cell cycle progression. Loss of *OSD1* function abolished the second meiotic cell division (d'Erfurth et al., 2009) and triggered endomitosis (Iwata et al., 2011); and a loss of *UVI4* function promoted endoreduplication (Hase et al., 2006; Heyman et al., 2011a). I further investigated cell cycle defects in loss of function mutants, double mutant and overexpression lines. Loss of *OSD1* function also had promoted endoreduplication, and *osd1*

*uvi4* double mutant had female gametophyte and zygote lethality. Overexpression of *OSD1* and *UVI4* each resulted in reduced endoreduplication which was also found in loss of function mutant *cpr5*. Epistasis analysis indicated that *cpr5* mutation suppressed endoreduplication defects in *uvi4* and *osd1-2* as well as the lethality of *osd1 uvi4*. CCS52A1 and CCS52B, two interacting proteins with OSD1 and UVI4 are required for the lethality of *osd1 uvi4*. Interestingly, *ccs52b* mutation completely suppressed the female gametophyte lethality but partially suppress the zygote defects of *osd1 uvi4*. *ccs52a1* and *ccs52b* mutations lead to the downregulation of APC/C activities in the degradation of cell cycle proteins. Overexpression of *CYCB1;1* also partially suppresses the lethality of *osd1 uvi4*, and *cpr5* mutation triggers activation of *CYCB1;1* expression by manipulating the activity of CDK-cyclin complex.

The remaining questions are which cyclins are misregulated in *osd1 uvi4* and lead to lethality. In my study, 35S promoter was used to overexpress *CYCB1;1* gene in *osd1 uvi4*, but the effect is yet to be confirmed. This promoter may not be appropriate to trigger a high expression of *CYCB1;1* in a cell cycle specific manner. When the promoter of *CDKA;1* was used to control the expression of *CYCB1;1*, the transgenic plants showed accelerated plant growth (Doerner et al., 1996). It might be a good idea to transform *pCDKA;1::CYCB1;1* into *osd1/OSD1 uvi4/uvi4* and analyze progenies to determine whether this construct has more robust effects. *CYCB1;1* has a homolog *CYCB1;2* whose ectopic expression triggered more mitotic cell division (Schnittger et al., 2002a). Therefore, it is worth testing the effect of higher expression of *CYCB1;2* on the lethality of *osd1 uvi4*.

During the isolation of suppressor of *bon1-1*, I isolated *sbo3* as an allele of *MOS1* (*Modifier of snc1, 1*) gene. The *mos1* mutation suppressed defense phenotype and morphological defects of *snc1-1*, and also resulted in a late flowering phenotype (Li et al., 2010). Loss of *MOS1*

function suppresses the disease resistance and dwarf phenotype of *bon1-1* through the repression of *SNC1* expression. The late flowering phenotype in *mos1-6* is due to the activation of *FLC* expression. Interestingly, the *mos1* mutation also promotes endoreduplication. Further studies found that *MOS1*, *MAD2* (Mitotic Arrest Deficient 2) and *SUF4* (*SUPPRESSOR OF FRIGIDA 4*) interacted with each other. SUF4 is a C2H2 zinc-finger transcription activator binding at *FLC* promoter region to activate *FLC* expression (Kim et al., 2006; Kim and Michaels, 2006). *SUF4* is required for both late flowering phenotype and promoted endoreduplication in *mos1-6*, indicating that MOS1 regulates gene expression through SUF4. The *MAD2* gene is required for endocycle defects of *mos1-6*, suggesting that MOS1, MAD2 and SUF4 may form an inactive complex to promote floral transition and mitotic cell cycle progression. MAD1 is another interacting protein of MAD2 (Gudmundsdottir and Ashworth, 2004; Van Leene et al., 2010), and it also interacts with SUF4. The *mad1* mutation causes slightly early flowering, partially suppresses the late flowering and suppressor phenotype of *mos1-6*, and completely suppresses the endocycle defects of *mos1-6*, suggesting that MAD1, MAD2 and SUF4 may form an active complex to antagonize the function of *MOS1*.

The remaining questions are how *MOS1* regulates the *SNC1* expression and whether *SUF4* plays a role in the regulation of S*NC1* expression. I generated a transgenic line containing CaMV 35S promoter-driven *MOS1* genomic DNA fused with GFP in *bon1 mos1-6*. This line recaptured bon1-1 phenotypes and could be used to isolate more MOS1-interacting proteins by the purification of *MOS1* complex. To understand the function of *SUF4* in the regulation of *SNC1* expression, I generated a *bon1 suf4* double mutant which had three different morphological phenotypes without alteration of *SNC1* expression: no suppression, moderate suppression and large suppression. These phenomena might be due to the strong activation of

*SNC1* by *bon1* mutation which masks the effect of *suf4* mutation. Therefore, I am generating another double mutant *snc1-1 suf4* because *snc1-1* has relatively weaker phenotype than *bon1-1*. In addition, I am generating the triple mutant *bon1 mos1 suf4* by crossing *bon1 mos1* and *mos1 suf4*. Whether *SUF4* has a role on the regulation of *SNC1* expression will be known with the analysis of *snc1 suf4* double mutant and *bon1 mos1 suf4* triple mutant. If *suf4* mutation suppresses the *snc1-1* phenotype, *SUF4* might also be an activator for *SNC1* expression. If *suf4* mutation enhances the *snc1-1* phenotype, *SUF4* might act as a repressor for *SNC1* expression. If *suf4* mutation partially or completely suppresses the suppressor phenotype of *bon1 mos1*, it would strongly support that *SUF4* is required for *MOS1* function in plant defense responses.

In my thesis research, I have explored associations among cell cycle regulations, plant defense responses and flowering time control. Under normal growth conditions, cell cycle controls cell proliferation and cell division in the plant growth and development. The interactions among MOS1, MAD2 and SUF4 facilitate the mitotic cell cycle progression and floral transition. Under biotic stress conditions, plant defense responses are activated. Consequently, plant growth is arrested and flowering time is shortened. This study could lead to a better understanding of the link among cell cycle progression, defense responses and flowering time control together. To explore this topic further, the following experiments can be carried out.

First, explore a general relationship between plant cell cycle regulation and pathogen invasion at local infection tissues and distal uninfected tissues. Second, collect more mutants with increased or decreased resistance phenotypes to allow an association analysis on defense, the flowering time and cell cycle progression. It is possible that cell cycle regulation plays a role in connecting plant defense responses and flowering time control. Third, test disease resistance and flowering time in mutants of cell cycle proteins. Cell cycle progression is associated with the

histone deposition and histone modification (Sanchez Mde et al., 2008). Fourth, collect mutants affecting histone deposition or modification and analyze their disease resistance, flowering time and cell cycle progression. These results may determine whether altered defense responses and flowering time by perturbed cell cycle progression are due to change of the deposition of histone marks at different cell cycle phase. Perturbed cell cycle regulation may activate the checkpoint machinery and consequently trigger PCD and disease resistance. Whether pathogen invasion affects the activation of checkpoint machinery needs to be determined. Fifth, collect mutants in checkpoint machinery and analyze the disease resistance to test a connection between DNA damages and plant immune responses.

All the studies will further expand our knowledge on how plant resistance genes are regulated and how plants fine-tune different signaling pathways to optimize their growth and development under stress conditions.

**Reference**

**d'Erfurth, I., Jolivet, S., Froger, N., Catrice, O., Novatchkova, M., and Mercier, R.** (2009). Turning meiosis into mitosis. PLoS biology **7,** e1000124.

**Doerner, P., Jorgensen, J.E., You, R., Steppuhn, J., and Lamb, C.** (1996). Control of root growth and development by cyclin expression. Nature **380,** 520-523.

**Gudmundsdottir, K., and Ashworth, A.** (2004). BRCA2 in meiosis: turning over a new leaf. Trends in cell biology **14,** 401-404.

**Hase, Y., Trung, K.H., Matsunaga, T., and Tanaka, A.** (2006). A mutation in the uvi4 gene promotes progression of endo-reduplication and confers increased tolerance towards ultraviolet B light. Plant J **46,** 317-326.

**Heil, M., and Baldwin, I.T.** (2002). Fitness costs of induced resistance: emerging experimental support for a slippery concept. Trends in plant science **7,** 61-67.

**Heyman, J., Van den Daele, H., De Wit, K., Boudolf, V., Berckmans, B., Verkest, A., Kamei, C.L., De Jaeger, G., Koncz, C., and De Veylder, L.** (2011). Arabidopsis ULTRAVIOLET-B-INSENSITIVE4 Maintains Cell Division Activity by Temporal Inhibition of the Anaphase-Promoting Complex/Cyclosome. The Plant cell.

**Hua, J., Grisafi, P., Cheng, S.H., and Fink, G.R.** (2001). Plant growth homeostasis is controlled by the Arabidopsis BON1 and BAP1 genes. Genes & development **15,** 2263-2272.

**Iwata, E., Ikeda, S., Matsunaga, S., Kurata, M., Yoshioka, Y., Criqui, M.C., Genschik, P., and Ito, M.** (2011). GIGAS CELL1, a Novel Negative Regulator of the Anaphase-Promoting Complex/Cyclosome, Is Required for Proper Mitotic Progression and Cell Fate Determination in Arabidopsis. The Plant cell.

**Kim, S., Choi, K., Park, C., Hwang, H.J., and Lee, I.** (2006). SUPPRESSOR OF FRIGIDA4, encoding a C2H2-Type zinc finger protein, represses flowering by transcriptional activation of Arabidopsis FLOWERING LOCUS C. The Plant cell **18,** 2985-2998.

**Kim, S.Y., and Michaels, S.D.** (2006). SUPPRESSOR OF FRI 4 encodes a nuclear-localized protein that is required for delayed flowering in winter-annual Arabidopsis. Development **133,** 4699-4707.

**Li, Y., Pennington, B.O., and Hua, J.** (2009). Multiple R-like genes are negatively regulated by BON1 and BON3 in arabidopsis. Mol Plant Microbe Interact **22,** 840-848.

**Li, Y., Tessaro, M.J., Li, X., and Zhang, Y.** (2010). Regulation of the expression of plant resistance gene SNC1 by a protein with a conserved BAT2 domain. Plant physiology **153,** 1425-1434.

**Menges, M., Hennig, L., Gruissem, W., and Murray, J.A.** (2002). Cell cycle-regulated gene expression in Arabidopsis. J Biol Chem **277,** 41987-42002.

**Menges, M., Hennig, L., Gruissem, W., and Murray, J.A.** (2003). Genome-wide gene expression in an Arabidopsis cell suspension. Plant molecular biology **53,** 423-442.

**Sanchez Mde, L., Caro, E., Desvoyes, B., Ramirez-Parra, E., and Gutierrez, C.** (2008). Chromatin dynamics during the plant cell cycle. Semin Cell Dev Biol **19,** 537-546.

**Schnittger, A., Schobinger, U., Stierhof, Y.D., and Hulskamp, M.** (2002). Ectopic B-type cyclin expression induces mitotic cycles in endoreduplicating Arabidopsis trichomes. Curr Biol **12,** 415-420.

**Van Leene, J., Hollunder, J., Eeckhout, D., Persiau, G., Van De Slijke, E., Stals, H., Van Isterdael, G., Verkest, A., Neirynck, S., Buffel, Y., De Bodt, S., Maere, S., Laukens, K., Pharazyn, A., Ferreira, P.C., Eloy, N., Renne, C., Meyer, C., Faure, J.D., Steinbrenner, J., Beynon, J., Larkin, J.C., Van de Peer, Y., Hilson, P., Kuiper, M., De Veylder, L., Van Onckelen, H., Inze, D., Witters, E., and De Jaeger, G.** (2010). Targeted interactomics reveals a complex core cell cycle machinery in Arabidopsis thaliana. Molecular systems biology **6,** 397.

**Yang, S., and Hua, J.** (2004). A haplotype-specific Resistance gene regulated by BONZAI1 mediates temperature-dependent growth control in Arabidopsis. The Plant cell **16,** 1060-1071.